Master Thesis, Department of Geosciences

Analogue Modelling of Detachment Zones and Structural Analysis of the Ringvassøy- Loppa Fault Complex, SW Barents Sea

Hanna Lima Braut

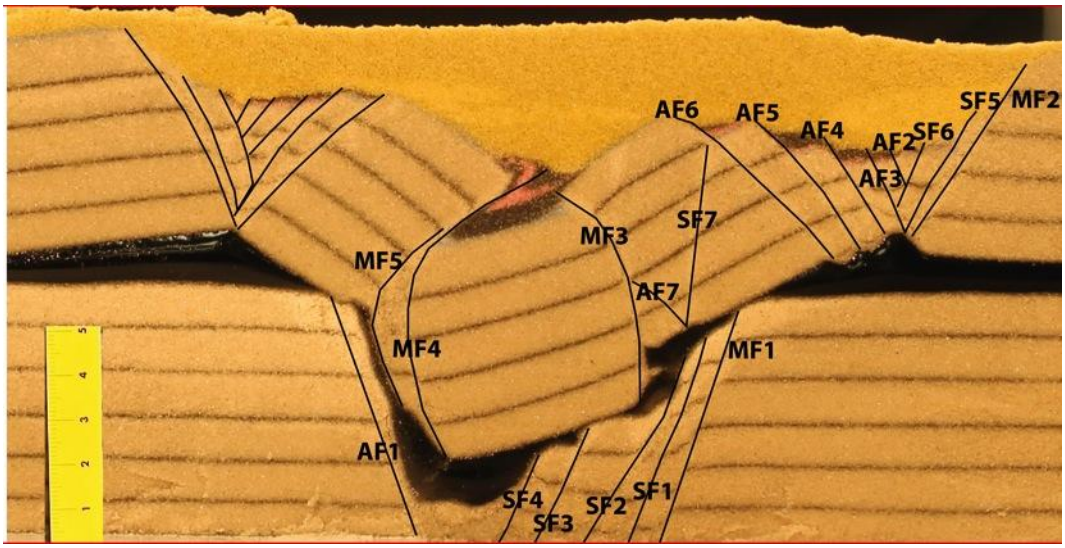

UNIVERSITY OF OSLO
FACULTY OF MATHEMATICS AND NATURAL SCIENCES

Analogue Modelling of Detachment Zones and Structural Analysis of the Ringvassøy- Loppa Fault Complex, SW Barents Sea

Hanna Lima Braut

Master Thesis in Geosciences

Discipline: Petroleum Geology and Geophysics

Department of Geosciences

Faculty of Mathematics and Natural Sciences

University of Oslo

June, 2012

© Hanna Lima Braut, 2012
Tutor(s): Roy H. Gabrielsen[i], Jan Inge Faleide[i] and Dimitrios Sokoutis[ii]

i) University of Oslo, UiO

ii) Vrije Universiteit, Amsterdam, the Netherlands.

This work is published digitally through DUO – Digitale Utgivelser ved UiO
http://www.duo.uio.no
It is also catalogued in BIBSYS (http://www.bibsys.no/english)
All rights reserved. No part of this publication may be reproduced or transmitted, in any form or by any means.

Abstract

The Southern part of Ringvassøy- Loppa Fault Complex is an extensional fault complex separating the Hammerfest Basin and the Tromsø Basin. Basement movements are believed to have caused the fault complex to work as a long-lived hinge line based on a deep seated zone of weakness, reactivated several times.

Structural analysis with special emphasize on detachment zones, fluid communication and periods of active faulting, is presented based on interpreting of 2D seismic lines are presented for this study. Analogue experiments were performed as a complementary part to understand the structural geometries developed during multiple extensions with presence of detachments.

Five extensional tectonic phases were distinguished in the sequences in the fault complex. The five phases were in Carboniferous?, Mid Jurassic- earliest Cretaceous, Early Cretaceous and Early Tertiary. Structures related to growth faults were identified in the seismic and established the active periods. These five observed tectonic phases are in correlation to the known regional tectonic phases in the South Western Barents Sea.

Three vertically separated levels were affected by faulting in the fault complex, namely the Late Permian level of faulting, Mid Jurassic- Early Cretaceous level of faulting and Early Tertiary level of faulting. Three possible detachments are proposed to separate the different levels of faulting.

Reactivation of faults during the tectonic events is likely to contain open fractures in the damage zone of the fault plane. Some of the faults in the fault complex appear to be reactivated and might affect the fluid communication in the area. Detachment zones are likely to have ceiling properties and consequently affect the migration path of hydrocarbons in the area.

Acknowledgements

I would like to give my supervisors, Prof. Roy Helge Gabrielsen and Prof. Jan Inge Faleide, great thanks for their patience, motivating discussions, guidance and time. Your help has been vital for the results of this thesis.

I will also give my special thanks to the Prof. Dimitrios Sokoutis and the TecLab staff at Vrije Universiteit, Amsterdam, for their warm welcome and great atmosphere during my stay.

Thanks to Dr. Michael Heeremans for loading all the acquired data for this study, and for helping out with problems and technical issues with the software.

TGS-NOPEC is acknowledged for making the seismic data available.

Thanks to my dear friends at Geo for good discussions, support and motivating talks. Finally thanks to all my friends and family for your patience and great support during the period of writing this thesis.

Table of Content

Chapter 1; Introduction

The Barents Sea is located in the north- western corner of the Eurasian continental shelf between Svalbard and Franz Josef Land in the north, mainland Norway and Russia in the south, the Norwegian- Greenland Sea in the west and Novaya Zemlya in the east, Figure 2.1 (Larssen, et al., 2005; Faleide et al., 1993a). It is bounded by two passive continental margins, Eurasia basin in the north and the Norwegian Greenland Sea in the west (Figure 1.1), which developed during the final continental breakup in Cenozoic time (Faleide et al., 1993a).

The structural pattern in the South Western Barents Sea is characterized by a composition of basins, highs and fault complexes connecting them (e.g. Gabrielsen et al., 1990). It is suggested that a deep- seated zone of weakness settled in the Devonian and even during the Caledonian Orogeny, caused the complex distribution of the structural elements (Gabrielsen et al., 1990; Gudlaugsson et al., 1998). Three main phases of rifting have affected the area from Late Paleozoic to Cenozoic and reactivation of long- lived fault zones are suggested during these events (Berglund et al., 1986; Gabrielsen et al., 1990; Faleide et al., 1993a). Ringvassøy- Loppa Fault Complex is one of these long- lived fault zones and the southern part of the fault complex makes out the study area of this study.

The study area has been extensively investigated in relation to petroleum exploration in more than 30 years. The Snøhvit field is located in the western part of the Hammerfest Basin and many wells and seismic surveys have provided the area with invaluable geological information.

The aim of this study is to investigate the structural geometries in the Ringvassøy-Loppa Fault Complex, identify active periods of faulting to correlate local tectonics to the regional tectonics, determine whether reactivation of faults have occurred and whether detachments are present or not in the study area. Also the affect of reactivated faults and the presence of possible detachments on the fluid communication in the area are emphasized.

Seismic interpretation of 2D seismic lines and the results of analogue experiments are the two complementary parts of the data set for this study. Wells were used to correlate the stratigraphic formation tops to the reflections in the seismic. The seismic interpretation was done on chosen Key Profiles to establish the structural geometries

and the tectonic history of the southern part of Ringvassøy- Loppa Fault Complex. The analogue models are used to investigate the interaction of multiple stages of deformation and the effect of stacked detachments.

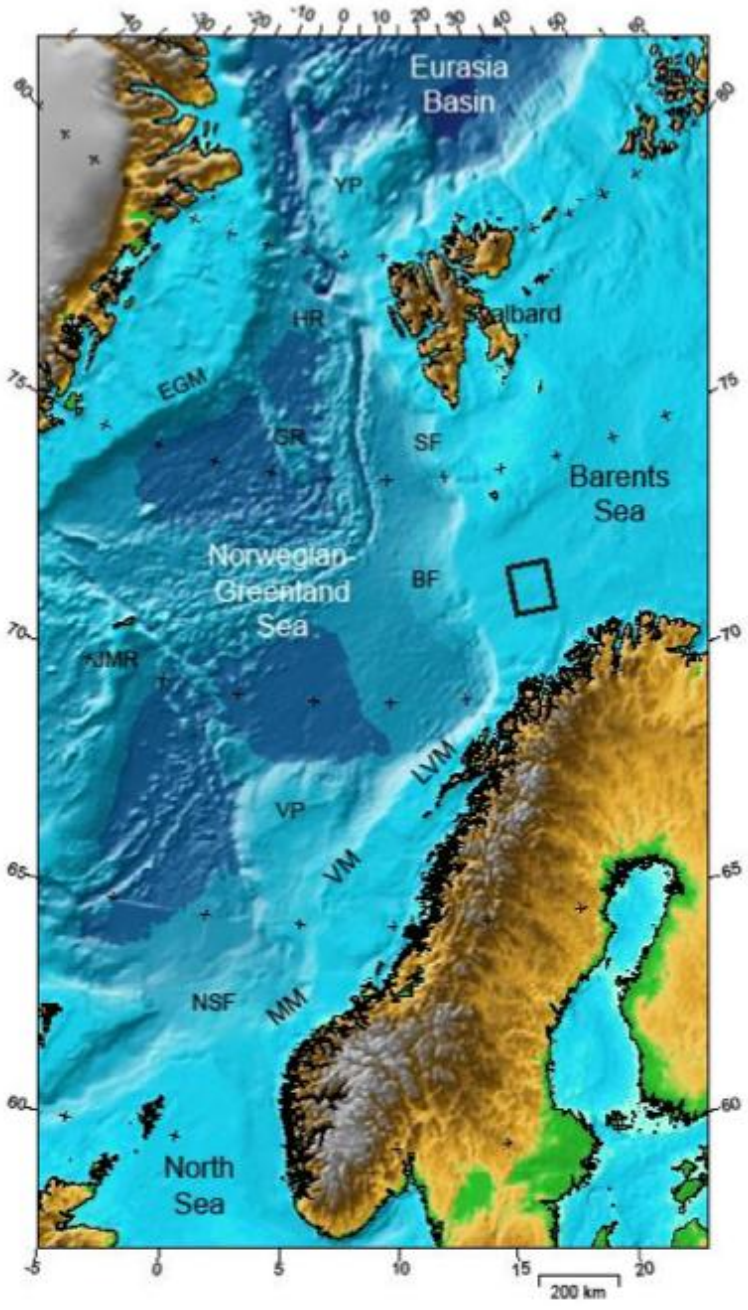

Figure 1.1: The Barents Sea is bounded by two passive continental margins, Eurasia basin in the north and the Norwegian Greenland Sea in the west. The study area is outlined by the black square (Modified from Faleide et al. 2008).

Chapter 2; Geological framework

2.1. Regional Setting

The structural evolution and the regional tectonic setting of the South Western Barents Sea have been studied by several authors (Rønnevik, 1981; Rønnevik et al., 1982; Rønnevik et al., 1984; Faleide et al., 1984; Gabrielsen, 1984 ; Ziegler, 1988; Gabrielsen et al., 1990; Dengo & Røssland, 1992; Faleide et al., 1993a; Faleide et al., 1993b; Gudlaugsson et al., 1998; Stemmerik, 2000; Faleide et al., 2008). The Barents Sea region has experienced several tectonic events since Paleozoic time. The Caledonian orogeny was followed by three main phases of rifting from Late Paleozoic to Cenozoic time, gradually migrating westwards (Gabrielsen et al., 1990; Faleide et al., 1993a). Salt tectonics influenced some areas in Mesozoic to Cenozoic time (Gabrielsen 1984), and massive glacial erosion was active in Neogene time (Gabrielsen et al., 1990; Nyland et al., 1992). The age of the sediments are ranging from Paleozoic to Cenozoic age, and they are distributed in correlation with tectonically created accommodation space.

The first rifting period in late Paleozoic time is proposed to have three major phases, Mid Carboniferous, Carboniferous- Permian and Permian- Early Triassic (Dóre et al., 1991; Faleide et al., 2008). This overall Paleozoic event was dominated by crustal extension and affected most of the Barents Sea. These structural features are covered by a thick sediment package farther west in the Barents Sea and have been influenced by several younger tectonic events in the Late Mesozoic and Cenozoic time. Two main phases affected the western Barents Sea in Mesozoic to Cenozoic time, Mid Jurassic - Early Cretaceous, and Early Tertiary. These two phases of rifting showed a gradually westward migration, and left the eastern part as a relatively tectonic stable platform (Gabrielsen et al., 1990; Faleide et al., 2010). The continental rifting along North Atlantic and Arctic, in relation to the break up of Pangea, was the source of these tectonic phases, and resulted in complex regional tectonic of both rifting and shearing (Faleide et.al., 1993a; Stemmerik, 2000).

Faleide et al. (1993a and 2010) divided the western Barents Sea into three geological provinces based on sedimentary infill, tectonic style and crustal structure, Figure 2.1.

1) The eastern part of the Barents Sea, and the Svalbard platform area. The area consists of mixed carbonate, evaporitic and clastic rocks of Late Paleozoic-Mesozoic time. The area has been relatively tectonic stable since the Paleozoic time.
2) The South Western Barents Sea, which is dominated by a complex pattern of subbasins and highs with a westward increasing structural relief. The eastern basins of this province (Hammerfest Basin, Fingerdjupet Subbasin) are containing sediments of Jurassic to Cretaceous age, and the deep Cretaceous-Tertiary western basins (Harstad, Tromsø, Bjørnøya and Orvestnaget) contain Paleocene – Eocene sediments. Several intrabasinal highs are located in the province (Senja Ridge, Veslemøy High and Stappen High)
3) The continental margin, Lofoten Basin and the Vestbakken Volcanic Province, developed during the final break up of the Norwegian Greenland Sea in Cenozoic time.

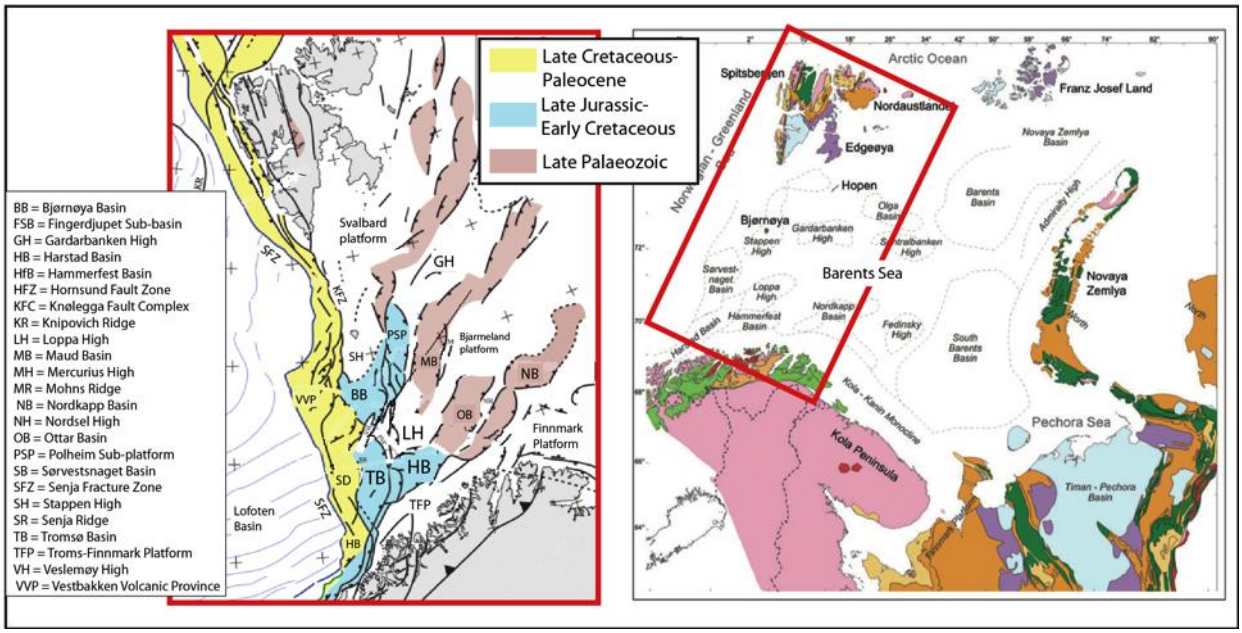

Figure 2.1: Right: The location of the Barents Sea (Worsley et al. 2008). Left: The main structural elements of the South Western Barents Sea. Colours show which structural elements were affected by different rift phases (Modified from Faleide et al. 2010).

The structural elements in the Western Barents Sea are in general ENE- WSW to NE-SW and NNE-SSW to NNW-SSE trending (Gabrielsen et al., 1990). It is suggested that younger tectonic events in the Barents Sea are affected by older structural trends established in Devonian and some during the Caledonian Orogeny (Gabrielsen et al., 1990; Gudlaugsson et al., 1998). Sediments in Devonian might have been deposited

in fault- bounded basins, which trailed already existing structural trends (Gabrielsen 1984; Gabrielsen, et al. 1990).

2.2. Structural elements

The southern part of Ringvassøy- Loppa Fault Complex is the study area of this study. To discuss and conclude on the deformational history and style of this fault complex, adjacent structural elements will here be described and put in a tectonic setting. The Ringvassøy- Loppa Fault Complex and the adjacent basins and highs have been exposed to a complex tectonic development where Ringvassøy- Loppa Fault Complex served as an important transition between two tectonically different regimes (Gabrielsen, 1984).

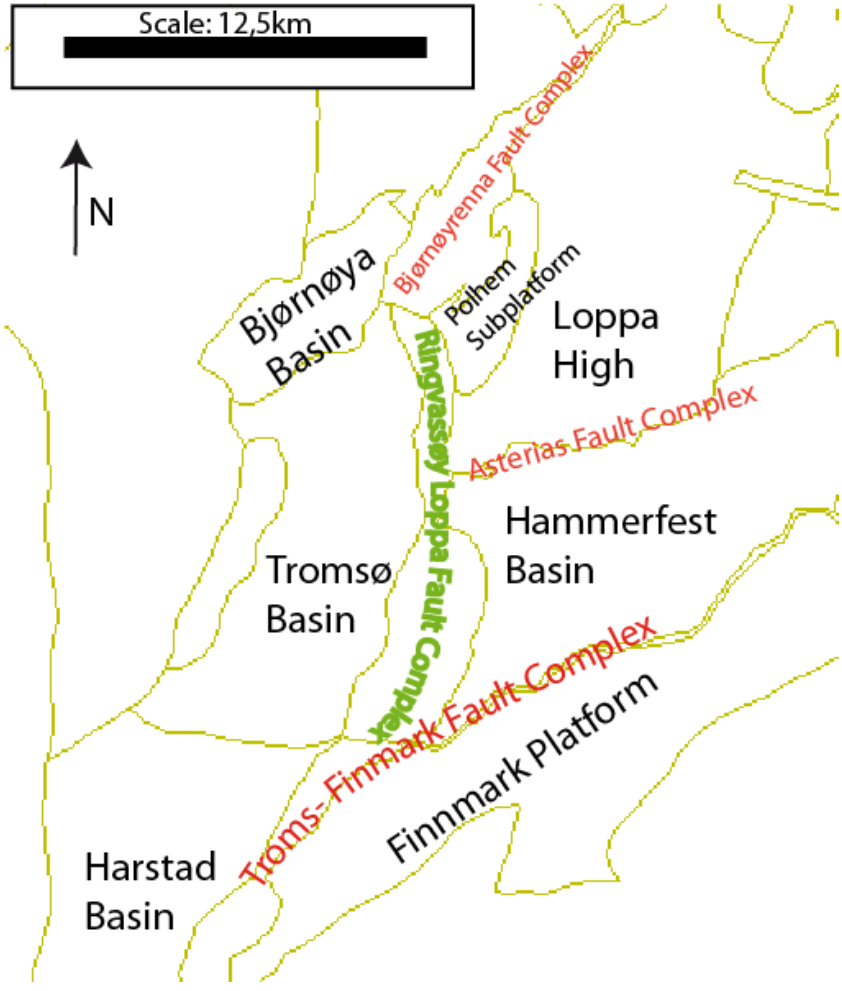

Figure 2.2: The location and relation between the structural elements adjacent to the study area.

The Hammerfest Basin

The Hammerfest Basin is located north of the Finnmark Platform, south of the Loppa High and east of the Tromsø Basin. Troms- Finnmark Fault Complex separates the Hammerfest Basin from the Finnmark Platform, Asterias Fault Complex makes out the transition towards the Loppa High, whereas Ringvassøy- Loppa Fault Complex separates it from the Tromsø Basin. The eastern limit of the basin is a flexure towards the Bjarmeland Platform. The basin is relatively shallow and has an axis trending ENE-WSW. The western part of the basin has a general western dip, and a structural dome that trend parallel to the basin axis (Gabrielsen et al., 1990). This dome was generated during Late Jurassic to Cretaceous in relation to the movements along the northern and southern boundary faults (Faleide et al. 1993a). Faults oriented E-W, ENE-WSW and WNW-ESE, are found in the centre of the western part and are known as the Hammerfest Basin Fault System (Gabrielsen 1984). The eastern part of the basin has not been much affected by faulting, and shows features of a sag basin. Generally the Hammerfest Basin contains deep, steep dipping faults along the margins, and intrabasinal listric normal faults detached above or within Permian sequences. Extension have been the main tectonic genesis causing the structures, but strike-slip movements in mid Jurassic to Cretaceous have also been suggested to have affected certain structures (Gabrielsen et.al. 1990)

The basin as known today was formed during the Mesozoic rift phase, but it started to develop already in the Devonian to Carboniferous time. The Troms Finnmark Fault Complex was then separating the basin from the Finnmark Platform (Gabrielsen et. al . 1990). The Hammerfest Basin together with the Loppa High experienced an easterly tilting during Late Carboniferous to Early Permian time. An E- W extensional regime was dominating the South Western Barents Sea during this time, and caused reactivation of underlying basement fault trends (Berglund et al., 1986). The locations of the main fault trends of the Hammerfest Basin are overlying deep basement grains that tend to have been reactivated through time. One such major fault zone between two basement blocks was located beneath the Ringvassøy- Loppa Fault Complex (Berglund et al., 1986).

The development of the Hammerfest Basin ceased during Early Cretaceous when Ringvassøy- Loppa Fault Complex separated it from the Tromsø Basin (Gabrielsen et al., 1990). Hammerfest Basin did not experience the Cretaceous to Tertiary basin subsidence like the basins farther west, and Cretaceous stratigraphic units have a general thickening trend from the Hammerfest Basin westward into the Tromsø Basin (Faleide et al., 1993a). Hammerfest Basin experienced erosion of 1000-1500m during uplift in Neogene (Nyland et al., 1992).

The Hammerfest Basin contains important petroleum reserves, which have provided extensive information through wells and seismic data in the area. The Snøhvit field is located in the Hammerfest Basin and consists of the three reservoir sandstone formations, Stø, Nordmela and Tubåen (Figure 2.4). Studies of quartz cementations, burial depth of the reservoir formations and the presence of open fracture communication, are some of the studies done based on information from the Snøhvit field. Quartz cementation and pressure solution stylolitization have destroyed the primary porosity and imply that the maximum burial depth was greater than the present burial depth (Olaussen et al, 1984; Berglund et al., 1986; Wennberg et al., 2008). Studies of open fractures in cores from the Snøhvit field done by Wennberg et al. (2008), are important when analysing the fluid flow in the area. A network of fractures is affecting an area around the fault core that is called the damage zone (Gabrielsen, 2010). The fractures are developed both parallel to, and cutting the main fault core. The width of the damage zone is proportional to the total fault throw, however the latest reactivation of the fault is more important in generation and preservation of fractures than the total displacement on a fault (Wennberg et al., 2008). Some of the faults in the Snøhvit field have been reactivated and are likely to have caused a network of open fractures (Wennberg et al. 2008).

The Tromsø Basin

The Tromsø Basin is bounded by the Ringvassøy- Loppa Fault Complex in the east, the Senja Ridge in the west and the intra basinal high, Veslemøy High, in the north. Troms Finnmark Fault Complex makes the southeastern boundary of the basin, while the southwestern boundary is not fully understood. The axis of the basin is trending NNE-SSW, and is defined by salt diapirs and the internal Tromsø Basin Fault System

in the south central part. The internal fault system is parallel to the basin axis and appears younger than the boundary faults, with activity as late as Eocene time (Gabrielsen et al., 1984). The salt is suggested to be evaporites deposited during Late Paleozoic time (Berglund et al., 1986; Faleide et.al., 1993a).

It is suggested that the basin did not exist before these evaporites (Gudlaugsson et al. 1998). The basin started to subside after the first rift event in Late Paleozoic time and the bounding faults of the basin show Early Carboniferous offset (Dengo and Røssland, 1992). After the second rifting from Mid Jurassic to Cretaceous time the basin experienced rapid subsidence, and a thick Cretaceous sediment package was deposited. The Tromsø Basin was at this time completely separated from the Hammerfest Basin by the Ringvassøy- Loppa Fault Complex. Depth to the basin floor is only measured in the northern part of the basin where it reaches 7-7,5 second *twt* (two-way traveltime) (Brekke og Riis, 1987; Gabrielsen et al. 1990).

The Loppa High

When introducing the Loppa High area in this study we make use of the terms used by Glørstad- Clark et al. (2011). The high as present in Late Paleozoic – Early Triassic time is termed the Selis Ridge, and was located beneath the western part of present day Loppa High. The high as defined in Late Triassic- Early Cretaceous, is termed Loppa High. The term Loppa High area refers to both structures in reference to tectonic movements, since no distinctions have been made in previous literature.

Three main fault complexes are bounding the present day Loppa High. The Bjørnøyrenna Fault Complex and the Ringvassøy- Loppa Fault Complex are respectively separating the Loppa High area from Bjørnøya Basin and Tromsø Basin in the west, whereas the Asterias Fault Complex is the delineation to the Hammerfest Basin in the south. The eastern and southeastern limit of the Loppa High area is marked by a monocline towards the Bjarmeland Platform and the Hammerfest Basin respectively. The Svans Dome, a salt structure, and the Maud Basin, the associated rim synclines of the salt, mark the boundary of the high in the northeast (Gabrielsen et al., 1990). The extent of the Loppa High area has also been associated by positive gravity anomalies from 0- 70mGal, and magnetic anomalies from 100- 900nT (Barrére et al., 2009). This is the effect of an

underlying Caledonian, shallow metamorphic basement in the western part of the high (Gabrielsen, 1984; Gabrielsen et al. 1990).

The Loppa High area has been influenced by repeated tectonic events since Devonian time. Several uplifts, subsidence, tilting and erosional events have affected the area. The first generation of the high was in Late Carboniferous time, but the first major uplift was in Late Permian (Dengo & Røssland, 1992). The high at this time, Selis Ridge, was a narrow N-S trending ridge located in the western part of present day Loppa High. The Loppa High area remained a positive structural feature until Early to Mid Triassic time. The High turned into a depocenter from Late Triassic to Mid Jurassic (Larssen et al., 2005). In Late Jurassic to Cretaceous time Loppa High area was again uplifted and eroded, due to footwall uplift along the fault complexes on the western margin (Faleide et al., 1993a). Onlap during the Early Tertiary shows that the high was part of a shallow Barents shelf until it was uplifted and eroded again in Neogen time (Wood et al., 1989; Faleide et al., 1993a, b). The result of several uplifts is the lack of post Jurassic sediments in the Loppa High area (Gabrielsen et al., 1990; Faleide et al., 1993a; Gabrielsen et al., 1993; Gabrielsen et al., 1997; Glørstad-Clark et al., 2011).

Polhem Subplatform

Polhem Subplatform makes out a block- faulted subplatform between the Loppa High area to the east, and the west bounding Ringvassøy- Loppa and Bjørnøyrenna Fault Complexes. The fault blocks are rotated and the faults are listric normal faults with a detachment zone deeper than Base Triassic. The faults got their listric geometry in Late Jurassic to Early Cretaceous time, and reactivation has occurred at later stages. The Jurassic rocks have been eroded from the platform (Gabrielsen et al., 1990). The bounding faults between the subplatform and the Loppa High area have been given the name Jason Fault Complex by Glørstad- Clark et al. (2011). This fault complex consists of N-S trending faults and is aligned with Leirdjupet Fault Complex to the north, and Ringvassøy- Loppa Fault Complex to the south. The faults are dominantly extensional with down-to-west displacement (Glørstad- Clark et al., 2011).

Ringvassøy- Loppa Fault Complex

Ringvassøy- Loppa Fault Complex has a general NNE- SSW strike. The southern part of the fault complex is the transition zone between a basin of Mesozoic age, Hammerfest Basin, and a basin that experience extensive subsidence in Cretaceous to Tertiary time, Tromsø Basin (Figure 2.3) (Faleide et al., 1993a). Farther north the fault complex develops into a narrower zone and makes the transition between the Tromsø Basin and the Loppa High, and farthest north the transition between the Tromsø Basin and Polhem subplatform. The Troms Finnmark Fault Complex and Bjørnøyrenna Fault Complex is the respectively southern and northern extension of Ringvassøy- Loppa Fault Complex (Figure 3.1) (Gabrielsen et al., 1990).

It is suggested that the fault complex was initiated already in Late Paleozoic time, and that basement movements have caused the fault complex to work as a long lived hinge line, based on a deep seated zone of weakness (Gabrielsen, 1984; Berglund et al., 1986). Other observations also suggest that the fault complex was active at this early stage. The western boundary faults of Loppa High show movements in Permian times (Gudlaugsen et al.,1998), and the eastern limit of the Paleozoic salt in the Tromsø Basin appear to be coincident with the Ringvassøy- Loppa Fault Complex. A slightly positive gravity anomaly is also supporting the presence of a deep zone of weakness in the fault complex (Gabrielsen et al., 1990). The main displacement along the fault complex happened in Mid Jurassic, in relation to significant subsidence of the Tromsø Basin to the west. The faults appear to be detached normal faults with listric geometry where their concave outline faces the Tromsø Basin. The faults farthest west show throw of more than 2,5 seconds twt with down-to-west throw, at Base Cretaceous level (Gabrielsen 1984).

Cretaceous and even Tertiary strata have been affected by faulting during several phases of extensional tectonics. Gabrielsen (1984) proposed that these faults appear to be detached from the Mid Jurassic level, and two detachment levels are proposed by the determination of listric normal faults. Fracturing initiated at the surface in relation with flexuring due to subsidence is suggested to be the genesis of these detachments.

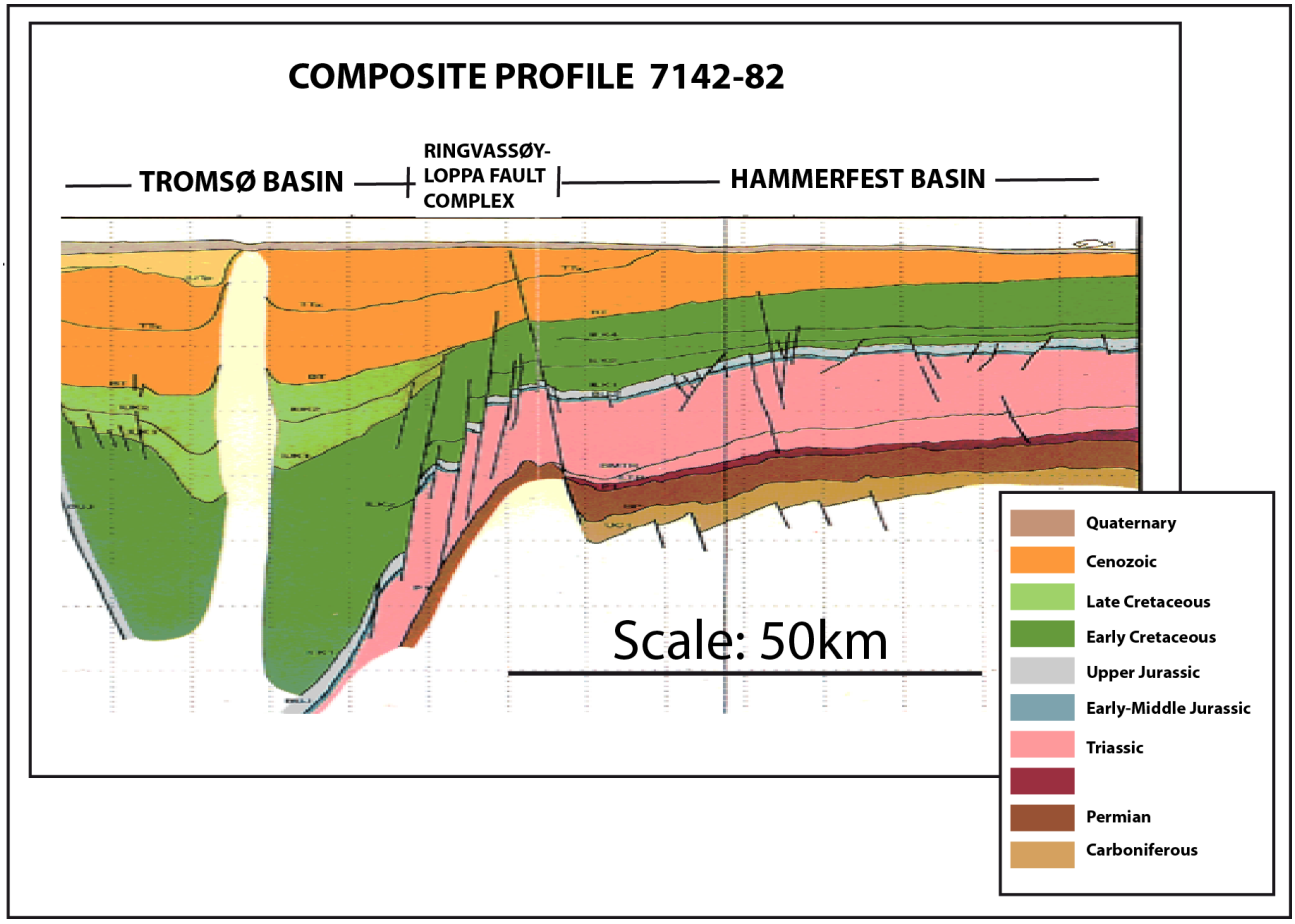

Figure 2.3: Composite profile showing Hammerfest Basin in the east, the Tromsø Basin in the west and Ringvassøy- Loppa Fault Complex as the transition between the two basins. Interpreted lithology is given by the coloured intervals (modified from Gabrielsen et al., 1990)

2.3. Interpreted reflections and lithostratigraphy

6 key reflections have been interpreted in this study. Top Kolmule Formation reflection, Top Kolje Formation reflection, Base Cretaceous reflection, Top Stø Formation reflection, Top Permian reflection and Intra Permian reflection. Their positions in the stratigraphic column are seen in Figure 2.4. The motivation for interpreting these reflections is the different rifting events that have affected the area. The two Permian reflections are affected by the Paleozoic rifting, while the four reflections of Mid Jurassic to Cretaceous (Top Kolmule Formation, Top Kolje Formation, the Base Cretaceous, Top Stø Formation), are affected by the Mesozoic- Cenozoic rifting events. The structural effects of these phases of rifting are investigated by looking at the behaviour of these interpreted reflections across the Ringvassøy- Loppa Fault Complex.

The reflections are correlated to be represented by the top surfaces of lithostratigraphic groups and formations. In the following chapter they will be presented with description from previous work. Age, lithology, depositional environment and lateral extent of each sequence, have been presented by several authors (Dalland et.al., 1988; Gudlaugsson et.al., 1998; Larssen et al., 2005).

The seismic sequence stratigraphy and the division into seismic sequences and Mega sequences are directly based on the work of Glørstad- Clark et al. (2011). The presented sequences are interpreted in the area around Loppa High and Selis Ridge, and have not been directly correlated to the southern part of Ringvassøy- Loppa Fault Complex. However, some of the information is regarded to be of regional importance, and is considered for this study.

Glørstad- Clark et al. (2011) have divided into Mega sequences, which are associated with erosion and deformation of underlying strata and correlated to major basin forming processes. These Mega sequences are further divided into seismic sequences that are bounded by surfaces that are extensive and easily mappable, but no significant deformation of the underlying units.

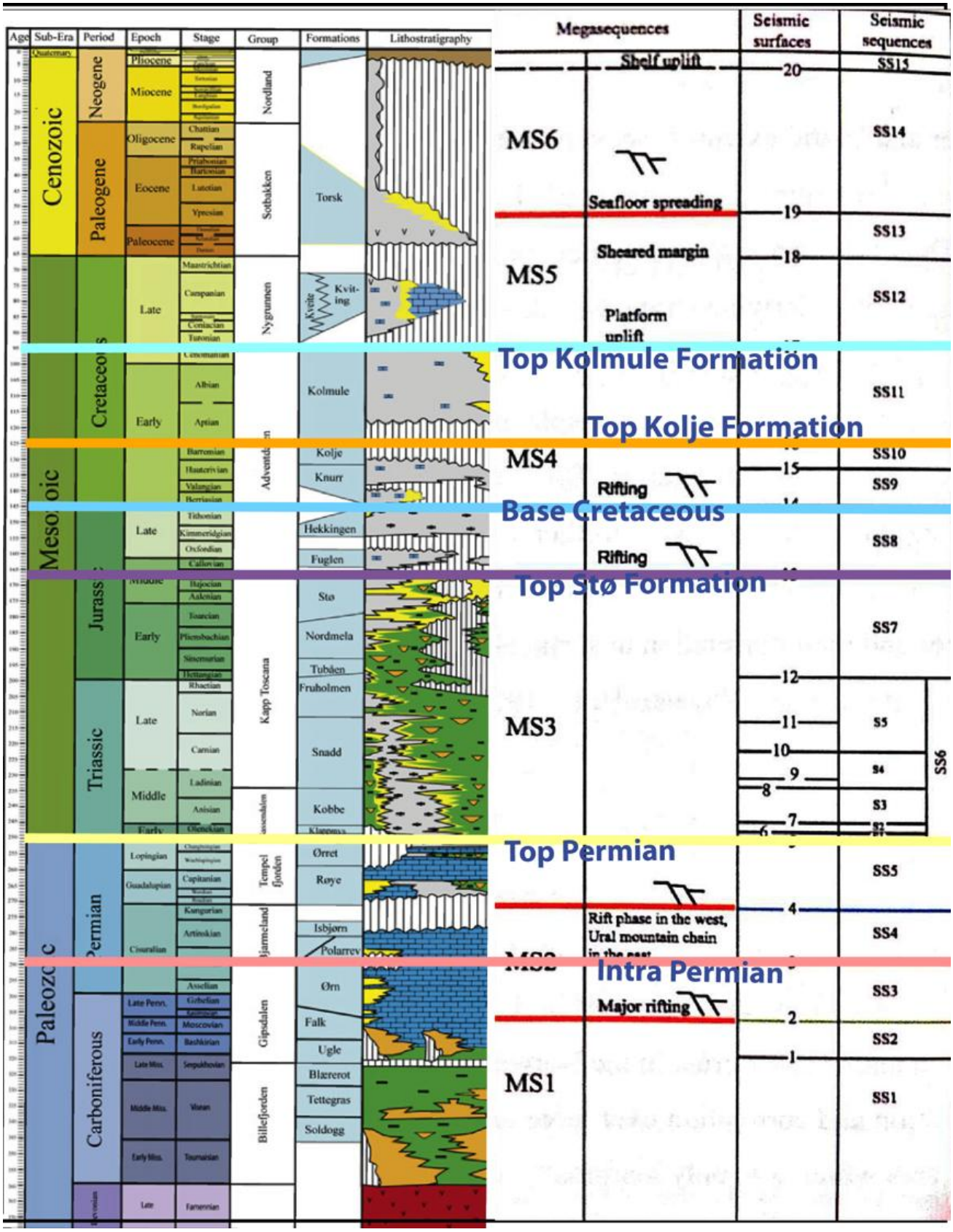

Figure 2.4: Lithostratigraphic column in The Western Barents Sea together with interpreted Mega Sequences and Seismic Sequences by Glørstad- Clark et al. (2011). Interpreted key reflections of this study is marked with their representing colours (Modified from Glørstad- Clark et al., 2011)

Ørn Formation (correlated to Intra Permian reflection)

Described by Larssen et al. (2005 p. 24).

***Group**:* Gipsdalen Group

Age: Late Moscovian/ Early Gzhelian to Early Sakmarian (Stemmerik et al. 1995; Bugge et al. 1995; Ehrenberg et al. 1998; Stemmerik et al. 1998, all as cited in Larssen et al.,2005).

Lithology: Shallow marine carbonates dominate the platform areas, while interbedded carbonates and evaporites dominate the distal ramp to basinal areas. Silisiclastics are rare for this formation.

Depositional environment: Shallow marine carbonate environment, with deposition on platforms is the dominating environment of this formation.

Lateral extent: The formation is thin on the inner platforms, and gets thicker more distally on the platforms.

Sequence stratigraphy: This formation has been correlated to the seismic sequence SS3, which is the lower seismic sequence of the Mega sequence MS2. The seismic facies of the sequence is characterized by a transparent, sub-parallel to chaotic lower part, and locally by strong parallel reflections in the upper part. Laterally extensive, high amplitude reflections within the unit are interpreted as carbonate platform deposits. Even though seismic resolution do not allow for stratigraphic correlation into the Tromsø Basin, the depositional setting is suggested to be similar here since the basin was part of an extensive epicontinental shelf at that time (Glørstad- Clark et al., 2011).

Tempelfjorden Group (correlated to Top Permian reflection)

Described by Larssen et al. (2005 p. 35).

Formations in the group: Ørret Formation and Røye Formation. Some wells in the southern Loppa High and the southern Hammerfest Basin are interpreted to show only the Røye Formation or an intercalation of the two formations.

Age: Mid- Late Permian

Lithology: The group is dominated by spiculites, spiculitic chert, silicified skeletal limestone and fine-grained silisiclastics. The silisiclastics include marls, calcareous claystones, shales and silt/sandstones in the offshore areas. Some coarse silisiclastic units are found in the southwestern part of Hammerfest Basin.

Depositional environment: The unit was deposited in a cool- water, temperate shelf, and most of the unit was deposited in distal marine, low-energy, moderate to deep basinal environments, during an overall transgression. In the Hammerfest Basin the depositional environment of the upper part of the unit is interpreted to be silisiclastic-dominated deltaic and lower coastal plain.

Lateral extent: The unit has a wedge-shape tendency with the greatest thickness in the basins. However, the group is thickest in the western part of the South Western Barents Sea.

Sequence stratigraphy: The seismic sequence SS5 is correlated to the group, which is the lowest seismic sequence in the Mega sequence MS3. Away from the Selis Ridge the lower boundary is conformably overlaying the strata of the seismic sequence SS4. The lower boundary of this unit is representing a climatic change towards cooler climatic conditions (Glørstad- Clark et al., 2011).

Stø Formation

Described by Dalland et al. (1988, p. 50)

Group: Kapp Toscana Group.

Age: Late Pliensbachian to Bajocian (Mid Jurassic)

Lithology: Moderate to well-sorted and mineralogical mature sandstone, with some interbedded thin layers of shale/siltstone.

Depositional environment: The sands in the formation were deposited in a prograding coastal environment, with many different clastic lithofacies represented. The thin layers of shale/siltstone were deposited during regional pulses of transgressions.

Lateral extent: the formation is thickest in the south western wells, and thins generally eastward.

Sequence stratigraphy: The Stø Formation is the upper part of the Mega sequence MS3. The upper boundary is an angular unconformity, and it is picked at 7 seconds twt in the Tromsø Basin (Glørstad- Clark et al., 2011, Faleide et al., 1993a,b).

Hekkingen Formation (correlated to Base Cretaceous reflection)

Described by Dalland et al. (1988, p. 51)

Group: Adventdalen Group

Age: Late Oxfordian/Early Kimmeridgian to Ryazanian (Late Jurassic)
Lithology: The formation consists of mainly shales and claystone, with some thin layers of limestone, dolomite, siltstone and sandstone.
Depositional environment: Marine, deep water with anoxic conditions.
Lateral extent: In the Hammerfest Basin the formation is thickest in the south, and thins northward towards the basin axis.
Sequence stratigraphy: Hekkingen Formation is the upper part of the seismic sequence SS8, in the Mega sequence MS4. This seismic sequence is characterized by wedge-shaped units where reflections are onlapping the underlying MS3. SS8 is mainly constricted to rotated fault blocks and *half grabens* (Twiss and Moores, 2007, p. 95), which points towards a syn-rift deposition. This is further supported by onlap onto the flanks of individual fault blocks. High amplitude and lateral continuity are characterizing the top reflection of the seismic sequence, which is interpreted to be a flooding surface (Glørstad- Clark et al., 2011).

Kolje Formation

Described by Dalland et al. (1988, p. 55)
Group: Adventdalen Group
Age: Early Barremian to Late Barremian/Early Aptian age (Early Cretaceous)
Lithology: Shales and claystones is the dominating lithology, with some internal layers of pale limestone and dolomite. A few layers of grey-brown siltstone and sandstone are present in the upper part of the formation.
Depositional environment: It was deposited in a distal open marine environment, with generally good water circulation but periods of more restricted environments.
Lateral extent: The general lateral trend is a westwards thickening, with a local thinning in the central part of the Hammerfest Basin.
Sequence stratigraphy: Kolje Formation is making out the seismic sequence SS10, in the Mega sequence MS4. The upper and lower boundaries are characterized by strong amplitude with a great lateral extent. Both boundaries are interpreted to be flooding surfaces. The seismic sequence is onlapping the central dome in the Hammerfest Basin, and has a westward thickening towards the Ringvassøy- Loppa Fault Complex and the Tromsø Basin. Transparent, sub-parallel reflections dominate the seismic facies of the sequence (Glørstad- Clark

et al., 2011).

Kolmule Formation.

Described by Dalland et al. (1988, p. 55)

Group: Adventdalen Group

Age: Aptian to Mid Cenomanian (Early- Late Cretaceous)

Lithology: Shales and claystones dominate the formation. Interbeds of siltstone, stringers of limestone and dolomite, and traces of glauconite and pyrite are present.

Depositional environment: Open marine environment. The base of the formation relates to a regional transgression.

Lateral extent: The formation shows a westward thickening towards and into the Tromsø Basin.

Sequence stratigraphy: Kolmule Formation is the upper part of the Mega sequence MS4, and is defined as the seismic sequence SS11. The upper boundary is characterized by a high amplitude and laterally extensive reflection, which has been interpreted to be a flooding surface. The lower boundary is seen as a continuous, high amplitude reflection in the Hammerfest Basin (Glørstad- Clark et al., 2011).

2.4. Nomenclature

The following nomenclature will be used for description of the study, and with the first use of the term in the text, a cross referenced to this subchapter will be given. The terms to be defined are given *italic* style.

A ***master fault*** is referring to the faults that have major amount of displacement, and is responsible for most of the deformation (Twiss and Moores, 2007, p. 95). The terms ***concave upward*** and ***convex upward*** are referring to the geometry of the fault plane of a listric fault (Gabrielsen, per. com., 2012). When the term ***listric fault*** is used without any specification of the fault plane geometry, it implies a concave upward listric fault (Twiss and Moores, 2007, p. 92). A ***terrace*** refers to the surface of a half graben. A ***detachment fault*** is a low angle fault that marks the transition between faulted rocks and non-faulted rocks (Twiss and Moores, 2007, p. 93). ***Soft linkage*** is the term used for faults that are linked laterally through ductile highly strained zones, and appear to be isolated from

each other on the scale in use. ***Hard linkage*** is the term used when faults directly link together (Walsh and Watterson 1991a, p. 194). ***Fault drags*** are seen as curved or folded reflections in relation to a fault. The fault drag is called ***normal drag*** when the reflection is convex in direction of slip, and ***reverse drag*** when the reflection is concave in the direction of slip (Hamblin, 1965). The term ***Thick-skin*** refers to basement-involved deformation, and ***thin-skin*** refers to sediment restricted deformation (e.g. Craigmann, 1989).

Chapter 3; Seismic interpretation

Seismic interpretation of 2D lines is one of two complementary analyses done in this study. The motivation for this seismic interpretation is to obtain a better structural understanding of the Ringvassøy- Loppa Fault Complex and the relation between the different extensional events in the area. The main objective is to study whether or not detachments exist in the Ringvassøy- Loppa Fault Complex, separating vertical units of contrasting fault geometry and mechanism (thin-skin and thick-skin) and to exploit the potential for fluid communication between the potential levels of fault families. Also the dynamic relations affiliated with the potential reactivation of older (thick-skin) faults will be discussed.

The southern part of the Ringvassøy- Loppa Fault Complex is the emphasized area for this study. When referring to "the study area" the southern part between the Hammerfest Basin and the Tromsø Basin is implied.

3.1. Data base, data quality and well ties

41 seismic 2D lines were put together to form a grid covering most of the Ringvassøy- Loppa Fault Complex. The lines are oriented E-W, NE-SW and SE-NW, Figure 3.1. The seismic lines are from different surveys and they are of different depth and seismic quality. The names of the surveys and the provider of them are given in Table 3-1. The surveys of TGS Nopec provides better resolution in the deeper parts of Permian age, and image down to 9000ms twt. Several providers on behalf of NPD shot the TTR surveys. The TTR surveys are imaging down to 5000ms twt and provide poor seismic quality deeper than Jurassic age.

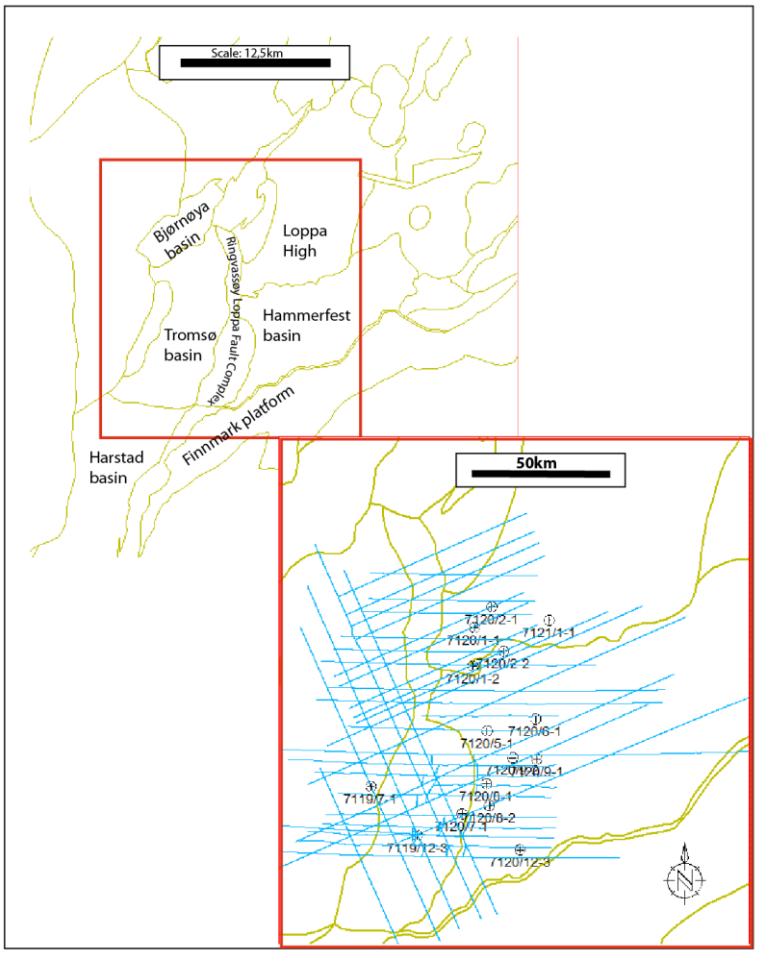

Figure 3.1: Map of regional location of Ringvassøy- Loppa Fault Complex and the location of the 2D seismic grid used in the study.

Table 3-1: Names, orientation and provider of the seismic surveys used in this study.

Orientation	Survey name	Provider
NE-SW	NBR08	TGS Nopec
	NBR07	TGS Nopec
	BBSS01	TGS Nopec
SE-NW	NBR08	TGS Nopec
	NBR07	TGS Nopec
E-W	TTR83R1	Unknown (NPD)
	TTR73R1	Unknown (NPD)
	TTR82R1	Unknown (NPD)
	TTR74R1	Unknown (NPD)

NH9702	TGS Nopec

Well data were supplied from the FactPage of Norwegian Petroleum Directorate (NPD, www.npd.no). 36 wells have been drilled in the Hammerfest Basin and at the Loppa High, and these served as an extra security when interpreting the key reflections. However, only four wells were used for seismic to well correlation, and special information about them are presented in Table 3-2.

Table 3-2: Information about the wells used for seismic to well correlation in this study. See Figure 2.4 for Lithostratigraphic column and time scale. See Figure 3.2 and Figure 3.4 for location of the wells.

Wellbore name	**7119/12-3**	**7120/7-1**	**7120/8-2**	**7120/9-2**
NS degrees	71° 14' 20.18'' N	71° 18' 36.29'' N	71° 20' 15.72'' N	71° 29' 40.81'' N
EW degrees	19° 44' 37.92'' E	20° 11' 22.21'' E	20° 27' 57.61'' E	20° 42' 5.38'' E
NS UTM [m]	7904727.31	7912388.54	7915359.17	7932809.50
EW UTM [m]	454909.86	471011.63	480927.89	489425.03
UTM zone	34	34	34	34
Drilling operator	Den norske stats oljeselskap a.s	Den norske stats oljeselskap a.s	Den norske stats oljeselskap a.s	Norsk Hydro Produksjon AS
Entry date	20.05.1983	31.07.1982	15.04.1982	18.04.1984
Completion date	12.09.1985	08.10.1982	29.07.1982	20.10.1984
Type	EXPLORATION	EXPLORATION	EXPLORATION	EXPLORATION
Status	P&A	P&A	P&A	P&A
Content	GAS/CONDENSATE	GAS	GAS	GAS
Discovery wellbore	YES	YES	NO	NO
1st level with HC, formation	Stø FM	Stø FM	Stø FM	Stø FM
Kelly bushing elevation [m]	29	25.0	25.0	23.0
Water depth [m]	211	233.5	245.0	293.0
Total depth (MD) [m RKB]	3314.0	2839.0	2590.0	5072.0
Final vertical depth (TVD) [m RKB]	3308.0	2839.0	2590.0	5069.0
Oldest penetrated age	EARLY JURASSIC	LATE TRIASSIC	LATE TRIASSIC	LATE PERMIAN
Oldest penetrated formation	NORDMELA FORMATION	TUBÅEN FORMATION	FRUHOLMEN FORMATION	RØYE FORMATION

Well 7120/8-2 is located in The Hammerfest Basin. The well penetrates down to Fruholmen Formation of Late Triassic age. Well 7120/7-1 is located in Ringvassøy- Loppa Fault Complex near the *master faults* (defined in subchapter 2.4) separating the fault complex from the Hammerfest Basin. Tubåen Formation

of Late Triassic age is the deepest penetrated formation. This well is important when correlating the key reflections of Mid Jurassic age from the Hammerfest Basin into the fault complex. Well 7119/12-3 is located farther into the fault complex towards Tromsø Basin, and Nordmela Formation of Early Jurassic age is the deepest penetrated formation. This well is also of great importance when picking the key reflections over the rotated fault blocks. These three wells are located in the Key Profile 2. Lithostratigraphic tops down to Mid Jurassic age have been picked in these three wells and allow for well to seismic tie across Ringvassøy- Loppa Fault Complex, Figure 3.2.

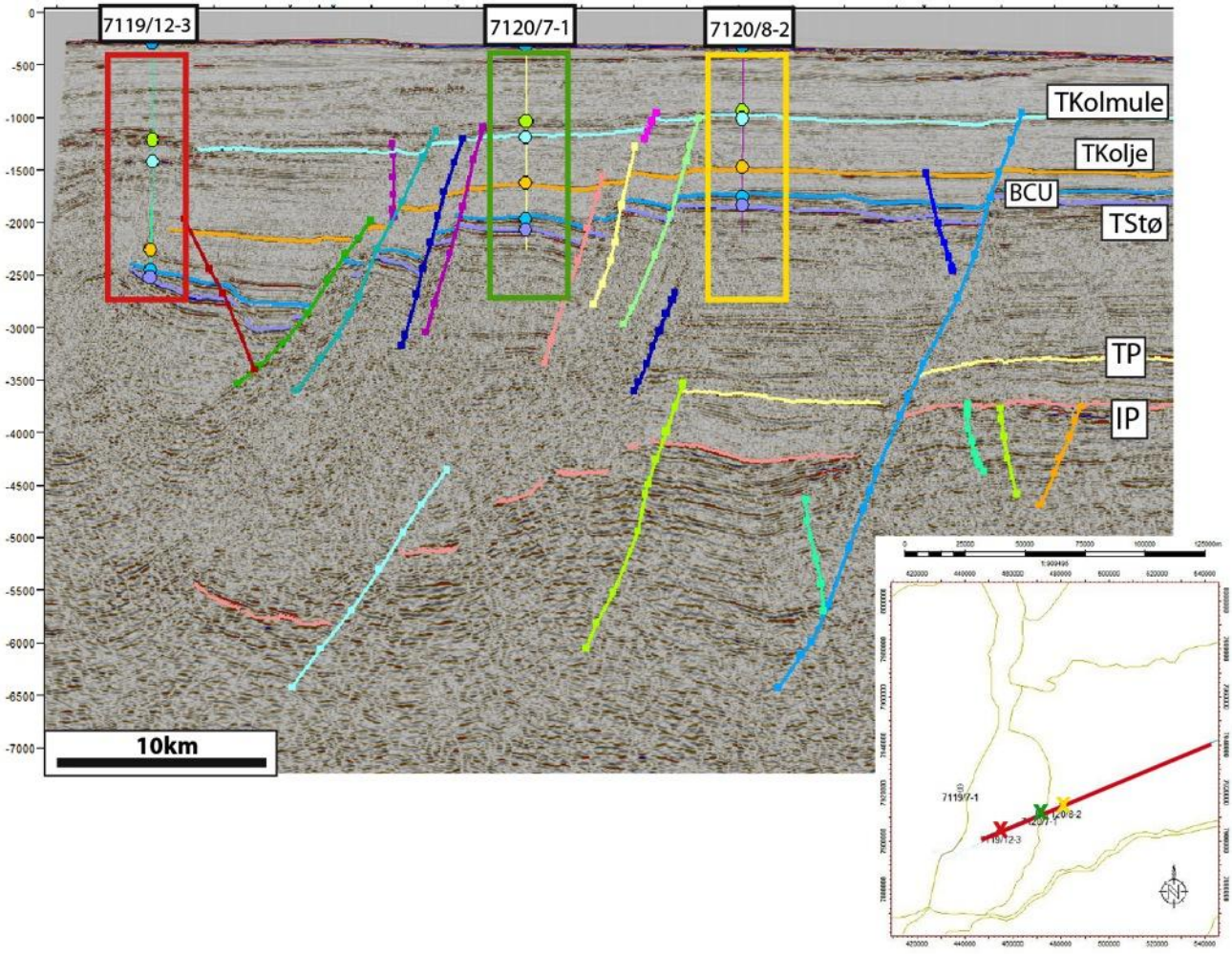

Figure 3.2: Seismic cross section showing location of the wells 7119/12-3, 7120/7-1 and 7120/8-2. Close-up of the wells can be seen in Figure 3.3.

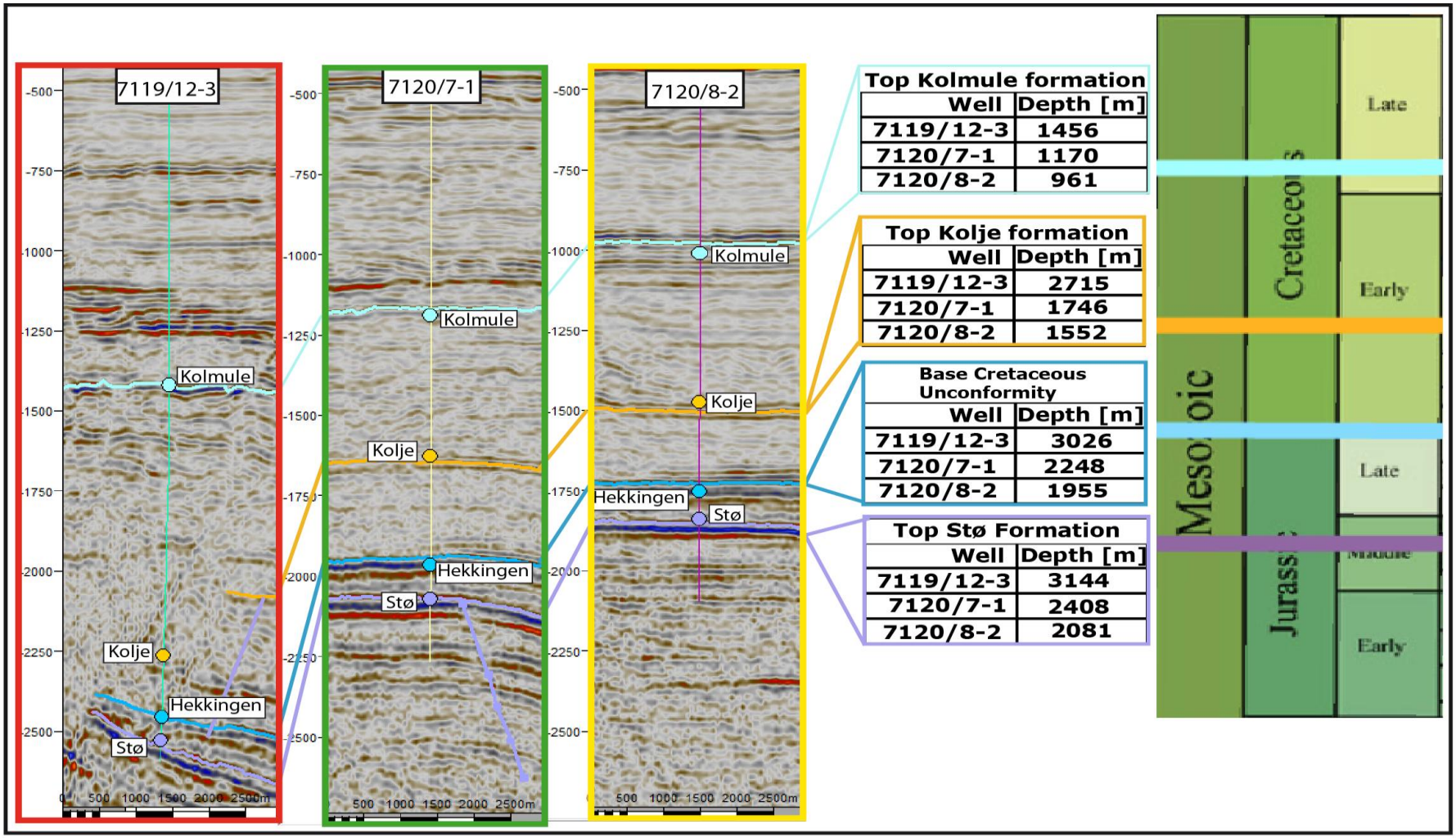

Figure 3.3: Well to seismic tie for the three wells 7119/12- 3, 7120/7-1 and 7120/8-2. None of the wells are penetrating any formations deeper than Late Triassic. Location of the wells is seen in Figure 3.2. Depths of the picked formations are taken from Norwegian Petroleum Directorate´s FactPage (NPD, www.npd.no).

Well 7120/9-2 is located in the Hammerfest Basin, and penetrates down to Røye Formation of Late Permian age, Figure 3.4. This is the only well in the study area that penetrates down to Permian age, and is therefore very important for the seismic to well correlation of the deepest key reflections.

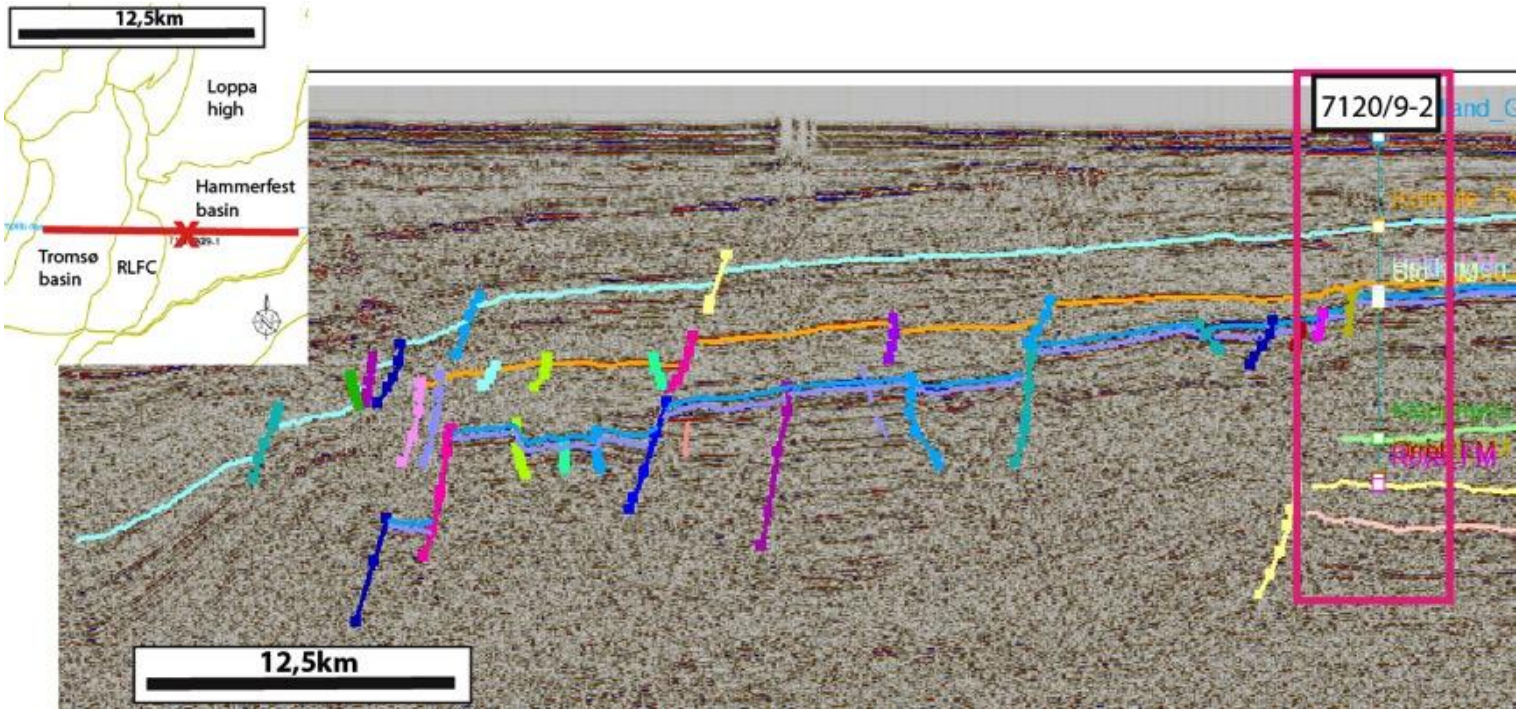

Figure 3.4: Seismic cross section showing location of the well 7120/9-2 .The well is seen in Figure 3.5.

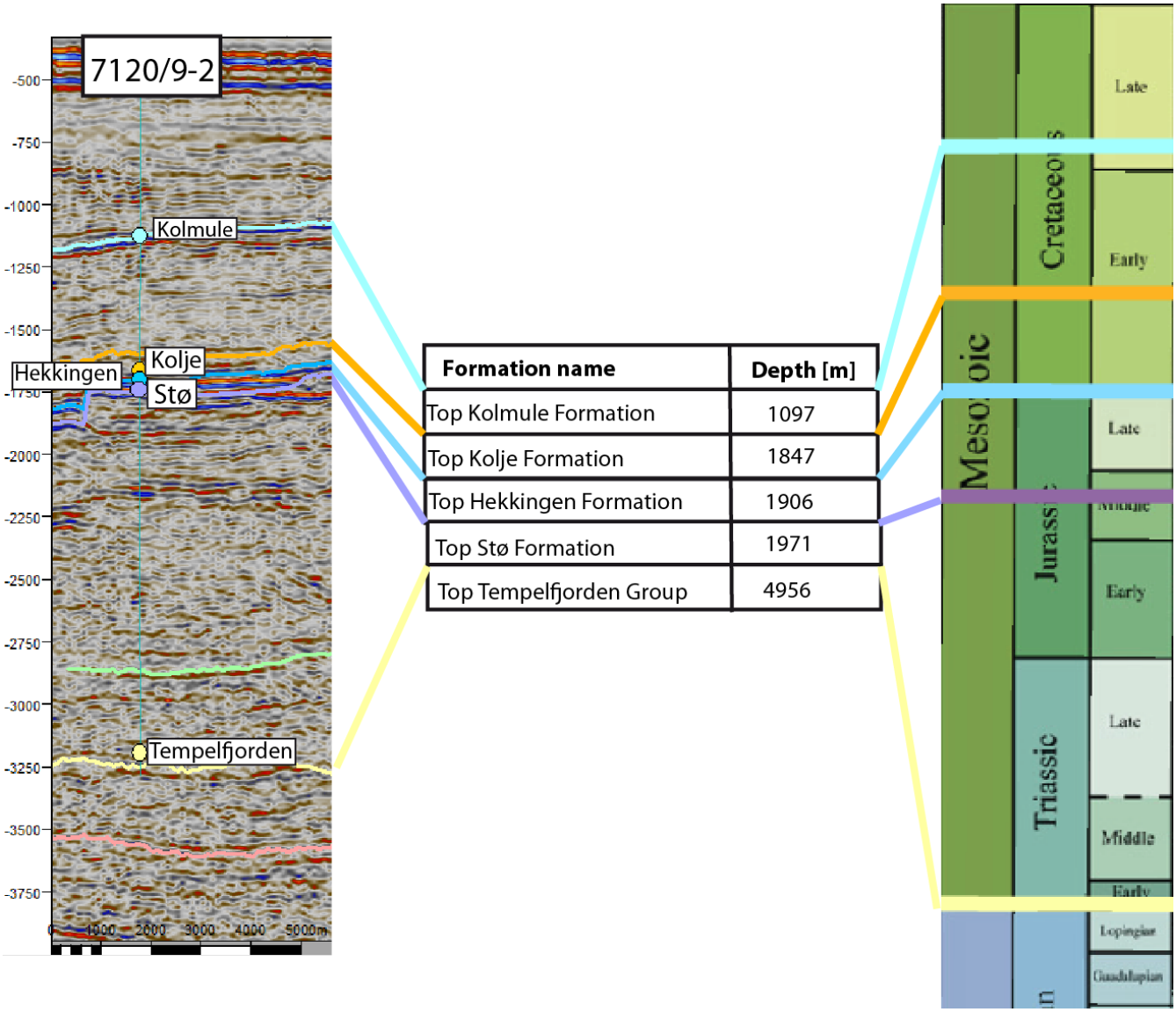

Formation name	Depth [m]
Top Kolmule Formation	1097
Top Kolje Formation	1847
Top Hekkingen Formation	1906
Top Stø Formation	1971
Top Tempelfjorden Group	4956

Figure 3.5: Well to seismic tie of well 7120/9-2. The deepest penetrated formation is Late Permian. Location of the well is seen in Figure 3.4. Depths of the picked formations are taken from Norwegian Petroleum Directorate´s FactPage (NPD, www.npd.no).

Key reflections

The Intra Permian reflection is only interpreted on a few seismic lines. The reflection is represented as a peak with medium amplitude. The underlying reflections have strong amplitudes and are relatively parallel. Faults are controlling the reflection with throws up to 650ms twt. Some of the faults appear to terminate at this reflection, while others are cutting farther up and affecting the Top Permian reflection. The interpretation has been done from 3700ms to 5821ms twt. The reflection was not picked in any well. The pick of this reflection was done based on the characteristics of the reflections described by Glørstad-Clark et al. (2011). Strong parallel reflections representing a climatic change from carbonate platform deposit to a cooler climate.

Top Permian reflection has only been interpreted on few lines and mostly in the Hammerfest Basin, due to limited seismic resolution. Where it can be recognised it appears as a peak with medium to strong amplitude. The overlying reflections have a tendency to downlap onto it, in the Hammerfest Basin. The reflection has been interpreted between 3100ms- 3700ms twt, and has been tied in well 7120/12-3 (Figure 3.4).

Top Stø Formation reflection is a negative reflection with high amplitude, and it can easily be correlated across the fault blocks of the study area. The reflection is strongly affected by faulting with small and large throws. Top Stø Formation reflection has been interpreted between 1740ms twt in the Hammerfest Basin down to 3900ms twt on the westernmost fault blocks of the fault complex. Overlying reflections onlap the horizon, and is evident in the most rotated fault blocks. The underlying reflections are conformable with the Top Stø Formation reflection. The reflection has been tied in wells 7119/12-3, 7129/7-1 and 7120/8-2 (Figure 3.2).

The Base Cretaceous reflection is correlated as the Top Hekkingen formation in the study area. The reflection is mainly conformable with the overlying reflections. Some of the faults in the fault complex are terminating at this reflection or below, but most of the master faults are cutting farther up in the overlaying sequences. The reflection is easily mapped and represented by strong negative amplitude in the Hammerfest Basin and Ringvassøy- Loppa Fault

Complex. However, the reflection cannot be followed into the Tromsø Basin. The reflection has been interpreted between 1650ms twt in the Hammerfest Basin down to 3800ms twt on the westernmost fault blocks of the fault complex. The reflection has been tied in wells 7119/12-3, 7129/7-1 and 7120/8-2 (Figure 3.2).

Top Kolje Formation reflection is a peak with medium to high amplitude. The reflection is relatively continuous in the east part, but becomes more uncontinous westward where limited seismic resolution and faulting are disturbing the reflection. The reflection has not been interpreted into the Tromsø Basin due to poor seismic quality. Some of the master faults of Mid Jurassic are cutting through the Top Kolje Formation reflection. Interpretation of Top Kolje Formation reflection has been done from 1300ms to 3400ms twt, and it has been tied in wells 7119/12-3, 7129/7-1 and 7120/8-2, (Figure 3.2).

Top Kolmule Formation reflection is visible as a trough with medium to strong amplitude. The reflection is relative continuous and represented by a strong amplitude in the Hammerfest Basin and half across the fault complex. Farther west the reflection becomes more faulted, less amplified and less continuous. Top Kolmule Formation reflection can be followed farther into the Tromsø Basin than the other interpreted reflections. Interpretation has been done between 950ms twt and 3300ms twt, and the reflection has been tied in wells 7119/12-3, 7129/7-1 and 7120/8-2 (Figure 3.2).

Faleide et al. (1993a) did a well correlation across the Ringvassøy- Loppa Fault Complex. When following the interpreted tops between the wells the general lateral trend of the Mid Jurassic and Cretaceous formations into the Tromsø Basin can be seen, Figure 3.6.

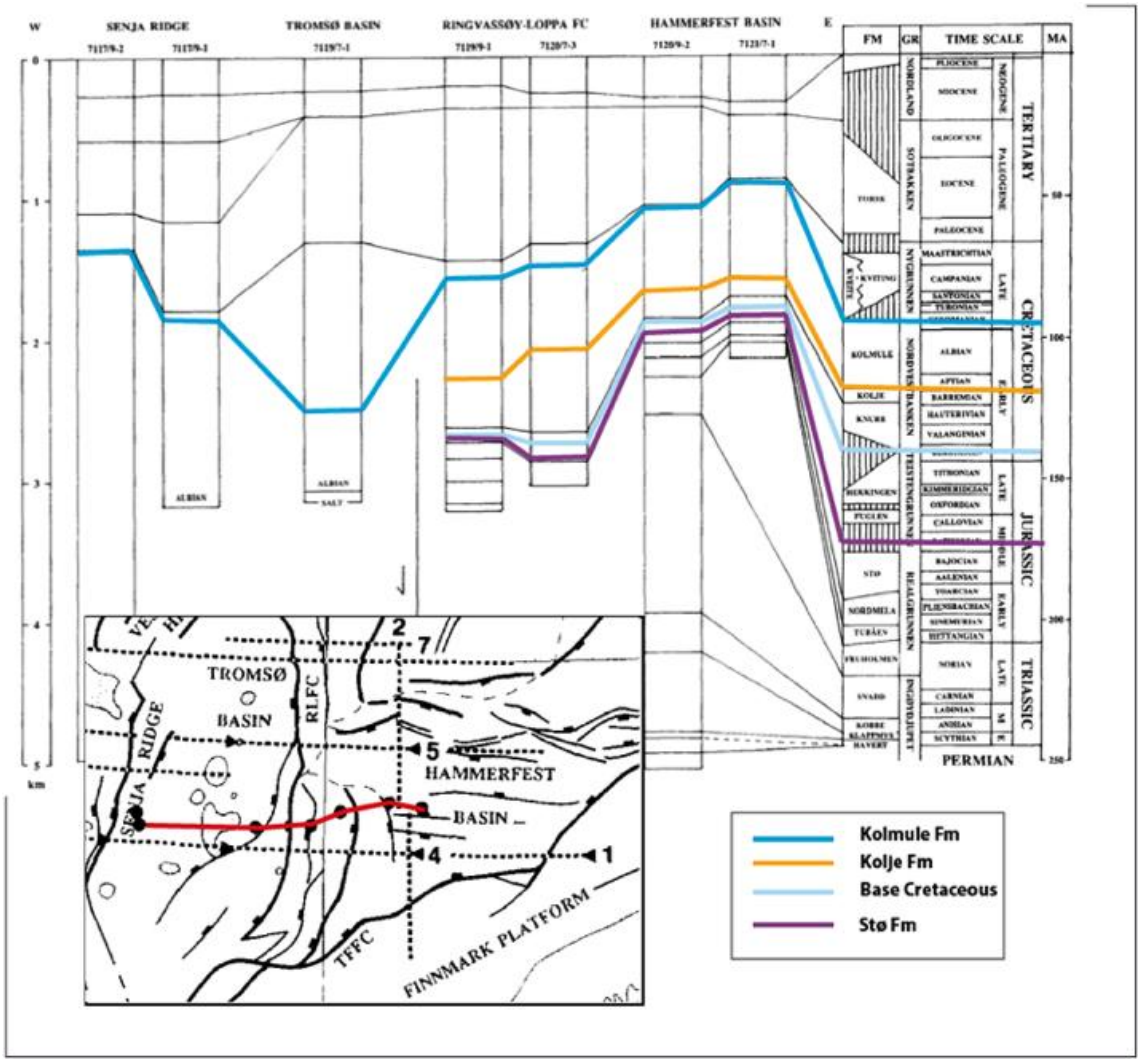

Figure 3.6: Seismic to well correlation in seven wells from the Hammerfest Basin across Ringvassøy- Loppa Fault Complex and into the Tromsø Basin, presented by Faleide et al. (1993a). Locations of the wells are seen in the map at bottom left. The key reflections of this study are marked with their representative colours (modified from Faleide et al., 1993a).

Kristiansen (2011) presented a contour map at the Top Stø Formation reflection that contains the western boundary faults of the Hammerfest Basin (Figure 3.7). The use of 3D data set, supplied by Statoil from the Hammerfest Basin (ST09M03), gave the opportunity to interpret the transitions between the master faults. This contour map is directly used in this study to make parts of the fault map at the Mid Jurassic- Early Cretaceous level of faulting (Figure 3.9).

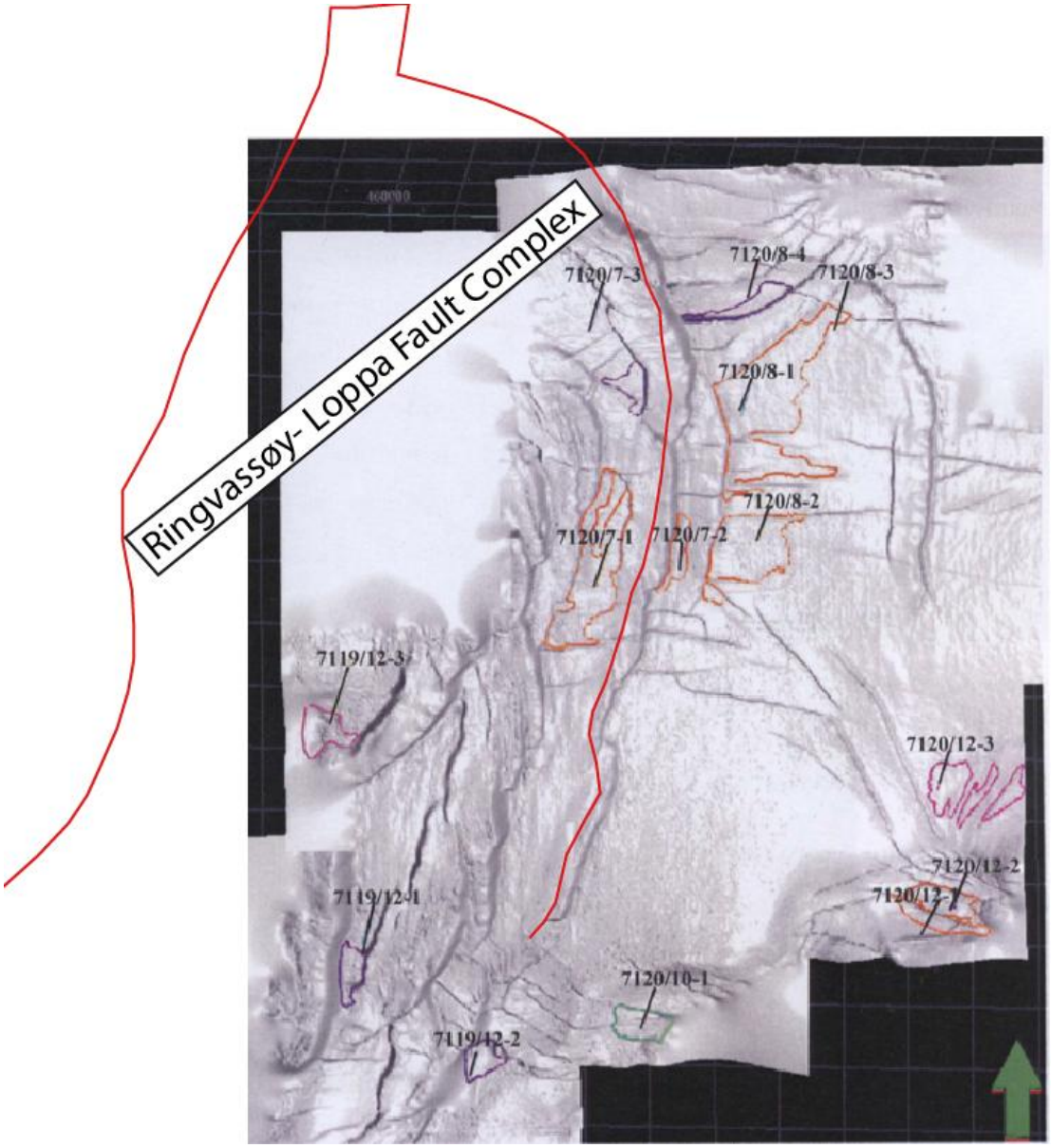

Figure 3.7: Contour map of the faults affecting Top Stø Formation reflection in the Hammerfest Basin and eastern part of Ringvassøy- Loppa Fault Complex (Modified from Kristiansen 2011).

3.2. The Interpretation procedure

The general procedure of the seismic interpretation was following the same workflow of other master thesis containing seismic interpretation (Figure 3.8) (e.g. Waqas, 2012; Fitriyanto, 2011).

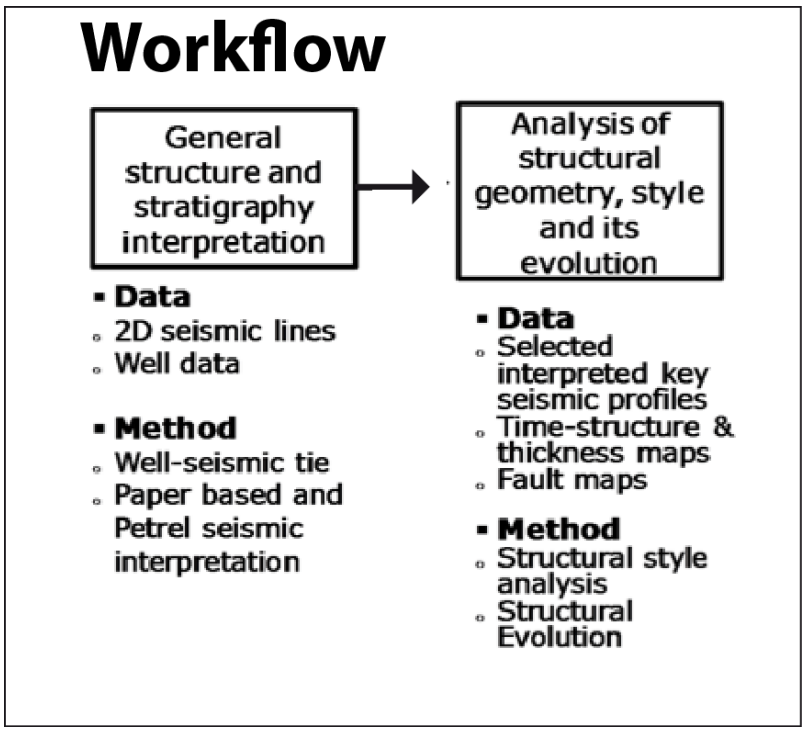

Figure 3.8: Scheme of the general workflow of the seismic interpretation procedure (Modified from Fitriyanto, 2011).

Three seismic lines were interpreted on hard copies, to get a regional understanding of the fault complex. Key reflections were picked to image the structural features and sediment infill. The main faults and the local faults were interpreted to illustrate different levels of faulting and the general geometries of the faults.

2D seismic lines were then interpreted in the seismic interpretation software PETREL, developed by Schlumberger. Petrel enables 2D and 3D seismic interpretation, 3D mapping and visualization, well correlation and several other applications that are helpful in the work of geoscientists (Schlumberger Petrel manual, 2010). The available well tops were tied to the seismic to identify the correct key reflections to interpret. The key reflections were interpreted on all the 2D lines were they could be identified. The faults were interpreted afterwards where the key reflections were not continuous.

Due to poor 2D seismic line coverage the quality of the maps became poor. However one structural map was made from the Top Stø Formation reflection, to show the depth relation of the area. Fault maps were made based on the map of Kristiansen (2011) and the measured throws across the faults in the 2D seismic lines.

After the interpretation was completed the fault complex was divided into sub-areas and segments based on the structural pattern across the fault complex and the outline of the master faults. Seismic key profiles were then chosen from each of the segments to describe the features of great importance and special interest.

3.3. Description of seismic data

In this chapter the description of the seismic interpretation will be presented. The overall structural trend, and sub-features of special importance will be described in detail. The study area will first be presented by one fault map and one cross section to highlight the most important structural elements. The study area is divided into segments and each of the segments will be described by cross sections termed key profiles. The structural geometries in the Mid Jurassic-Early Cretaceous level of faulting are divided into sub-areas in E- W direction, to illustrate structural areas with similar internal structural geometries. The Structural map of Top Stø Formation reflection will be presented in the end.

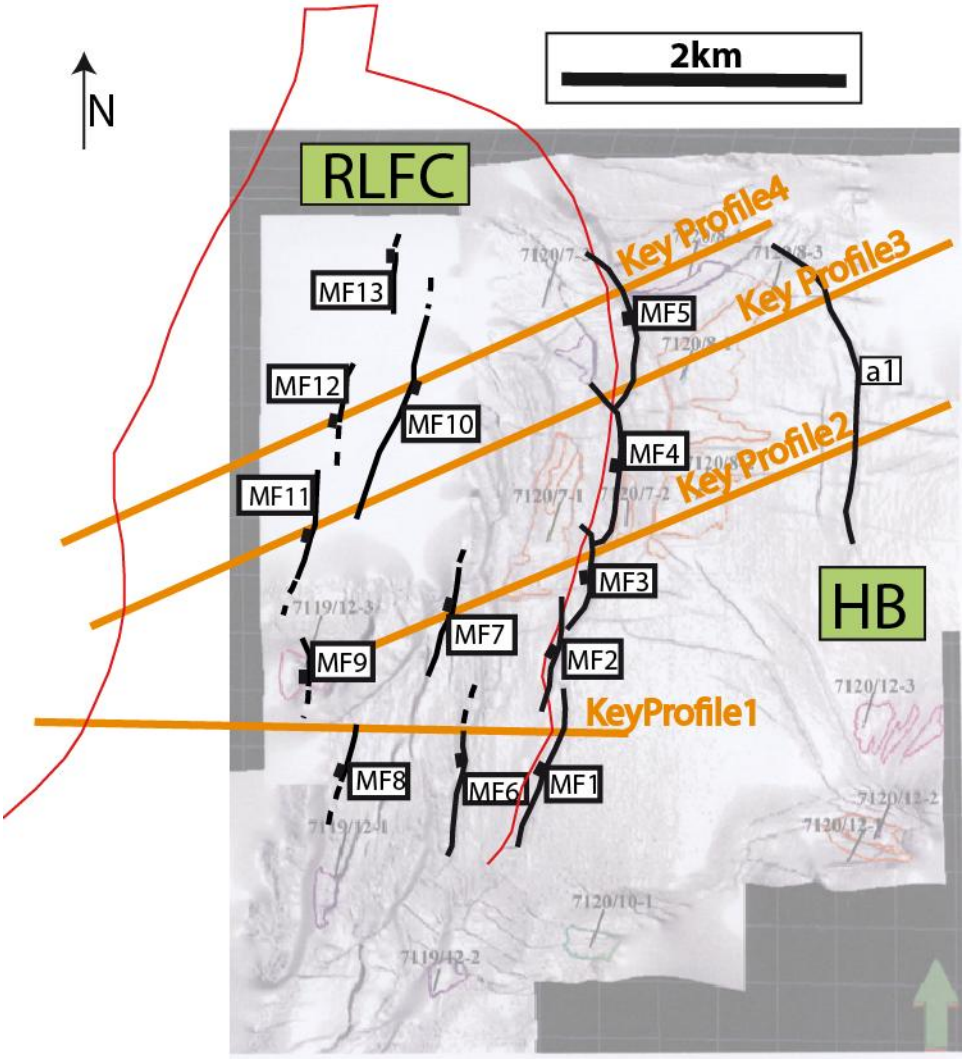

Figure 3.9: Fault map containing the master faults and other faults affecting the Mid Jurassic- Early Cretaceous level of faulting. Locations of the key profiles are also marked (partly based on the contour map in Figure 3.7). (Modified from Kristiansen 2011)

The study area was divided into three structural segments based on the contrasting structural geometries and the five master faults that define the transition between the Hammerfest Basin and the Ringvassøy- Loppa Fault Complex. The five master faults are affecting the Triassic to Early Cretaceous sequences, and are termed MF1, MF2, MF3, MF4 and MF5 (Figure 3.9). The master faults are *normal faults* (Twiss and Moores, 2007, p. 91) with *listric geometry* (chapter 2.4) and a down-to-west displacement. MF1 makes out segment 1, MF2 and MF3 make out segment 2 and MF4 and MF5 make out

segment 3, Figure 3.10. Segment 2 and segment 3 contain two master faults each, because the main structural elements are the same for the master faults.

13 master faults as defined on the Mid Jurassic level of faulting were included in this part of the study area (Figure 3.9). They are normal faults that represent important transitions between the different structural sections along the fault complex. The contour map of Kristiansen (2011) was directly used to divide the five master faults making the western boundary of the Hammerfest Basin (Figure 3.9). The outline of the rest of the master faults have been interpreted on the theory that displacement on a single fault usually dies out in both strike and dip direction from a centrally located maximum (e.g Barnett et al. 1987). Faults with similar outline and geometry in different seismic lines have been divided into individual faults by measuring the throw on each fault in each seismic line.

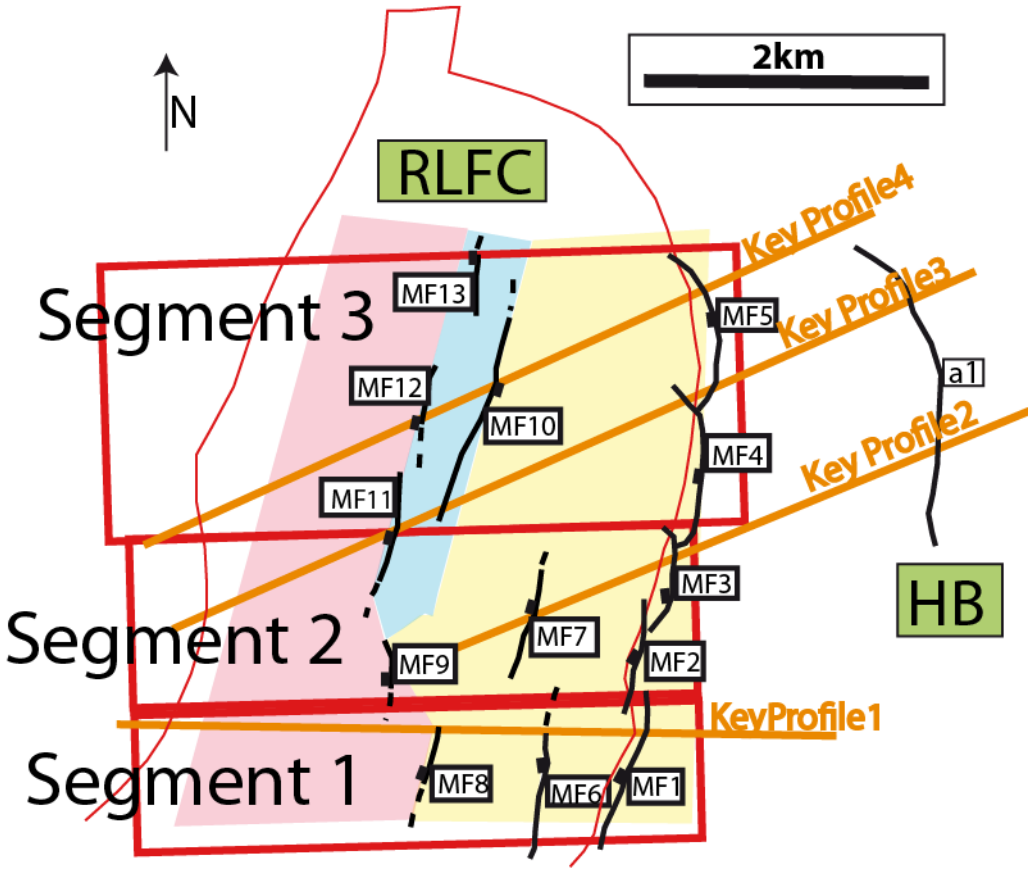

Figure 3.10: The three red boxes show the three defined segments of the study area. The three sub-areas defined at Mid Jurassic- Early Cretaceous level of faulting are shown by filled colours of yellow (Sub-area A), blue (sub-area B) and red (sub-area C). (Modified from Kristiansen 2011)

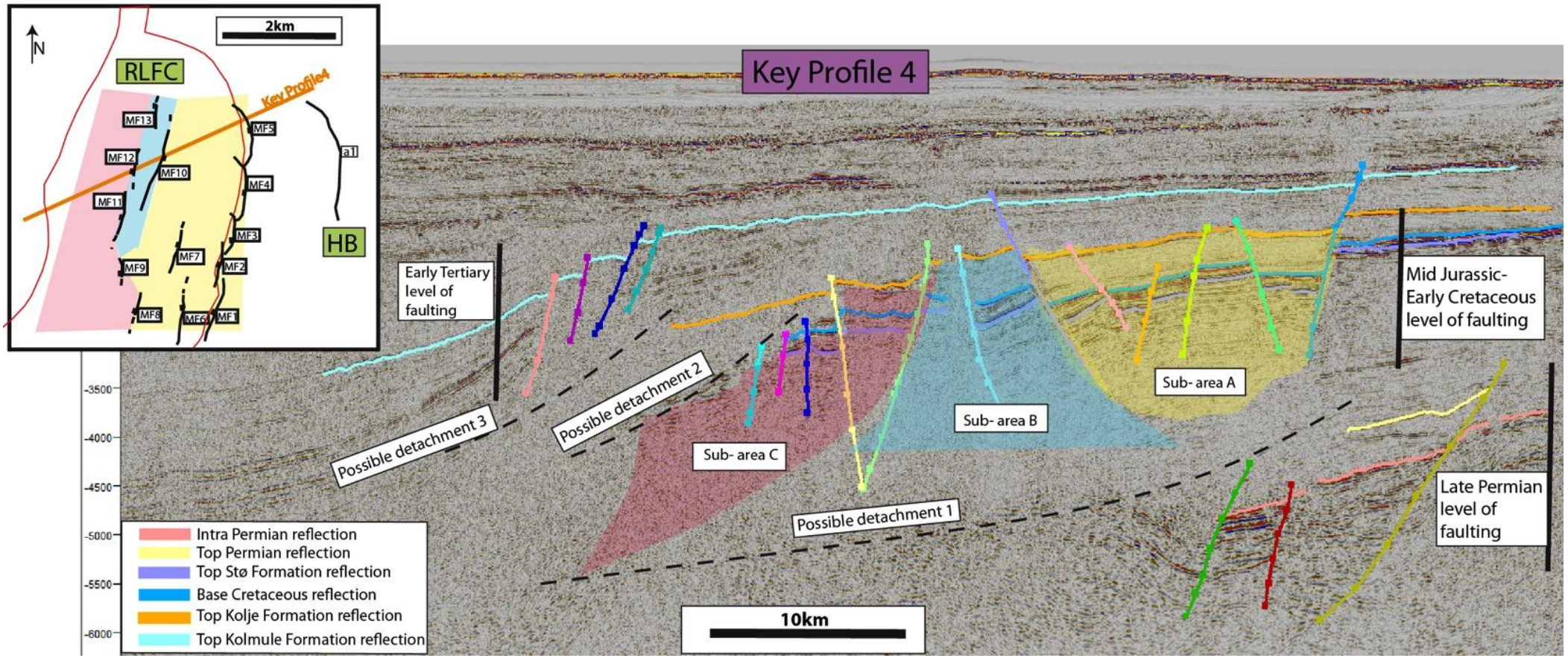

Figure 3.11: 2D seismic line illustrating the most important structural features of the study area. Position of the line is seen in the map in upper left corner. Three vertically separated levels are affected by faulting, called the Late Permian level of faulting, the Mid Jurassic-Early Cretaceous level of faulting and the Early Tertiary level of faulting (the affected sequences are marked by a black vertical line for each level of faulting). Three possible detachments are proposed to separate different levels of faulting. Three sub-areas are defined at the Mid Jurassic- Early Cretaceous level of faulting to illustrate areas with similar structural geometries (yellow filled area, sub-area A; blue filled area, sub-area B; red filled area, sub-area C). A legend of the interpreted key reflections with representing colours is presented in the bottom left corner.

The study area was further divided into three sub-areas in E- W direction by the characteristics of three important structural elements at Mid Jurassic- Early Cretaceous level of faulting (Figure 3.11). Sub-area A is bounded by the master faults MF1- MF5 to the east and the master faults MF8, MF9 and MF10 to the west. Sub-area A is an overall *graben* (Twiss and Moores, 2007, p. 95), between the footwall block of the eastern bounding fault of the Hammerfest Basin and the adjacent sub-area in the west. Sub-area A is characterized by *synthetic* and *antithetic* (Twiss and Moores, 2007, p. 95) normal faults making out fault blocks in an overall *horst and graben system* (Twiss and Moores, 2007, p. 95), with the most down dropped fault block towards west in the overall graben. Both listric geometry and near planar geometry are found among the synthetic and antithetic faults, and the individual fault blocks show different amount of rotation away from the centre of the graben. Sub-area B is bounded by the master faults MF10 in the east and MF11, MF12 and MF13 in the west. Sub-area B is a horst with two normal faults with listric geometry dipping opposite direction. The internal reflections are near horizontal. The area west of Sub-area B into the Tromsø Basin is termed sub-area C. Sub-area C has not been fully interpreted due to restricted seismic resolution in that area. Even though it is hard to map out exactly the key reflections and the faults of sub-area C, it is clear that the key reflections rapidly drops into the Tromsø Basin and that several faults affect the sub-area.

Three main levels have been affected by faulting in the study area. The faulting affecting the two Permian reflections is referred to as the Late Permian level of faulting. The faulting affecting Top Stø Formation reflection, Base Cretaceous reflection and most often Top Kolje Formation reflection is referred to as Mid Jurassic- Early Cretaceous level of faulting. The faulting affecting the Top Kolmule Formation reflection is referred to as the Early Tertiary level of faulting.

Three possible detachments have been interpreted based on termination of faults and the geometry of individual fault planes and fault blocks. Possible Detachment 1 is located between the Late Permian level of faulting and the Mid Jurassic- Early Cretaceous level of faulting. Possible Detachment 2 is located in the far west between Base Cretaceous reflection and the Top Kolje Formation

reflection. The Possible Detachment 3 is located between the Top Kolmule Formation reflection and the Top Kolje Formation reflection. These will carefully be discussed in the discussion later.

3.4. Key profiles

4 regional 2D seismic lines have been selected as key profiles to present the three segments. Three of them are striking NE-SW and the last one is striking E-W. Most of the interpretation of the faults and reflections was done on the E- W striking seismic lines to make the map, and to be able to correlate between the available 2D seismic lines. This was done because their orientation nearly give a cross- sectional view of the Mid Jurassic- Early Cretaceous structures in the fault complex. However, the NE-SW striking lines have a better seismic resolution in the deeper parts, and make it possible to look at the structures in the Permian reflections in relation to the younger structures. The NE- SW trending lines were therefore best to be presented as key profiles.

The key profiles will be described in order to establish the general geometry of each segment and to demonstrate the geometrical variations of the sub-areas between the segments.

The three defined levels affected by faulting will be described from the oldest (Late Permian) to the youngest (Early Tertiary). The three possible detachments will be described in the discussion. The key reflections in each level of faulting will be described in an older- younger approach. The sequence between the key reflections will be presented, and then the faults in that level are described. The present sub-areas of each Key Profile will be outlined before the description of the Mid Jurassic- Early Cretaceous level of faulting are presented.

The master faults will be denoted MFx, as in the fault map, and they represent the same faults interpreted in map view. The other faults are not given names in the fault map, and the given names is only given for one key line and cannot be related to local faults with the same names in other key profiles. The faults in the Permian level of faulting will be denoted with a small capital letter a. The local faults of Top Stø Formation reflection and Base Cretaceous reflection are denoted with a small capital b, the local faults of Top Kolje Formation reflection

with a small capital c, and the local faults in Top Kolmule Formation reflection with a small capital d. Those faults that cut more than one reflection will get the letter from the oldest affected level of faulting.

Key profile 1

Key Profile 1 is the southernmost segment in the study area, and the orientation of the profile is E-W (Figure 3.10). The Permian reflections and structural features of the Late Permian level of faulting have not been interpreted in this key profile. The profile is presented in Figure 3.12.

Sub-Area A is present in this Key profile from MF1 to MF8, with the graben centre between MF6 and b1. Sub-area B is not present as the elevated fault block between b1 and MF8 is interpreted as a part of the Sub-area A. Sub-area C is present west of MF8 as the Top Stø Formation reflection and Base Cretaceous reflection are dropping fast into the Tromsø Basin.

Four fault blocks are interpreted in the Mid Jurassic- Early Cretaceous level of faulting. The Top Stø Formation reflection has an eastward tilt inside all the fault blocks. Base Cretaceous reflection also have a general eastward tilt but less tilted than for the Top Stø Formation reflection due to difference in lateral thickness in the sequence between the two reflections. Base Cretaceous reflection has normal drag towards b1 in both footwall and hanging wall block.

The sequence between the Top Stø Formation reflection and Base Cretaceous reflection is decreasing in thickness towards MF1 from the east in the footwall block. A clear wedge-shape sequence is seen between the two reflections in the fault block between MF1 and MF6, with the thickest part towards MF1. The fault block between MF6 and b1 has a thicker sequence of sediments between the two reflections compared to the other fault blocks. The fault block between b1 and MF8 are seen as a small horst, and the sequence between the Top Stø Formation reflection and Base Cretaceous reflection has a small wedge-shape with the thickest part towards b1. In the fault block between MF8 and b3 the wedge-shape of the sequence between the two reflections is clearest. The sequence has a thickness difference of 165ms twt with the thickest part towards MF8 and the thinnest part towards b3. The eastward tilt of the Top Stø Formation reflection is up to 20° in some of the fault blocks in this key profile.

Top Kolje Formation reflection is cut by the same faults as the Top Stø Formation reflection and Base Cretaceous reflection. The reflection has normal drag towards MF6 in the hanging wall block, and a domal feature is recognised towards that fault in the footwall block. Normal drag in Top Kolje Formation reflection is also seen towards MF8 in the hanging wall block.

The sequence between Top Kolje Formation reflection and Base Cretaceous is thickening westward east of MF1.

All the faults of the Mid Jurassic- earliest Cretaceous level of faulting are normal faults with near planar geometries. All the faults show an increase in throw with increase in depth. All the faults in this level except b1 have down-to-west displacement.

Top Kolmule Formation reflection is chaotic in this key profile. The reflection has an overall westward tilt. The reflection is clearly affected by faulting on the distal part of the platform, but only five faults were identified. d1, d2, d3 and d4 are normal faults with near planar geometries. d4 is a *reverse fault* (Twiss and Moores, 2007, p. 115), with near planar geometry. F1 is a low angle fault that cuts b3, and the reflections above are onlapping onto the fault.

The sequence between Top Kolmule Formation reflection and The Top Kolje Formation reflection is thickening westward.

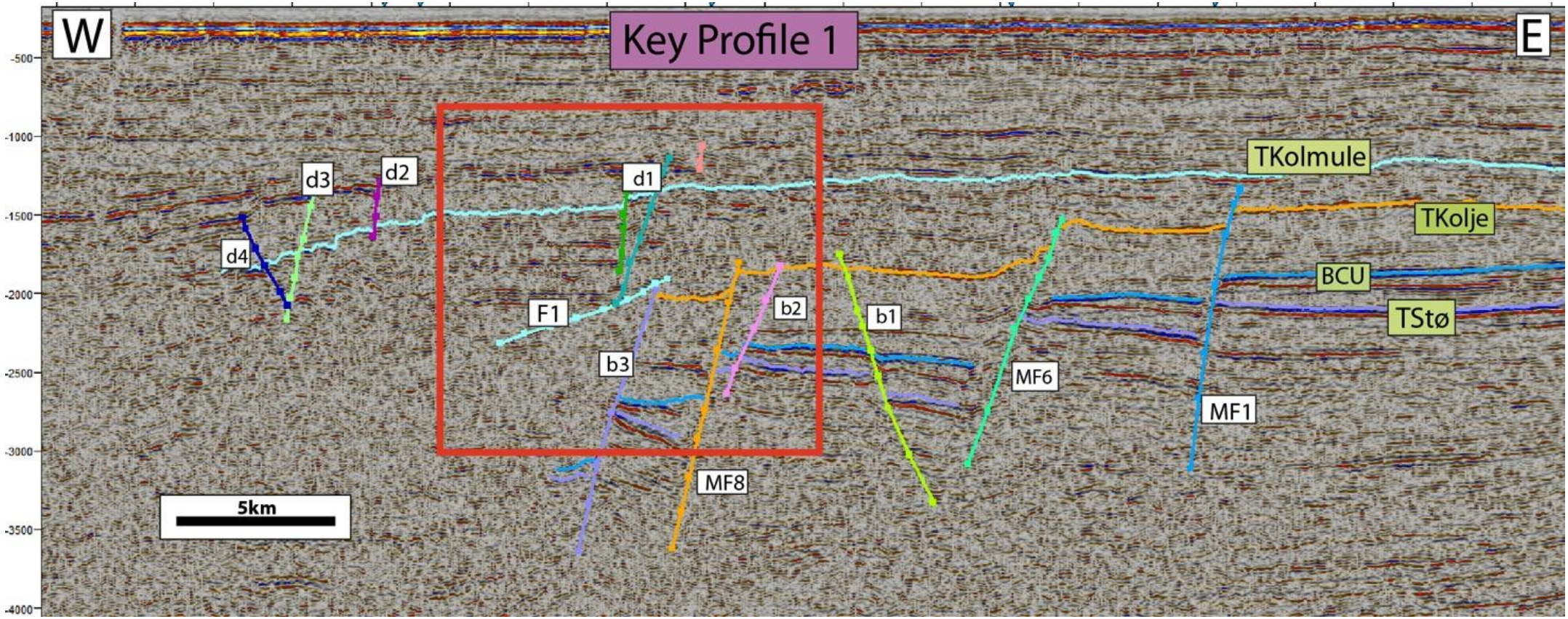

Figure 3.12: Key profile 1, see Figure 3.9 for location of the line. TStø: Top Stø Formation reflection, BCU: Base Cretaceous reflection, TKolje: Top Kolje Formation reflection, TKolmule: Top Kolmule Formation reflection. Red square show the position the focused area in Figure 5.4

Key profile 2

This key profile is oriented NE- SW and is located in segment 2 (Figure 3.10). The Key Profile is presented in Figure 3.13.

The Intra Permian reflection has a westward dip farthest east in the Key Profile. The reflection show normal drag in the footwall block towards a1. The Intra Permian reflection has a downward flexure between a1 and a2. The reflection is more disturbed between a2 and a3 and the exact fault planes are not interpreted. However, it is clear that the reflection is faulted and abruptly increases with 1700ms twt over 6km horizontal distance. The reflection changes between being near horizontal and steep dipping westward. The reflection is tilted eastward west of a3.

The Top Permian reflection has a westward tilt in the east of the key profile towards a1. The reflection has an eastward tilt in the fault block between a1 and a2. The reflection has a normal drag towards a1 in the hanging wall block.

The sequence between the Intra Permian reflection and the Top Permian reflection is thinning from east to west towards a1 in the east of the key profile. The sequence increases in thickness across a1, and it thickens towards the middle of the fault block.

Some local faults are cutting the Intra Permian reflection in the footwall block of a1. a1, a2 and a3 are the main interpreted faults in the Late Permian level of faulting. a1 is affecting the deepest reflections and all the way up to Top Kolmule Formation reflection, and shows an increase in throw with depth. a2 and a3 appear to affect the Permian reflections only. All three faults are normal faults with down-to-west displacement and near planar geometry. However, a1 have listric geometry in the deepest part.

Sub-area A is the only present sub–area in this key profile, since the seismic line only reaches half across the fault complex. MF4 marks the eastern boundary of sub-area A and the graben centre is between b5 and b6.

Top Stø Formation reflection is tilted towards east in all the fault blocks except between b3 and b4 and between b5 and b6, and the tilt ranges from less than 2°

east of MF4, to 20° between b4 and MF7. Normal drag is seen in both hanging wall and footwall block of b6.

Base Cretaceous reflection is following the same trend as the Top Stø Formation reflection but with less degree of tilt in the fault blocks. Normal drag is seen in both hanging wall and footwall block of b6, and in the hanging wall block of b2.

The sequence between Top Stø Formation reflection and Base Cretaceous reflection has a wedge-shape in all the fault blocks where the Top Stø Formation reflection has an easterly tilt. The thickest part is towards the eastern boundary faults of the fault blocks. The sequence is thickest between b5 and b6.

Top Kolje Formation reflection is more horizontal than the two deeper reflections but an eastward tilt of less than 3° is seen east of MF1 and west of b5. An upward flexure is present between b2 and b3 and a downward flexure is seen between b4 and MF7. Normal drag in the footwall block of both b2 and b5 are present. The sequence between Top Kolje Formation reflection and Base Cretaceous reflection shows a general thickening westward from MF1 (230ms twt) to b5 (650ms twt).

The faults of the Mid Jurassic- Early Cretaceous level are normal faults and affect Top Stø Formation reflection, Base Cretaceous reflection and Top Kolje Formation reflection. All faults except b6 have a down-to-west displacement. MF1, b3, b4 and MF7 are affecting all reflections up to Top Kolmule Formation reflection. MF1, b1, MF7 and b5 have listric geometry and b2, b3, b4 and b6 have near planar geometries. All faults show an increase in throw with increasing depth, except MF7. The throw at the Top Kolje Formation reflection is bigger than for the Base Cretaceous reflection across MF7. In general the throw across the faults is increasing from east to west.

The Top Kolmule Formation reflection has a general westward tilt. The reflection has an eastward tilt between MF7 and d2 with a normal drag towards d2. The sequence between Top Kolmule Formation reflection and Top Kolje Formation reflection is increasing in thickness towards west

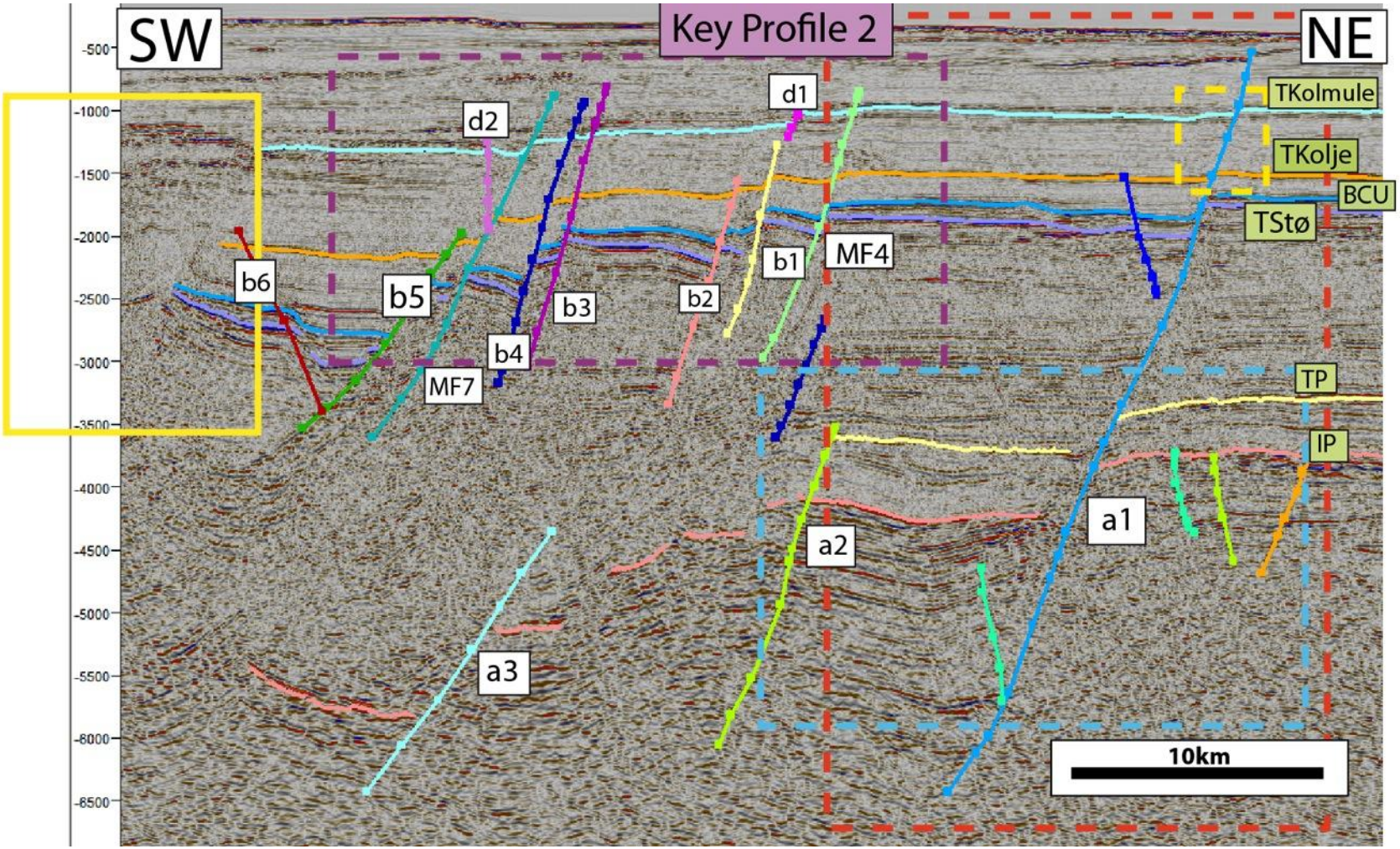

Figure 3.13: Key profile 2, see Figure 3.9 for location of the line. TStø: Top Stø Formation reflection, BCU: Base Cretaceous reflection, TKolje: Top Kolje Formation reflection, TKolmule: Top Kolmule Formation reflection. The coloured squares show the positions of focused area. Blue dashed square: Figure 5.6; Purple dashed square: Figure 5.9; Yellow dashed square: Figure 5.10; yellow full square: Figure 5.11; red dashed square: Figure 5.12.

Key profile 3

This key profile is oriented NE-SW and is located in segment 3 (Figure 3.10). The key profile is presented in Figure 3.14.

The Intra Permian reflection is near horizontal in the east, it gets a westward tilt when moving across the faults towards west. In the farthest west where it is interpreted the reflection has an eastward tilt. The reflection shows a structural sag between a1 and a2. The Top Permian reflection has a normal drag towards a1 in the footwall block, and is onlapping the fault in the hanging wall. The reflection dips westward near a1 before it gets more horizontal 1,5 km farther southwest.

The sequence between Top Permian reflection and the Intra Permian reflection is thinning towards a1 in the footwall block. The sequence has a wedge-shape between a1 and a2 with a thick part near a1, then a thinner part where the Top Permian reflection starts to flatten out, and gradually becomes thicker again in the deepest part of the structural sag of the Intra Permian reflection.

a1 and a2 are normal faults with near planar geometries and down-to-west displacement. a1 is affecting all interpreted key reflections and has an increase in throw with increasing depth.

The sub-area A is present between MF5 and MF10, with the graben centre between b7 and b8. The sub-area B is present between MF10 and MF11 with near horizontal internal reflections. Sub-area C is present southwest of MF11.

Top Stø Formation reflection is heavily faulted and have an eastward tilt in all fault blocks except in the fault block between b7 and b8, and west of b11. Base Cretaceous reflection has the same trend as the Top Stø Formation reflection but the Base Cretaceous reflection is less tilted. Normal drag is seen in the hanging wall block towards MF5, b2, b3, b4, b5 and b6.

The sequence between Top Stø Formation reflection and the Base Cretaceous reflection is wedge-shaped in several fault blocks, but it is most evident between b4 and b5 and between b10 and b11.

Top Kolje Formation reflection has a general westward tilt. Normal drag is seen in both hanging wall block and footwall block of MF5. A structural sag is seen between MF12 and b9.

The sequence between Top Kolje Formation reflection and the Base Cretaceous reflection is thickening westward. Top Kolje Formation reflection is affected by a1, MF5, b4, b5, b6, MF12, b9 in addition to the four faults interpreted locally on the reflection, c1- c4.

The faults are normal faults and the majorities have a down-to-west displacement. b8, b9 and MF10 have a down-to-east displacement. b11 is a reverse fault, or a normal fault with *convex upward listric geometry* (defined in subchapter 2.4). MF5 and b1- b6, b8, MF10 have listric geometries, whereas b7, MF12, b9 and b10 have near planar geometries.

Top Kolmule Formation reflection has a general westward tilt. The reflection has normal drag in the footwall block of MF5, but is only slightly affected by faulting before far out on the platform where c3 and c4 are located. c3 and c4 are normal faults with listric geometries.

The sequence between Top Kolmule Formation reflection and Top Kolje Formation reflection is thickening westward.

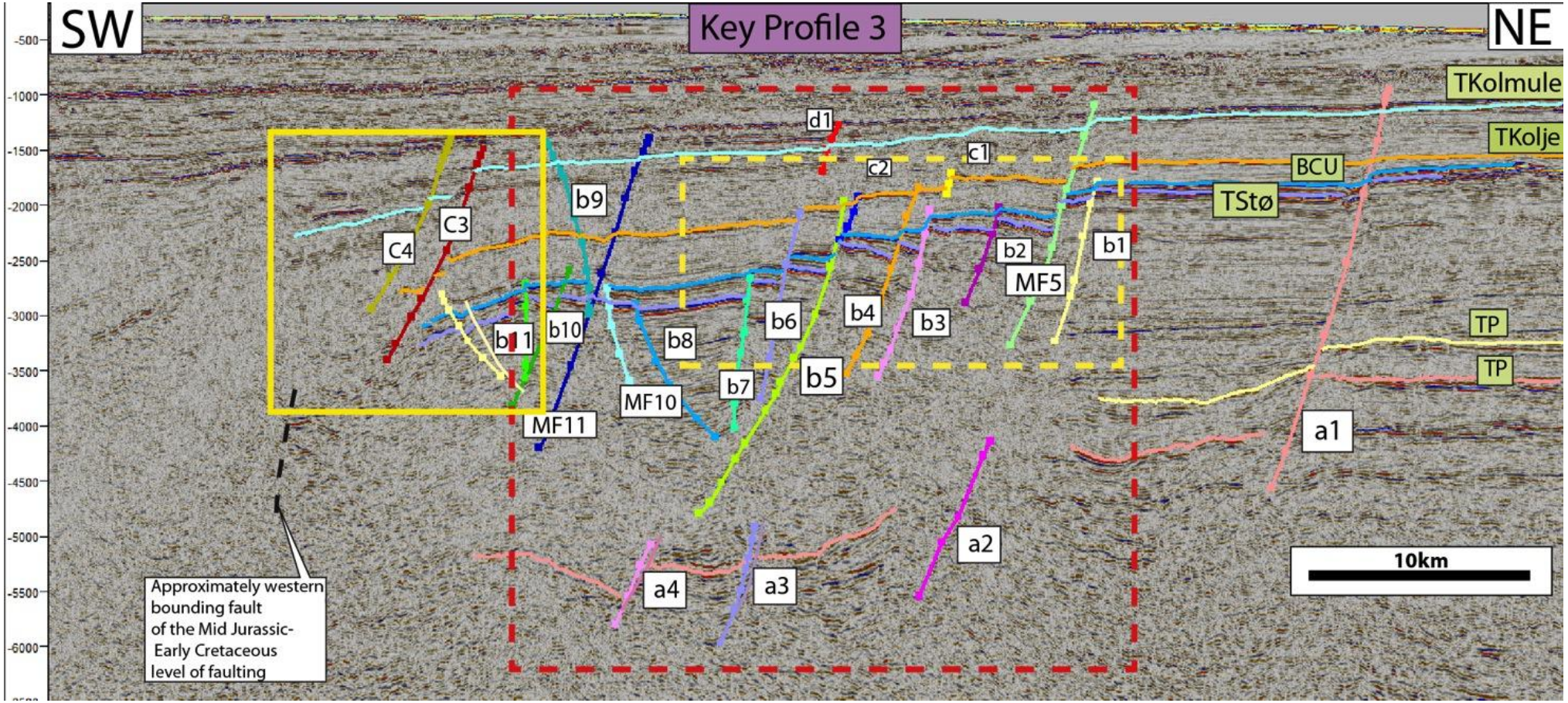

Figure 3.14: Key profile 3, see Figure 3.9 for location of the line. TStø: Top Stø Formation reflection, BCU: Base Cretaceous reflection, TKolje: Top Kolje Formation reflection, TKolmule: Top Kolmule Formation reflection. The coloured squares show the positions of focused area. Red dashed square: Figure 5.2; yellow full square: Figure 5.3; yellow dashed square: Figure 5.8

Key Profile 4

Key profile 4 is oriented NE-SW and is the northernmost key profile in segment 3 (Figure 3.10). The Key Profile is presented in Figure 3.15.

The Intra Permian reflection and Top Permian reflection are only interpreted in a limited area where they can be identified. The Intra Permian reflection has a general south western tilt and throws up to 111ms twt across the faults. Top Permian reflection has not been correlated from the footwall to the hanging wall block of a1, and is only interpreted between a1 and a2 with a southwestward tilt. The reflection shows a normal drag towards a1 with a structural sag connected to the normal drag. The sequence between the Intra Permian reflection and the Top Permian reflection shows a small thickening towards southwest.

Three normal faults are affecting the Intra Permian reflection. a1 has listric geometry and a dip of 55° towards SW. a2 and a3 have near planar geometries with steep dips towards SW of 70-80°.

Sub-area A is defined between MF5 to MF10 with the graben centre between b3 and b4. MF10 and MF12 make out the horst of sub-area B. Sub-area C is located west of MF12.

The fault blocks of the Mid Jurassic-Early Cretaceous level of faulting are from 1-4 km in NE-SW direction measured at the Base Cretaceous reflection. The dips of the Top Stø Formation reflection are ranging from being near horizontal in the horst of sub-area B to have a westward dip in most of the fault blocks. The western dips in the fault blocks in sub-area A, gets gradually steeper in each fault block towards west. The Top Stø Formation reflection and Base Cretaceous reflection are showing an abrupt increase in depth across the sub-area C, which is a distance of about 6km. Normal drag folds are seen in Top Stø Formation reflection in the hanging wall block of b5 and b7, and reverse drag is seen towards b7 in the footwall block. The Base Cretaceous reflection is having the same dip trend in the fault blocks as the Top Stø Formation reflection, but with lower degree of dips. Normal drags are seen in Base Cretaceous reflection in the hanging wall block of MF5, b1, b2, MF10, b5, b7 and MF12, and in the footwall block of b6.

The sequence between Top Stø Formation reflection and Base Cretaceous reflection is thickest in the fault block between b4 and b5, which is the most down faulted fault block of sub-area A. Clear wedge-shaped sequences are seen between the two reflections in the two fault blocks between b4 and b5, with the thickest parts towards southwest.

Top Kolje Formation reflection has a general southwestward tilt, and the sequence below the reflection shows westward thickening. The sequence between Base Cretaceous reflection and Top Kolje Formation reflection is thickening in both directions from the centre of the fault block between MF12 and b6. Normal drags are seen in the hanging wall block of b5 and MF12, and in the footwall block of b6.

All the faults of the Mid Jurassic- Early Cretaceous level of faulting are normal faults. b6 is interpreted to be a normal fault with convex upward listric geometry, since the reflections indicate this by their drag folds. MF10, b5 and MF12 have listric geometries, whereas the rest of the faults have near planar geometries. B1, b4, MF10, b5 and b6 have down-to-east displacement, and the rest of the faults have down-to-west displacement. MF5 and MF10 are affecting all reflections from Top Stø Formation reflection up to Top Kolmule Formation reflection. b1, b2, b4, b5, MF12 and b6 are affecting the reflections from Top Stø Formation reflection up to Top Kolje Formation reflection. b3 and b7- b9 are only affecting Top Stø Formation reflection and Base Cretaceous reflection. All faults are showing an increase in throw with increasing depth.

Top Kolmule Formation reflection is only affected by the master faults MF5 and MF10, from the underlying levels of faulting. The reflection shows a small sag directly above the fault block between MF5 and b1 in Mid Jurassic- Early Cretaceous level of faulting. A structural dome is seen in Top Kolmule Formation reflection just above the horst between MF10 and MF12. The reflection has a gradually tilt towards southwest and affected by faulting near the boundary towards the Tromsø Basin. The fault planes of d1- d4 have not been interpreted in depth, but they appear to be near planar since no distinct relative rotation between the hanging wall blocks and the footwall blocks can be seen. d1 and d2

have a westward dip of 66-67°. d3 and d4 are more steep- dipping with dips of 77-79°. A small structural dome is seen on the west side of d4.

The sequence between Top Kolmule Formation reflection and Top Kolje Formation reflection is generally thickening towards southwest.

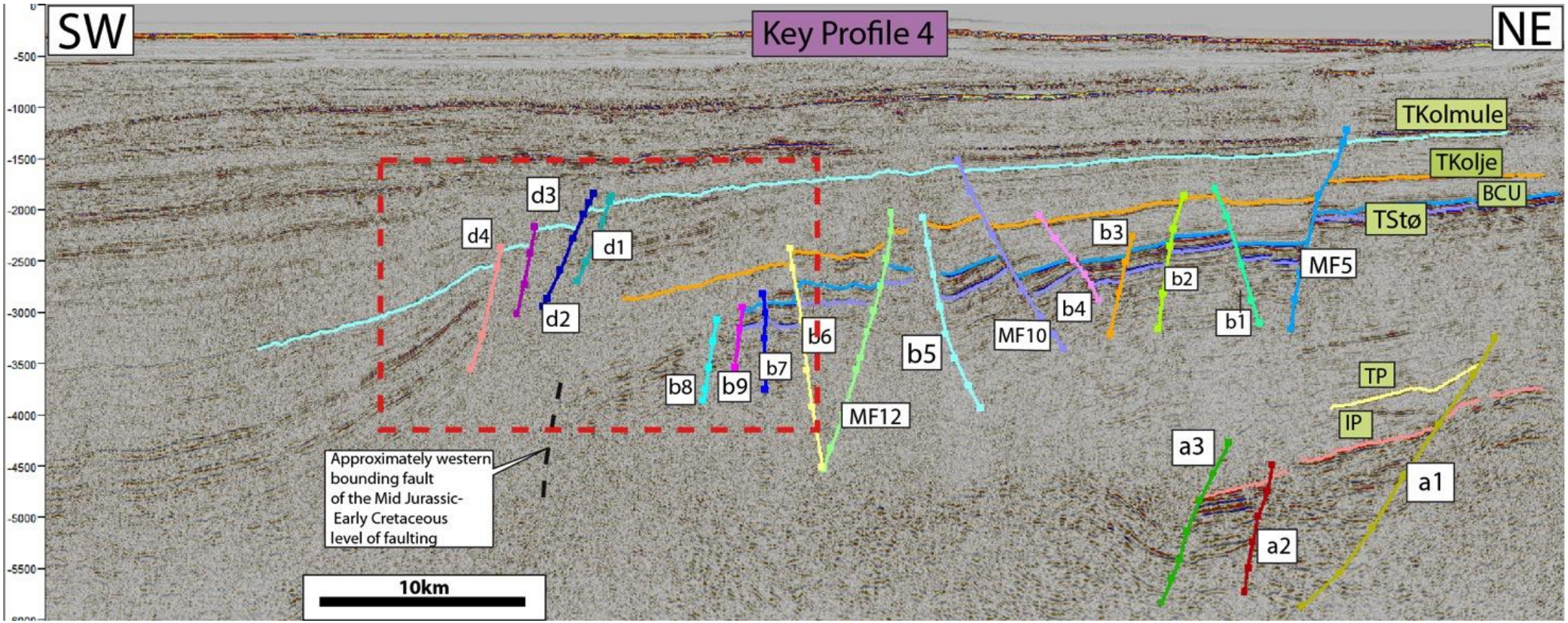

Figure 3.15: Key profile 4, see Figure 3.9 for location of the line. TStø: Top Stø Formation reflection, BCU: Base Cretaceous reflection, TKolje: Top Kolje Formation reflection, TKolmule: Top Kolmule Formation reflection. The coloured squares show the positions of focused area. Red dashed square: Figure 5.3 and Figure 5.5

3.5. Time-Structure map

One time-structure map of Top Stø Formation reflection was included to show the depth relation in the area (Figure 3.16). The reflection ranges from 1800ms twt in the Hammerfest Basin down to more than 3400ms twt in the western part of the Ringvassøy- Loppa Fault Complex. The general trend of the contour lines shows that the reflection becomes deeper farther east in the southern part of the study area than in the northern part. A structural high can be distinguished between MF10 and MF12 and MF13, which correlated to the sub-area B in the cross sections.

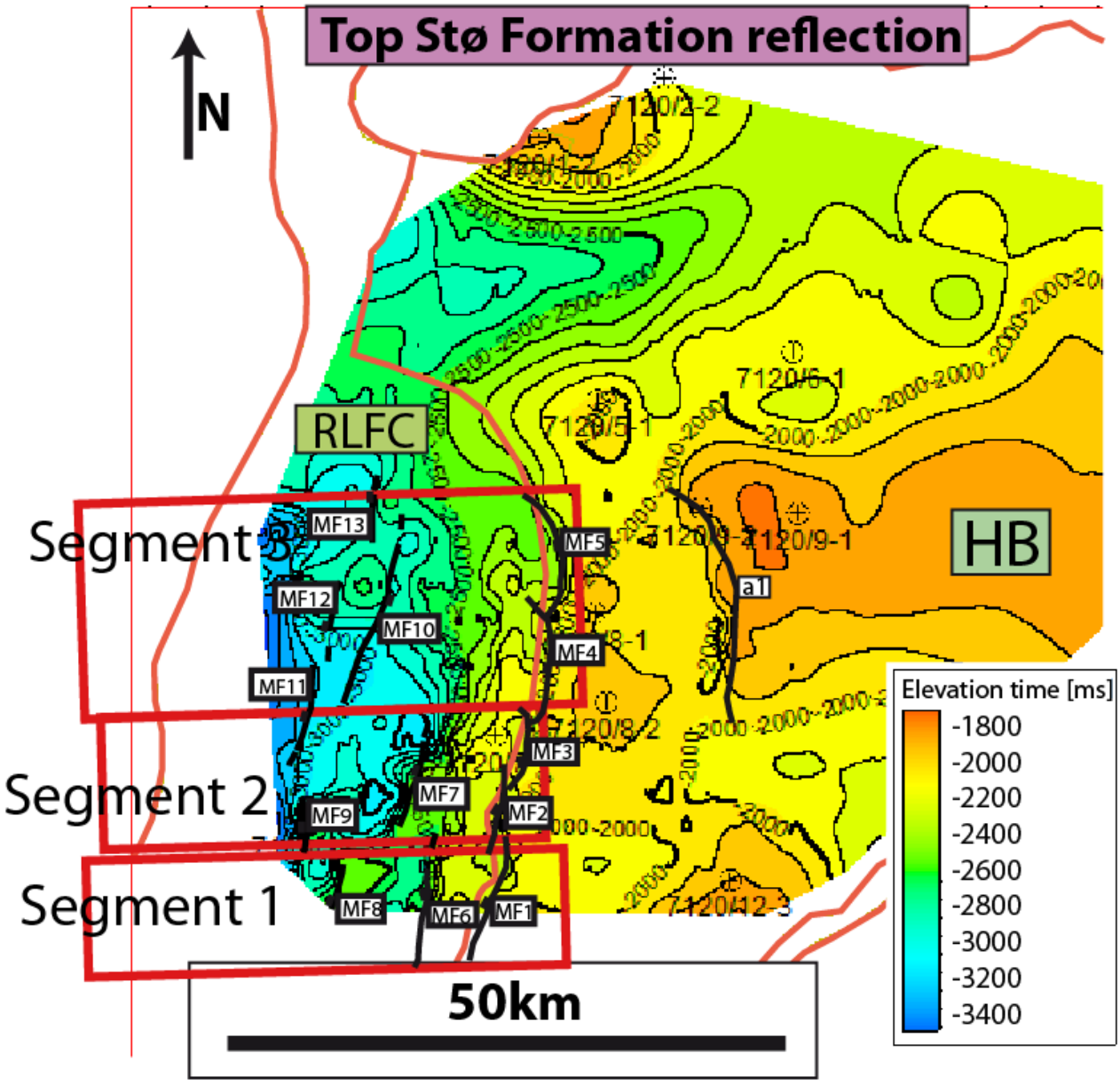

Figure 3.16: Time-structure map of Top Stø Formation reflection.

Chapter 4; Analogue experiments

4.1. Background

Seismic interpretation and analogue mechanical experiments are the two complementary parts of this thesis. The analogue models are used to investigate the interaction of multiple stages of deformation and the effect of stacked detachments, Figure 4.1.

Three analogue models were built with different sediment layers and performed with different numbers of extensions. The purpose of contrasting setups was: 1) to see how detachments effect the geometrical configuration of the fault zone; 2) whether multiple detachments can promote or suppress the bulk fluid communication on the fault zone.

The results and observations from the analogue models are also applied in connection with the seismic interpretation and allow for a better understanding of the development of the fault complex seen on the seismic lines.

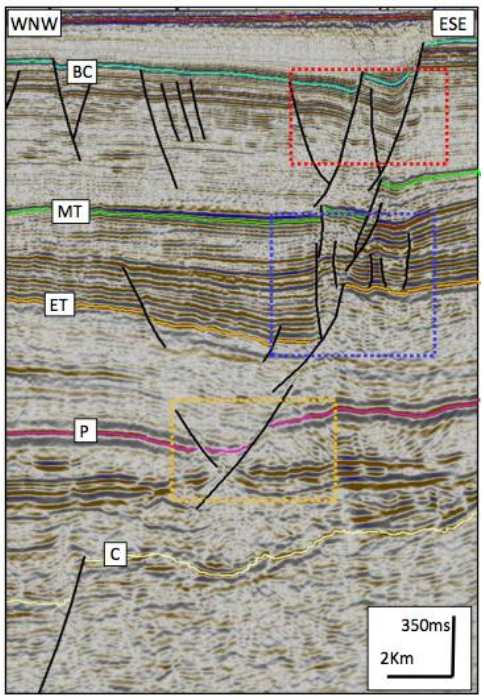

Figure 4.1: Illustration of stacked detached levels of faulting (Waqas, 2012).

4.2. Experimental set up

The analogue models were made at the tectonic laboratory, TecLab, at the Vrije Universiteit (VU) Amsterdam, the Netherlands. Sand, silicon putty, scanners, cameras, different mechanical machines and software are used to solve different kinds of tectonic problems on both lithospheric and crustal scale, at this laboratory. The mechanical machines can be set up to perform compression, extension and strike- slip movements.

The mechanical machine used for the experiments of this study is called a squeeze box. The machine contains an engine and moveable walls. The squeeze box is able to perform strike-slip, shortening and extension, symmetrical and asymmetrical for upper crustal scale (Vrije Universiteit Amsterdam, 2012). This squeeze box will be referred to as a motor driven machine in the following descriptions.

Several other workers have presented analogue experiments with relevance to the experiments presented here. Sand models, with similar set ups have been performed at TecLab (e.g. Zalmstra, 2011; Van Nunen, 2011). Results of experiments performed at other laboratories have proven to be interesting. The plaster experiments made by Gabrielsen and Clausen (2001) are interesting when looking at fluid communication along and across the fault zone. Plaster experiments done by Fossen and Gabrielsen (1996) on extensional fault systems, and the relation of these experiments to detachment zones in The North Sea by Fossen et al. (2000), are comparable for this study. The result of the sand/ silicon putty experiments in McClay et al. (1990), and Brun et al. (1993) both show the structural development when brittle and ductile layers are interacting. The studies of Ellis et al. (1988) and McClay et al. (1987) show the evolving geometries of the developing faults during extension.

Method

The experiments represent asymmetric extension on a crustal scale. Sand and silicon putty were used to build the models, and their properties are listed in Table 4-1.

Table 4-1: Properties of the sand (Willingshofer & Sokoutis, 2005), and properties of the silicon putty (Passchier & Sokoutis, 1993) used in the experiments.

Material	Grain size [μm]	Critical angle of repose [°]	Internal friction	Density [Kg m^{-3}]	Viscosity [Pa s]
Quartz	300	42	0,9	1510	
Silicon putty				970	5x10^{4}

The sand represented the brittle layers, and the silicon putty represented a ductile detachment zone in the experiments. The purpose of including the silicon putty layer was to create a simulation of the different fault deformation above and below the detachment zone (Figure 4.2). These contrasting geometries in the sand above and below are expected when an area is undergoing multiple rifting events with a developing detachment zone in between.

Figure 4.2: Showing the concept of two vertical separated systems of faulting with a detachment in between (Modified from Gabrielsen, 1984).

The alternating layers of black and white sand will be referred to as pre-rift strata for all three experiments. During the extension of model #1 and model #2 the developing features were filled with differently coloured sand to be able to see how the structures developed upwards during the experiments. The activation of the different structural features could then be interpreted on the top view images with support from the final cross sections. In the description of these two experiments, these layers of coloured sand will be referred to as the syn-rift strata. Infill of black sand was done during the second rifting of experiment #3, and this layer is referred to as syn-rift strata. However, infill of the developing structure of the first rifting in experiment #3 was only done after the rifting was finished. This infill will be referred to as post-rift strata in relation to the first rifting, but will be pre-rift strata in reference to the second rifting. After the rifting in Experiment #1, #2 and second rifting in experiment #3 the developed structural reliefs were filled completely with one colour sand to make a flat top surface, and this part of the models will be referred to as the post-rift strata.

The dimension of the models was 40x40 cm, with a height of 9,6 cm. A thin mobile plate was placed in the bottom of the model, covering half of the model. This mobile plate was pulled by hand and by a motor driven machine. The general set up can be seen in Figure 4.3c. Three fixed walls were built up by metal bars. Each bar had a thickness of 0,8cm and each new layer contained one very thin layer of black sand at the start and was filled to the rim of the framing bars with white sand, and repeated like that for each new set of bars. A thin blue layer was put on top of the complete model and a mesh was made with white sand. The mesh had a separation of 5 cm (Figure 4.3a). This blue coloured sand was only used at the top of the models, which makes it possible to look for the blue sand to see which parts that remained unaffected by the rifting.

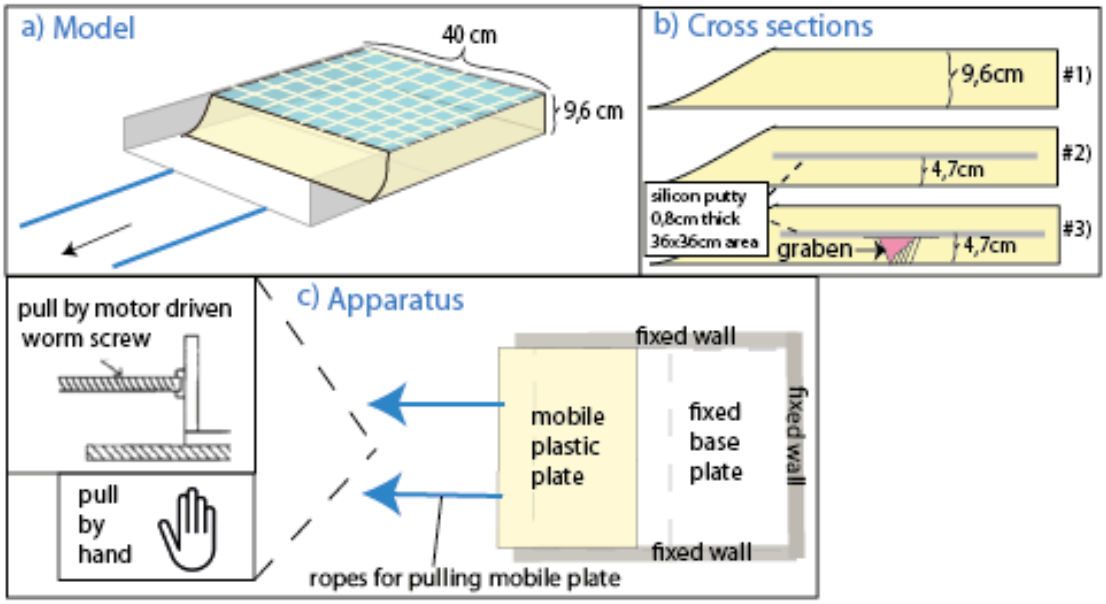

Figure 4.3: a) General dimensions of the sand models B) Cross sectional view of the three experiments to show the contrasting elements and dimensions of the three experiments. C) The model seen from above with three fixed walls, mobile plate pulled either by motor driven worm screw or by hand.

After the experiments were performed the models were soaked in water. By letting the models rest for some hours the water distributed throughout the model. The cross sections were cut from left to right when looking into the open wall of the model. The position of a cross section will then be described by distance in cm into the model from the left side of the model. A sharp knife was used to cut the model to get cross sectional images. The knife cut through the model at the wanted position of the cross section and the sand on the left side was removed to get a clear view. The cross section was finalized by using a small sharp knife to clean the cross section.

Asymmetrical extension was performed on all three models, by pulling the mobile plate with constant angle of 90° direction to the graben axis. The pulling was done either by hand, 1cm at a time, or by a motor driven machine with a fixed deformation velocity of 1cm/h, Figure 4.3c.

Three experiments were performed with variable setups. Experiment #1 had a homogeneous sand column, and extension was performed by hand to a total displacement of 9cm. This experiment was performed to serve as a reference model for the study. Experiments #2 and #3 was both built with a silicon putty layer after 4,7cm (Figure 4.3b). The dimension of the silicon putty layer was 36x

36x 0,8 cm. The motor driven machine was used to perform Experiment #2 to a total extension of 4,7cm. Experience #2 was performed with only one rifting to show the contrasting structural development above and below the detachment zone. Experiment #3 was first built up to 4,7 cm and then an extension of 4 cm was performed by hand. The structures that formed were filled with pink sand as post-rift strata, before the silicon putty layer was placed in the model. The model was then completed with additional layers of sand before the motor driven machine performed a second extension of 4,6cm. Experiment #3 was performed with two phases of rifting to observe how structures from the first extension was reactivated and further developed in the second extension.

In order to relate the analogue experiments to the structural features seen on the 2D seismic lines the pictures of the models will be oriented with the extensional force from the left in the following description. The extensional force in The Barents Sea acted from the west in the seismic lines, which is viewed towards north. Only the eastern part of the rift is represented on the seismic lines and hence the corresponding right part of the experiments will be emphasized in this study. Thus, the open wall in the sand models where the extension was performed will be referred to as west.

Notes and photographs were taken for documentation of the models. Top view photographs were taken of the experiments before, during and after extension. Photographs of the cross sections were taken from the left side of the model when looking into the open wall, since the cross sections were made from that side. This means that the photographs of the cross sections from the models are oriented opposite of the extensional direction we want to simulate. The photographs have therefore been flipped horizontally before they were interpreted.

4.3. Description of the experiments

The structural features in the three experiments will be described in an organized way, starting with the motivation and particular setup for the experiment. Description of the final stage in map view will then be presented with all the structural features seen at the surface. One cross section that

illustrates the dominating structural geometry and features for all the cross sections, is chosen as a reference cross section. The structural features in the reference cross section are given names and described in detail. All cross sections taken along the model is then presented together with the reference-cross section, and the structural features in the reference cross section is identified in each of the other cross sections. The general similarities between the cross sections are shortly given before the difference in each cross section is emphasized. The structural development versus extensional distance is then presented in a diagram to show when the structures were activated. A general direction or trend of the structural development is presented based on the diagram.

Grabens are given numbers according to their sequential development, where GR1 was the first to be formed. The analysis of their relative development was made based on the top view pictures taken during the extensions.

Only the structural features in the eastern part, Graben 1 and 3 with internal features will be described in the cross sections of experiment #2 and #3. This is because these are the interesting parts that can be compared to structures seen in Ringvassøy- Loppa Fault Complex.

It is not possible to determine the relative timing of activation for all the faults. The faults are therefore named and numbered based on their location, from bottom to top, right to left, in the cross sections. Certain abbreviations are given to imply their regional importance (Table 4-2).

The interpretation of the fault development through time is based on the photographs in map view taken during the extension, and which syn-rift layers are disturbed or even present in each fault block seen in the cross sections. The photographs taken regularly during the performance of the experiments were investigated and faults in each image were interpreted. By plotting the faults visible in one photograph according to when the photograph was taken, a schematic figure were made to show the activation of the different structural features and how long they were active. The blind faults that cannot be recognized in the top view images have not been taken into the diagram of fault

timing. The information in the diagram is limited since there is no continuous documentation to tell the exact activation of the faults during the extension.

Table 4-2: The main fault types used in the interpretation of the analogue models with abbreviation and their regional importance.

Abbreviation	Short description
GR	**Graben** - Regional structural feature
MF	**Master fault** -Regional importance
SF	**Synthetic faults** -Local importance
AF	**Antithetic faults** -Local importance
BF	**Branching fault** - Local importance

Experiment # 1

Experiment #1 was performed to serve as a reference model for the other two experiments. The dimension and style of the developed structural features will be important when discussing the development in the other experiments. The developed features of experiment #1 are representing the fault system underneath a detachment zone, the green square, seen in Figure 4.2. Extension was performed on a homogenous package of sand, which gives the opportunity to look at how the graben developed independent of the silicon putty and the load of overburden.

Only one graben developed during experiment #1. An asymmetric geometry of the graben was recognised where the deepest part was located towards west in relation to the centre of the graben. Terraces combined by *relay ramps* (Twiss and Moores, 2007, p. 86) dominated the eastern part of the graben. The terraces were relatively horizontal, and showed rotations less than 2° on the individual terraces. The uppermost terraces were wider than those near the graben axis.

The western boundary of the graben was dominated by one steep dipping slope into the graben. Traces of several antithetic faults could be identified in the slope.

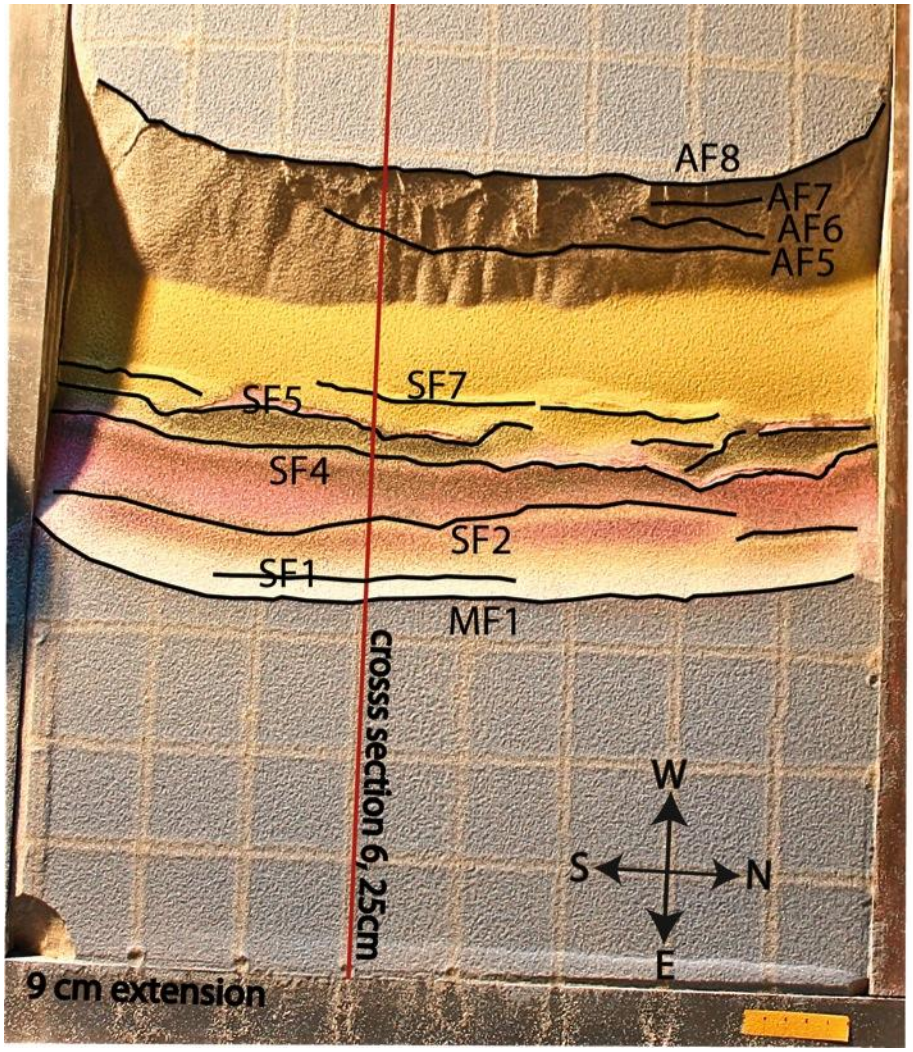

Figure 4.4: Top view image of experiment #1 after complete extension of 9 cm. Location of reference cross section is marked with red line.

The asymmetric graben structure was further investigated in the cross section (Figure 4.5). Cross section 6 was chosen as the reference section because this cut represented the dominating structures in a neat way. The master fault MF1, made out the eastern boundary of the graben. This was a near planar normal fault. Five fault blocks were bounded by planar normal faults. These normal faults were steeply dipping 73-76°, and were synthetic in relation to the master fault. The throws of the faults decreased from the uppermost fault block in east towards the centre of the graben. The fault blocks had rotations less than 2°. SF3 and SF6 were not cutting through all the syn-rift layers. Two fault branches, BF1 and BF2, developed from SF 1 and SF 5, and terminated respectively towards SF2

and internal in the fault block between SF5 and SF7. These branching faults were normal faults with convex upward listric geometry. An unknown number of nearly planar antithetic normal faults were making out the western side of the graben. They had steep dips of 80-84°.

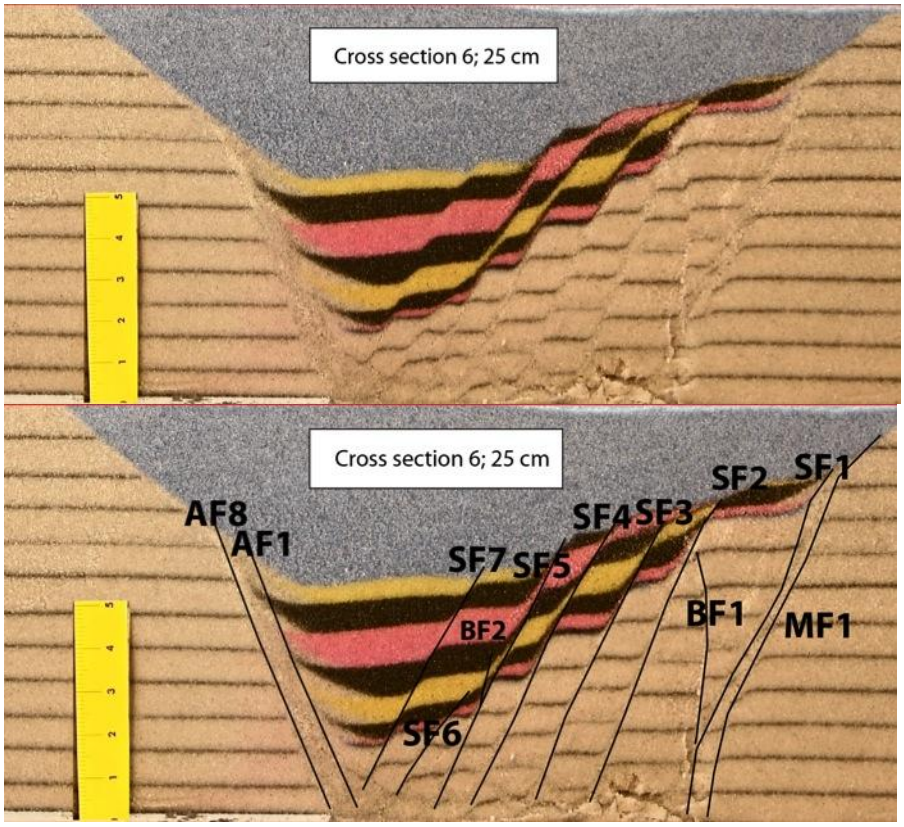

Figure 4.5: Uninterpreted (top), and interpreted (bottom) image of the reference cross section 6. Location of the cross section in the model is marked in Figure 4.4.

8 cuts along the model were made, and they are presented in Figure 4.6.

All the cuts showed the same general structural trend as the reference cross section. All of them had three- five fault blocks bounded by synthetic normal faults on the eastern side of the centre. Antithetic faults were bounding the western side of the graben.

Cross section 1 had four developed fault blocks on the eastern side. The throw on the synthetic normal faults were less than in the reference cross section. The antithetic faults were less steep with dips of 59 to 63°. One fault block developed on the western side of the graben centre, with an increase in throw with depth.

Cross section 2 had three well- developed fault blocks. SF3 was branching out and terminated before it cut through all the syn-rift layers. The antithetic faults were steeper compared to the cross section 1. The western fault block was also present in this cross section but less developed.

Cross section 3 had four fault blocks. The branching fault BF1, developed from SF1 seen in the reference cross section, was well developed in this cross section. This fault was here making out a tilted fault block together with another branching fault farther east. The layers in this fault block had westward dips. The western fault block seen in cross section 1 and 2, were seen in the pre-rift layers but not in the syn-rift layers in this cross section.

Cross section 4 had four fault blocks, and all the faults in the reference cross section could be identified. Some more branching faults developed between SF1 and SF2 in this cross section.

Cross section 5 was very similar to the reference cross section with five fault blocks.

Cross section 7 had four fault blocks where SF5 was the fault that bounded the central part of the graben. SF7 did not develop in this cut.

Cross section 8 had four fault blocks on the eastern side. One western fault block was present. Many branching faults were seen in the deep where most of them terminated before they reached any other faults.

The timing of activation of each fault can be seen in Figure 4.7. The development of the eastern side of the graben started with the bounding master fault. During the extension, new synthetic faults were created frequently towards west. For each new activated synthetic fault the older ones seemed to be left relatively inactive. New antithetic faults were frequently made on the western side of the graben. AF1 was the first fault to be activated and the younger faults were created regularly towards west. These antithetic faults appeared to be active from the onset to the end of the extension, and together they made out a zone of deformation. Thus, the general direction of structural development was from east towards west.

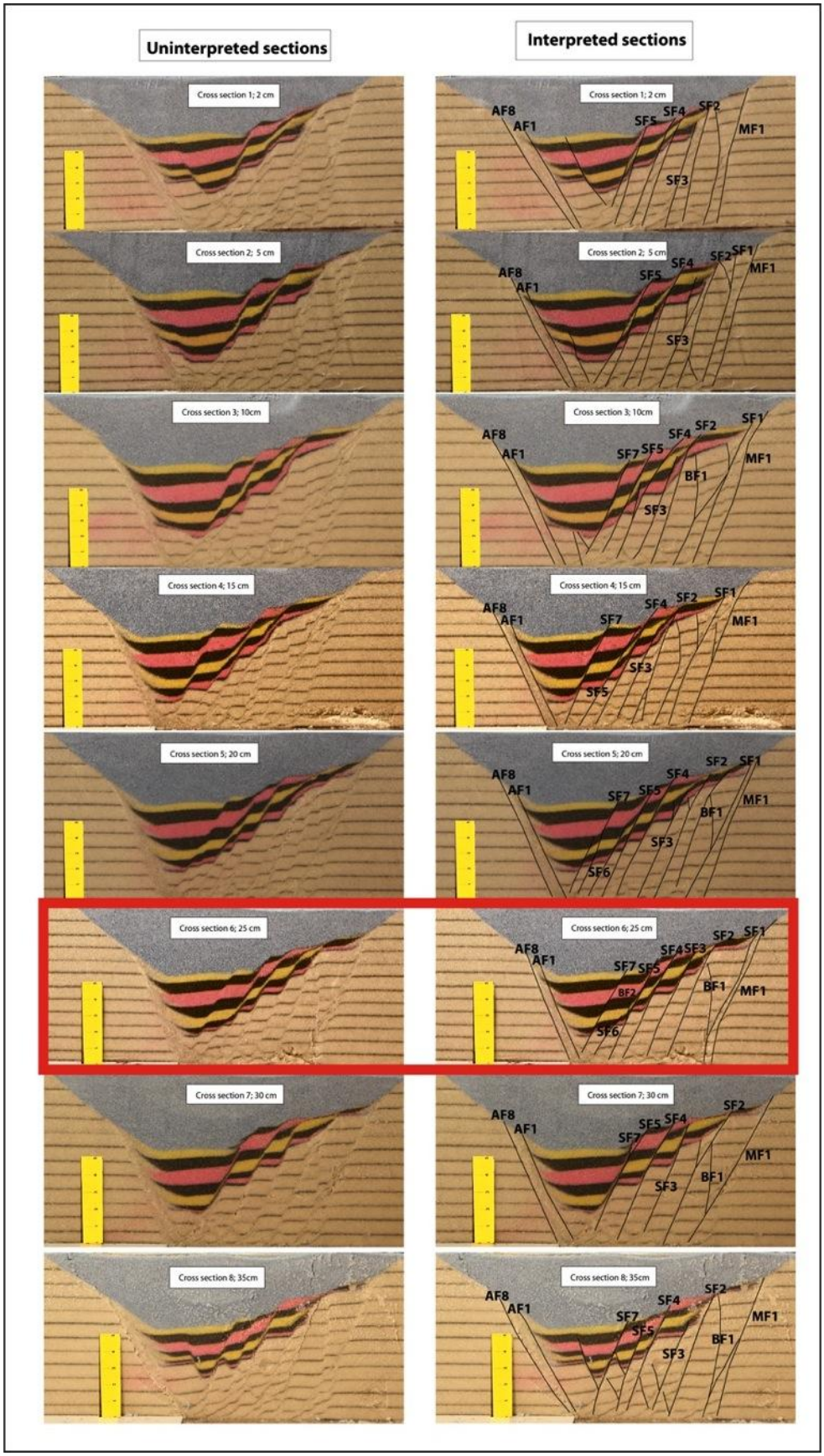

Figure 4.6: Uninterpreted (left) and interpreted (right) images of all cross sections of Experiment #1. Position of the cross sections in cm into the model is given in each image. Reference cross section 6 is marked by the red square.

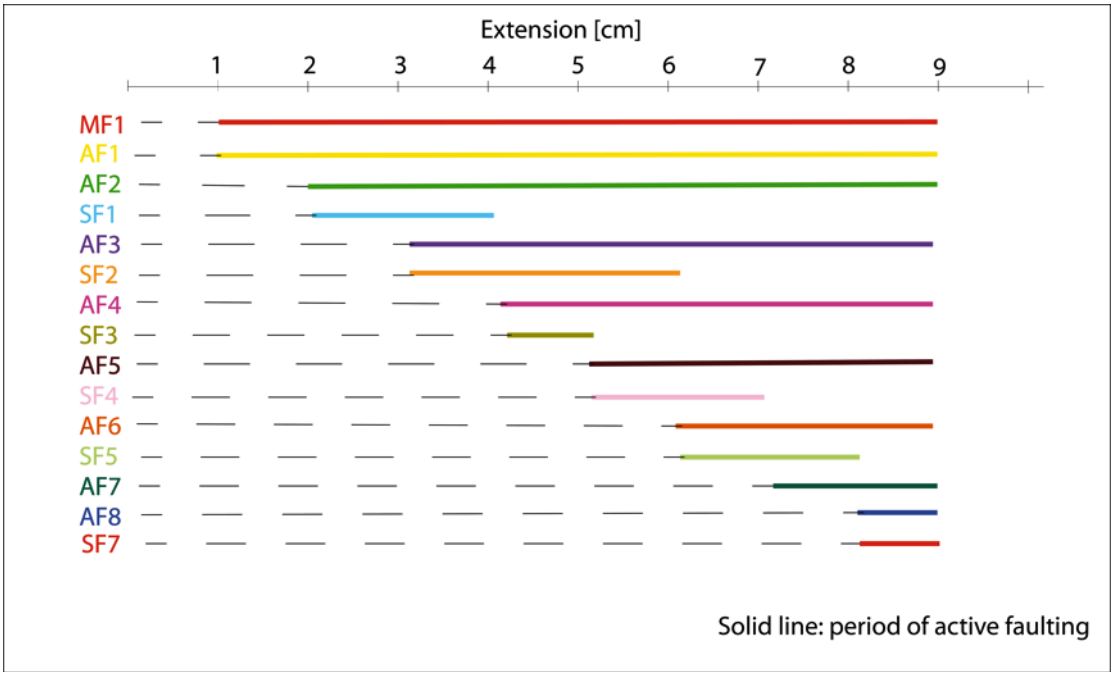

Figure 4.7: Timing of activation and development of structural features of Experiment #1. Total extension was 9 cm for this rifting.

Experiment #2

In experiment #2, a layer of silicon putty was placed in the middle of the model. This silicon putty is simulating a detachment zone, and Figure 4.2 is illustrating the wanted simulation. The experiment was performed with only one event of deformation, and the main motivation of this experiment was the contrasting developing structural features above and below the silicon putty. The deformation was performed by a motor driven machine, with a deformation velocity of 1cm/hr. The total extension of the experiment was 4,7cm.

Four grabens developed during this experiment, Figure 4.8. Two steep slopes were dipping towards Graben 1. There was no exact visible eastern boundary of *Graben 1*, and the western boundary appeared to be a reverse fault MF5, when seen in the map view. However, further investigation of the cross sections showed that the master fault was a normal fault with convex upward listric geometry. *Graben 2* was only developed in the southern part of the model, and had few internal faults. The throw of the bounding faults of Graben 2 was decreasing northwards. *Graben 3* was bounded by the faults, MF2 and AF5. The eastern slope was steep with traces of synthetic faults. Terraces with few relay ramps dominated the western part of Graben 3. The western and uppermost

terrace was wider than the other terraces. *Graben 4* had two bounding master faults and internal faults made out terraces. The internal faults in Graben 4 were less developed and had a less evident relief across the terraces. The western part of Graben 4 was less dominated by terraces, while the eastern part had some fault bounded terraces.

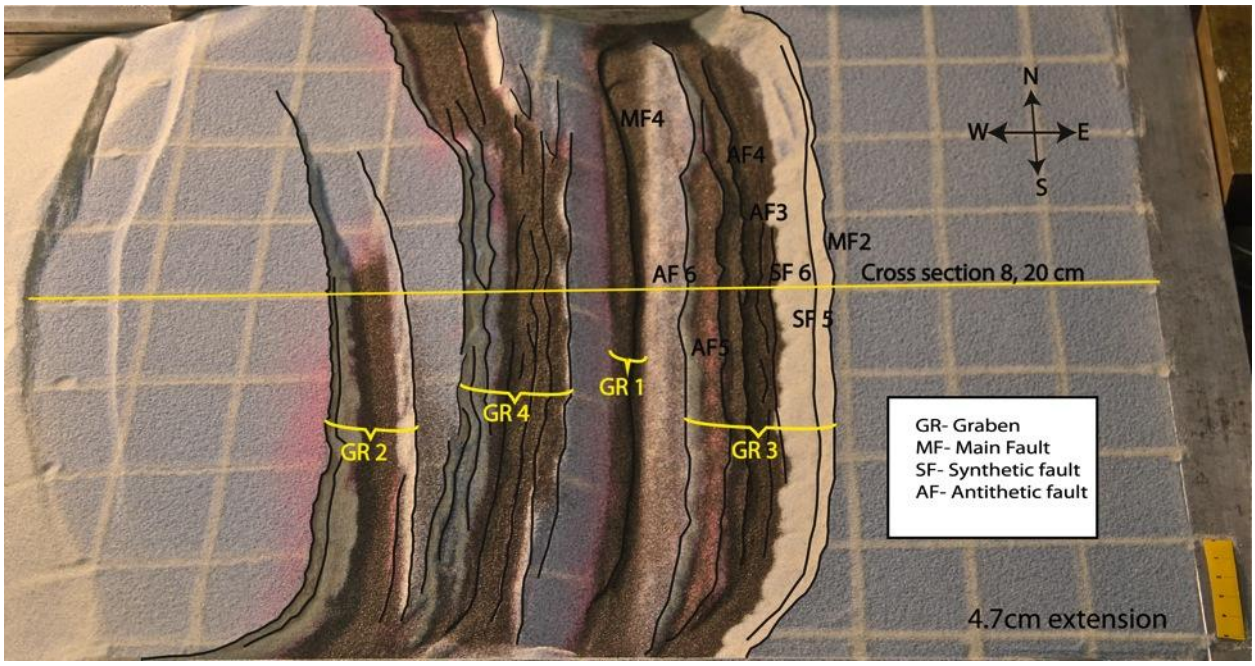

Figure 4.8: Top view image of experiment #2 after complete extension of 4,7 cm. Location of reference cross section is marked with yellow line.

Cross section 8 was chosen as the reference cross section for this experiment (Figure 4.9). One graben developed under the silicon putty, and will be referred to as the Deeper Graben. The description of this cross section is presented in Table 4-3.

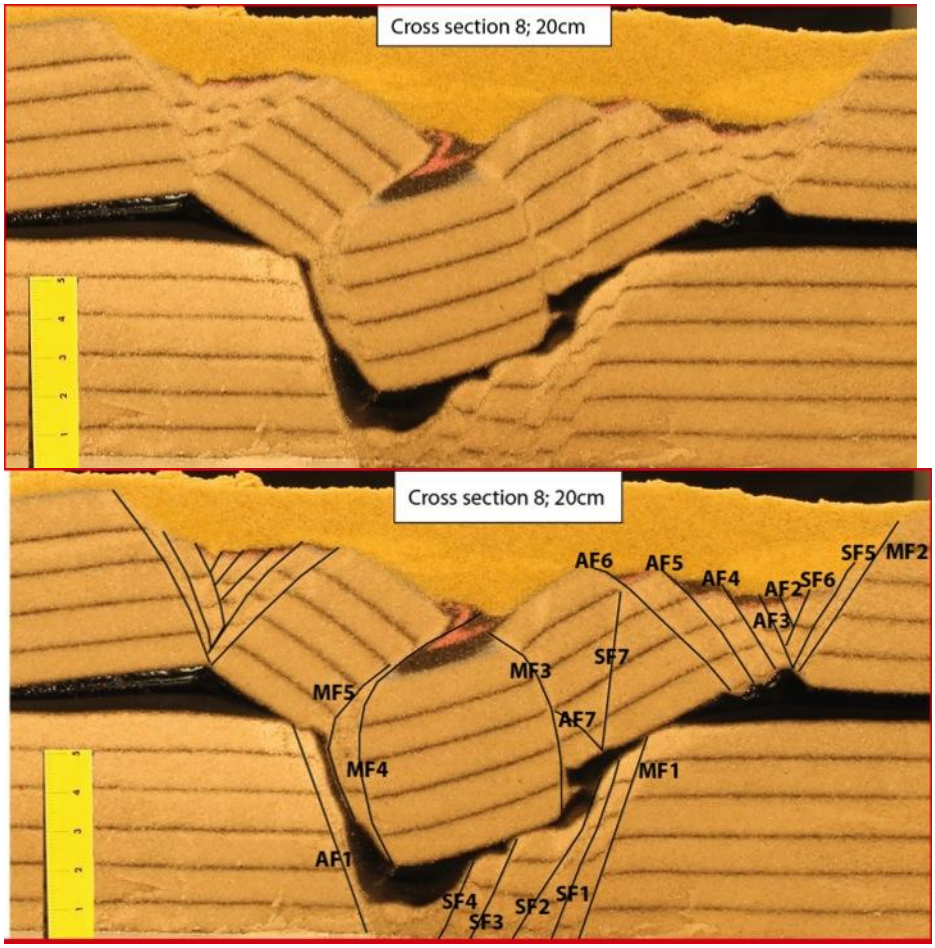

Figure 4.9: Uninterpreted (top), and interpreted (bottom) image of the reference cross section 8. Location of the cross section in top view is marked in Figure 4.8

Table 4-3: Description of the reference cross section 8 organized in individual grabens with comprising structures.

Main structures		Structures and description
The Deeper Graben -Generally the same structures and geometries as the graben described in Experiment #1	Eastern boundary	MF1: - Normal fault, nearly planar
	Western boundary	AF1: - Normal fault, nearly planar
	Location of deepest part	Towards west
	East of deepest part	SF1-SF4: - Normal faults, nearly planar - Made out four fault blocks, with less than 2° rotation
	West of deepest part	- Dominated by westward migrating development of antithetic faults. - Traces of older antithetic faults were overridden by the silicon putty
Graben1	Eastern boundary	MF3 - Normal fault - Convex upward listric geometry

		- The *fault trace* (Twiss and Moores, 2007, p. 82) was buried by syn-rift sediments
	Western boundary	MF5 - Normal fault - Convex upward listric geometry - Development of *fault propagation fold* (Twiss and Moores, 2007, p. 121) in syn-rift layers
	Comments: - Not a normal graben, but a down dropped fault block - Internal layers were tilted towards west with a dip of 15°. However the layers in the horst between Graben1 and Graben3 had a westward dip of 32°	
Graben2	Only interpreted in top view	
Graben3	Eastern boundary	MF2 - Normal fault, nearly planar
	Western boundary	AF6 - Normal fault - Slightly convex upward listric geometry
	Location of deepest part	Towards east
	East of deepest part	SF5-SF6: - Normal faults, nearly planar - No fault blocks - It appeared to be a deformation zone with a westward migration of developing synthetic faults
	West of deepest part	AF2-AF5: - Normal faults, nearly planar - Made out four rotated fault blocks where the westernmost fault block had the greatest rotation (23° dip towards west)
Graben4	Only interpreted in top view	
Other structures	SF7	- Synthetic normal fault, nearly planar - Terminated towards AF6
	AF7	- Antithetic normal fault, nearly planar - Terminated towards MF3

10 cross sections were made of Experiment #2. These are presented in Figure 4.10.

All cross sections, except cross section 1, showed the general structural trend described in the reference cross section with the Deeper Graben with fault blocks on the eastern side, and antithetic faults on the western side, the Graben 3 with different amount of developed rotated fault blocks, and a down dropped block making out Graben 1.

Cross section 1 was not well developed. The Deeper Graben was seen as a nearly symmetric graben with fault blocks on each side of the graben centre. Graben 3 did not develop and was only marked by MF2 and SF5. Graben 1 was not broken off along MF 4, and a downward flexure in the layers was instead present at that point.

Cross section 2 had a less developed Graben 3 with only one fault block on the western side, but two fault blocks on the eastern side bounded by synthetic normal faults. The eastern fault blocks showed rotation less than 2°, whereas the western fault block had dip similar to the reference cross section. The down dropped fault block of Graben 1 was less rotated than in the reference cross section, and the slopes adjacent to Graben 1 was less steep dipping. The fault propagation fold was not well developed in this cross section, and the syn-rift layers were covering a wider surface area than in the other cross sections.

Cross section 3 had the same Graben 3 as cross section 2. The fault propagation fold was seen at the surface of Graben 1 in this cross section.

Cross section 4 had the Graben 3 with three eastern fault blocks and two western fault blocks.

Cross section 5, cross section 6 and ***cross section 7*** looked the same, where Graben 3 had two synthetic fault blocks and two antithetic fault blocks.

Cross section 9 had the same structural features of Graben 3 as in the reference cross section.

Cross section 10 had a simple Graben 3 with two antithetic fault blocks and one synthetic fault block.

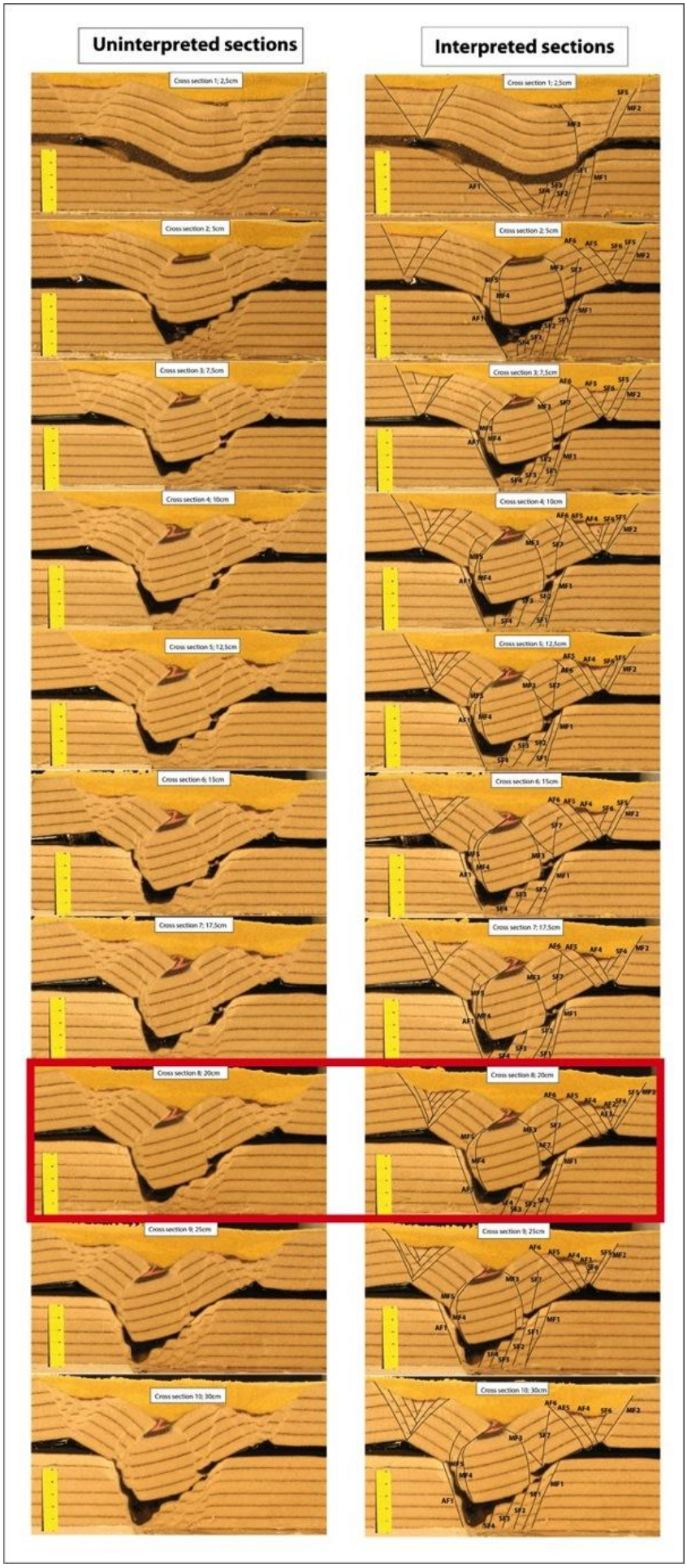

Figure 4.10: Uninterpreted (left) and interpreted (right) images of all cross sections of Experiment #2. Position of the cross sections in cm into the model is given in each image. Reference cross section 8 is marked by the red square.

The activation and the active period of the individual structures of this experiment can be seen in Figure 4.13. Not all the faults were included in this diagram, since it was not possible to interpret the activation for all of them. This is especially the case for the internal faults of Graben 3, and the Deeper Graben. All the structural features appear to have been active throughout the extension after they were activated.

The general development of the experiment has been divided into four major stages.

Stage 1: After 1cm extension, a uniform depression of approximately 3 cm was developing orthogonal to the direction of extension. This depression was defining Graben1.

Stage 2: After 2cm extension the outlines of Graben2, Graben3 and Graben4 could be seen as a structural sag, and GR1 had subsided more, Figure 4.11.

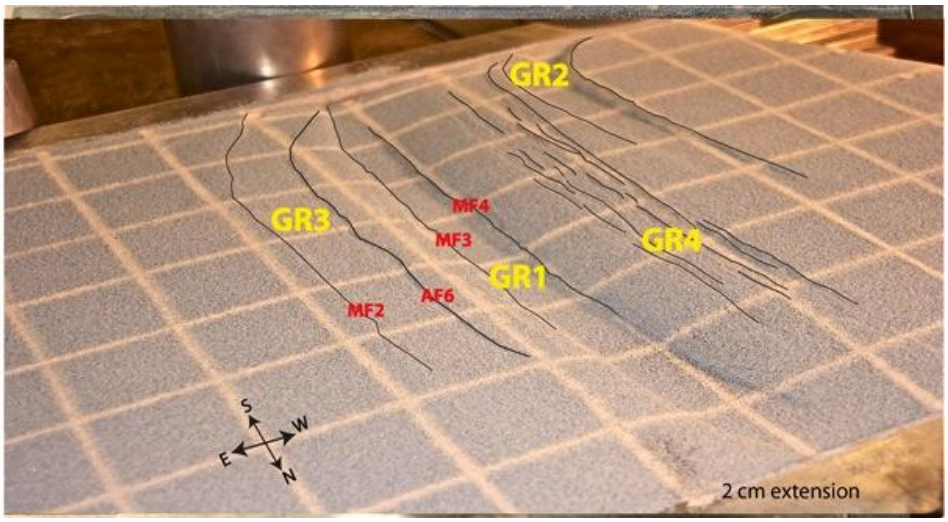

Figure 4.11: Top view image of Experiment #2 after 2cm extension, called stage 2 of the development of Experiment #2.

Stage 3: After 2,7cm of extension, internal, random, branched faults were visible in Graben3 and Graben4, Figure 4.12.

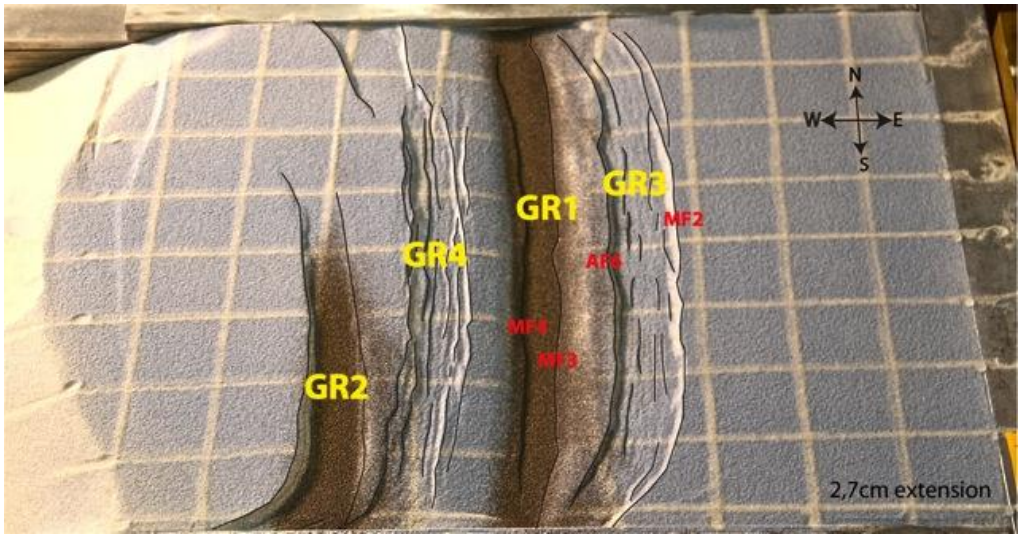

Figure 4.12: Top view image of Experiment #2 after 2,7cm extension, called stage 3 of the development of Experiment #2.

Stage 4: The random internal faults in Graben3 and Graben4 became organized and formed terraces with interconnecting relay ramps, when the extension reached 4,7cm of extension.

The general development of the structures in experiment #2 seen in top view started with the bounding faults of each individual graben. Internal uncontinous faults developed at the surface in the grabens with increasing extension. The uncontinous internal faults in the grabens became linked and developed into terraces with persistent extension.

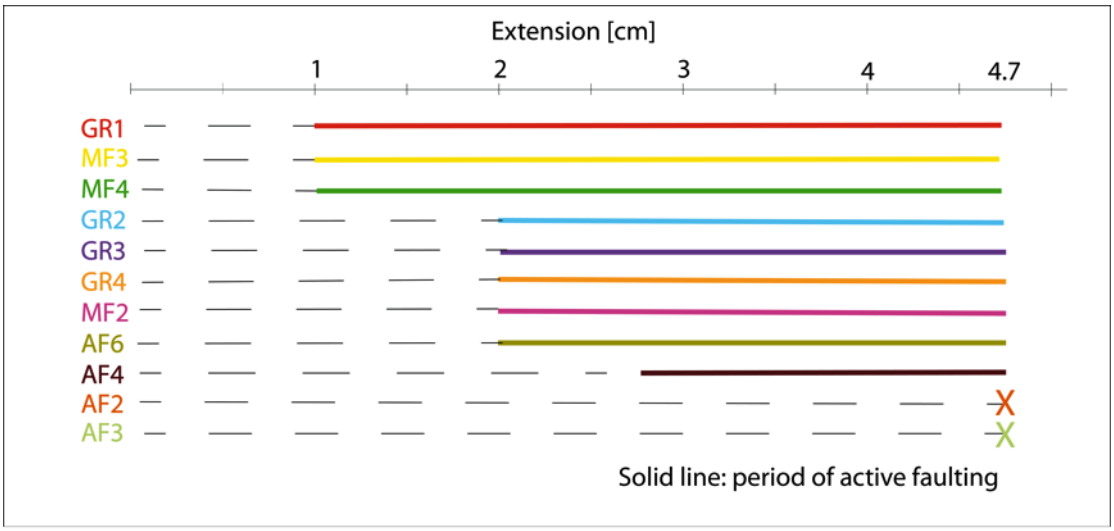

Figure 4.13: Timing of activation and development of structural features of Experiment #2. Total extension was 4,7 cm for this rifting.

Experiment #3

Experiment #3 was performed with two phases of extension. The first extension was performed when the model was built to 4,7 cm, to a total extension of 4 cm. The developing structures were filled with sand and a silicon putty layer was placed upon. The model was then built to the uppermost bar, before a motor driven machine performed the second extension. The displacement velocity of the second rifting was 1cm/hr, and the total extension was 4,6cm. Thus, the total extension of the two phases of rifting was 8,6cm. The motivation for this experiment was to observe how two phases of rifting affect the structural features above and below the silicon putty.

5 grabens could be seen from top view (Figure 4.14). Graben 1 had the same configuration as Graben 1 in Experiment #2. Graben 2 was similar to Graben 4 in experiment #2 but the affected area was up to 3 cm wider, and the throw of the bounding faults of the graben was up to 1 cm larger in this experiment. Graben 3 was similar to Graben 3 in Experiment #2, both in width and throw of the faults. Graben 4 was seen as two poorly developed arms that were mainly controlled by boundary effects. Graben 5 was a narrow graben of approximately 3 cm width, with one distinct eastern bounding master fault, and a less distinct western bounding antithetic fault. No internal structures could be identified in Graben 5.

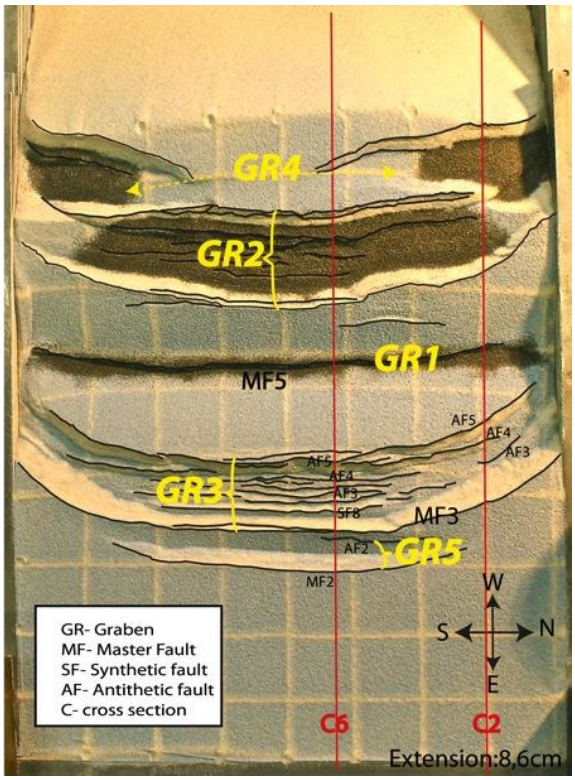

Figure 4.14: Top view image of experiment #3 after two phases of rifting and a total extension of 8,6 cm. Location of reference cross sections are marked with red lines. Abbreviations are given in the table in the bottom left corner.

Cross section 2 (Figure 4.15) was chosen as reference cross section described in detail in Table 4-4. However, Cross section 6 (Figure 4.16) was described for Graben5 and adding some information on Graben1, since not all structural features were present in cross section 2.

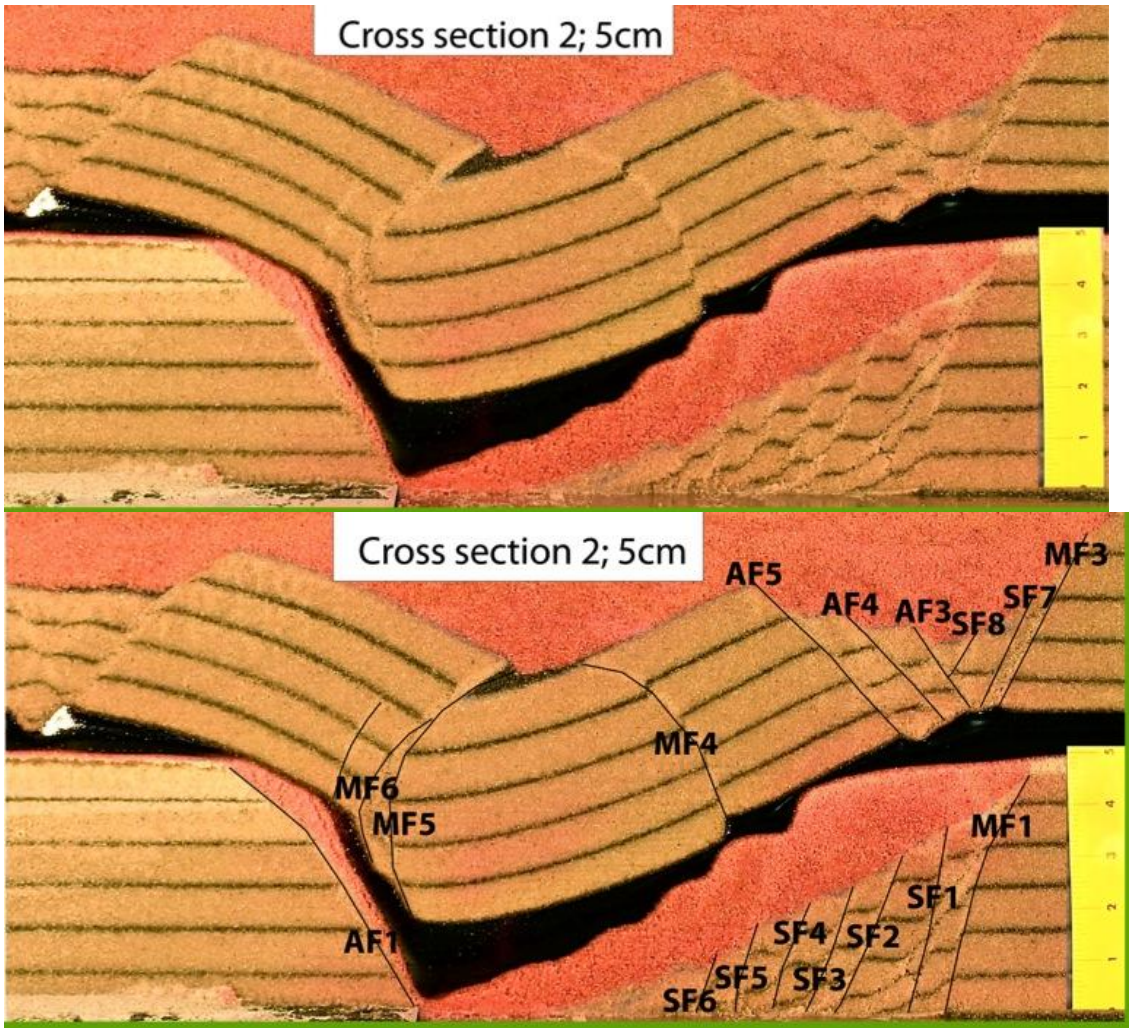

Figure 4.15: Uninterpreted (top), and interpreted (bottom) image of the reference cross section 2. Location of the cross section in the model is marked in Figure 4.14, and is taken 5 cm into the model.

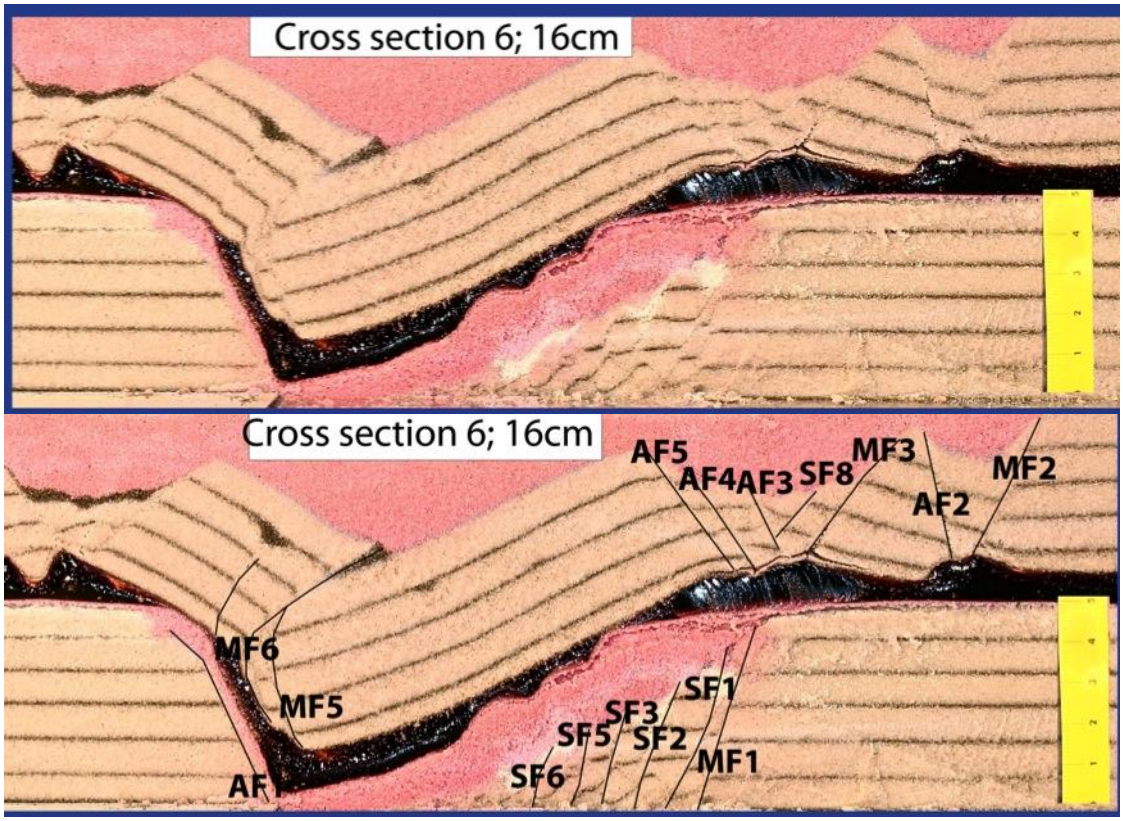

Figure 4.16: Uninterpreted (top), and interpreted (bottom) image of the reference cross section 6. Location of the cross section in the model is marked in Figure 4.14, and is taken 16cm into the model.

Table 4-4: Description of the reference cross sections 2 and reference cross section 6 organized in individual grabens with comprising structures.

Main structures		Structures and description
The Deeper Graben -Generally the same structures and geometries as the graben described in Experiment #1	Eastern boundary	MF1: - Normal fault, nearly planar
	Western boundary	AF1: - Normal fault, nearly planar
	Location of deepest part	Towards west
	East of deepest part	SF1-SF6: - Normal faults, nearly planar - Made out six fault blocks, with less than 2° rotation
	West of deepest part	- Dominated by westward migrating development of antithetic faults.
Graben1	Eastern boundary (only in cross section 2, not present in cross section 6)	MF5 - Normal fault - Convex upward listric - The fault trace was buried by syn-rift sediments
	Western boundary	MF5 - Normal fault - Convex upward listric - Development of a fault propagation fold in

	syn-rift layers	
	Comments: - In ***cross section 2*** this graben was similar to Graben1 described in Experiment #2 (dip on layers inside fault block: 15°, dip on layers in horst between Graben1 and Graben3: 27°). - In ***cross section 6***, the graben was only defined by MF5 in the west, and by a downward flexure of the layers towards east.	
Graben2	Only interpreted in top view	
Graben3	Eastern boundary	MF3 - Normal fault, nearly planar
	Western boundary	AF5 - Normal fault, nearly planar geometry
	Location of deepest part	Slightly towards east
	East of deepest part	SF7-SF8: - Normal faults, nearly planar - One fault blocks - It appeared to be a deformation zone between SF7 and MF3 with a westward migrating development of synthetic faults during deformation
	West of deepest part	AF3-AF4: - Normal faults, nearly planar - Made out two rotated fault blocks where the westernmost fault block had the greatest rotation (20° dip towards west)
Graben4	Only interpreted in top view	
Graben5 Present in ***cross section 6,*** not present in ***cross section 2***	Eastern boundary	MF2: - Normal fault, nearly planar
	Western boundary	AF2: -Normal fault, nearly planar
	Comments: - No internal structures, but an eastward dip of the layers (11-14°) - The horst between Graben5 and Graben3 had an eastern dip of 14-16°	

7 cross sections were made through the model of experiment #3, and are presented in Figure 4.17.

Cross section 1 and 2 had the same structural features seen in Experiment #2 with the Deeper Graben, Graben3 and the down dropped fault of Graben1. In ***Cross section 3- cross section 7*** the down dropped fault block had not been cut off from the horst separating it from Graben3, and an additional graben, Graben5 was present east of Graben3.

Cross section 1: Graben3 was not well developed, and no antithetic fault blocks could be outlined.

Cross section 2: Described in Table 4-4.

Cross section 3: The eastern bounding fault of Graben1, MF5, was a blind fault in this cross section. Graben 5 had developed but had a small throw and less dip on the internal layers than in Cross section 6. The Deeper Graben could not be interpreted properly due to loose sand.

Cross section 4: MF5 could not be identified in this cross section. Graben5 and the Deeper Graben were as in cross section 3.

Cross section 5: The same structural features as in cross section 6.

Cross section 6: Described in Table 4-4.

Cross section 7: Graben 3 in this cross section had one antithetic fault block and two synthetic fault blocks.

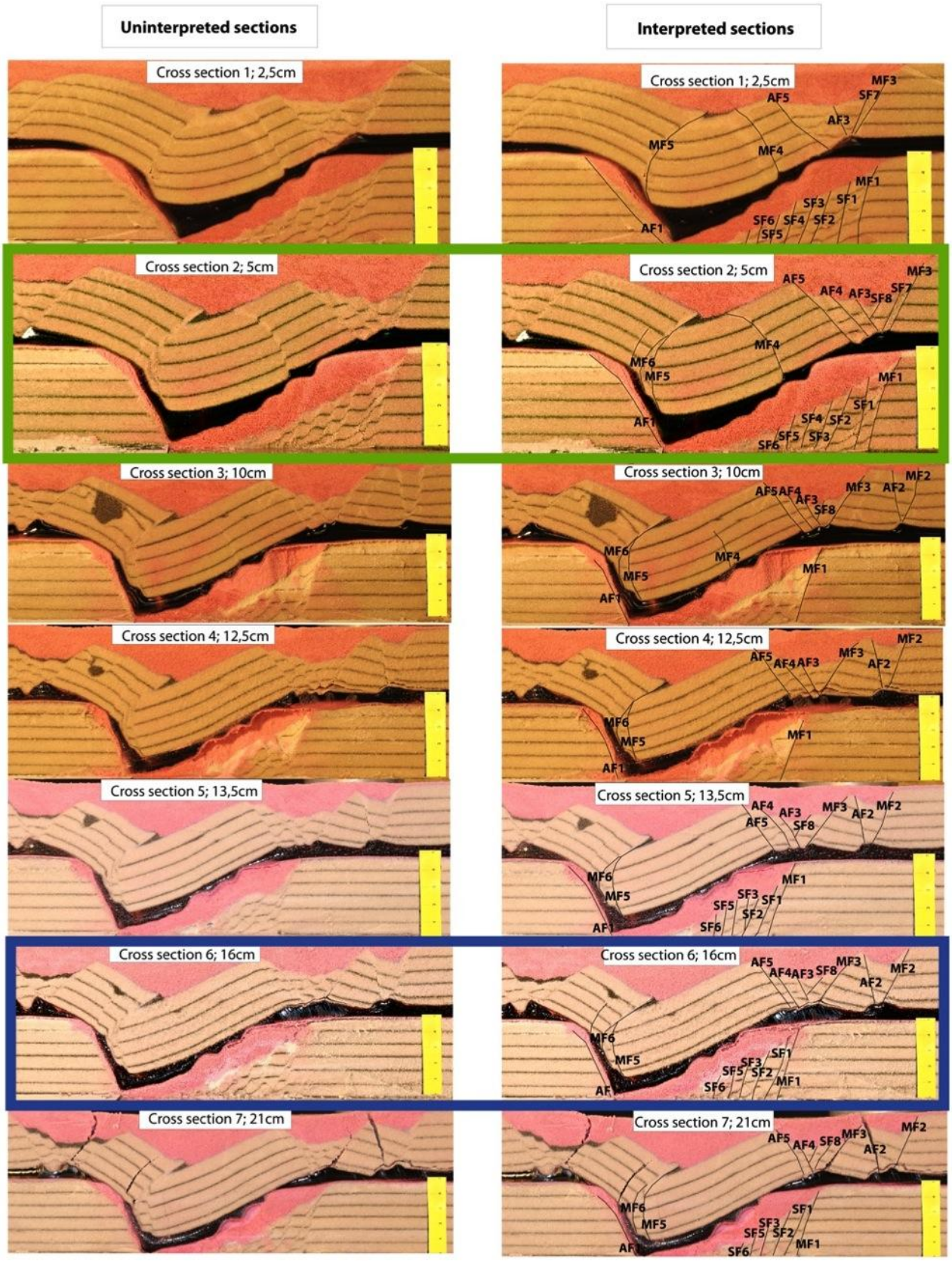

Figure 4.17: Uninterpreted (left) and interpreted (right) images of all cross sections of Experiment #3. Position of the cross sections in cm into the model is given in each image. Cross section 2 is marked by the green square, and cross section 6 is marked with the blue square.

The development of Experiments #3 was divided into two parts, related to the two phases of extension. The structural development during the first extension (Figure 4.18) was following the same pattern as the structures in Experiment #1. The antithetic faults appeared to be active from their development and throughout the rest of the extension. The synthetic faults were active in a short time before an older fault was left behind due to activation of a younger fault. The overall development of the structures was from east towards west.

The second phase of extension (Figure 4.19) was similar to the development seen in Experiment #2. The structures seemed to be active from their development and throughout the rest of the extension.

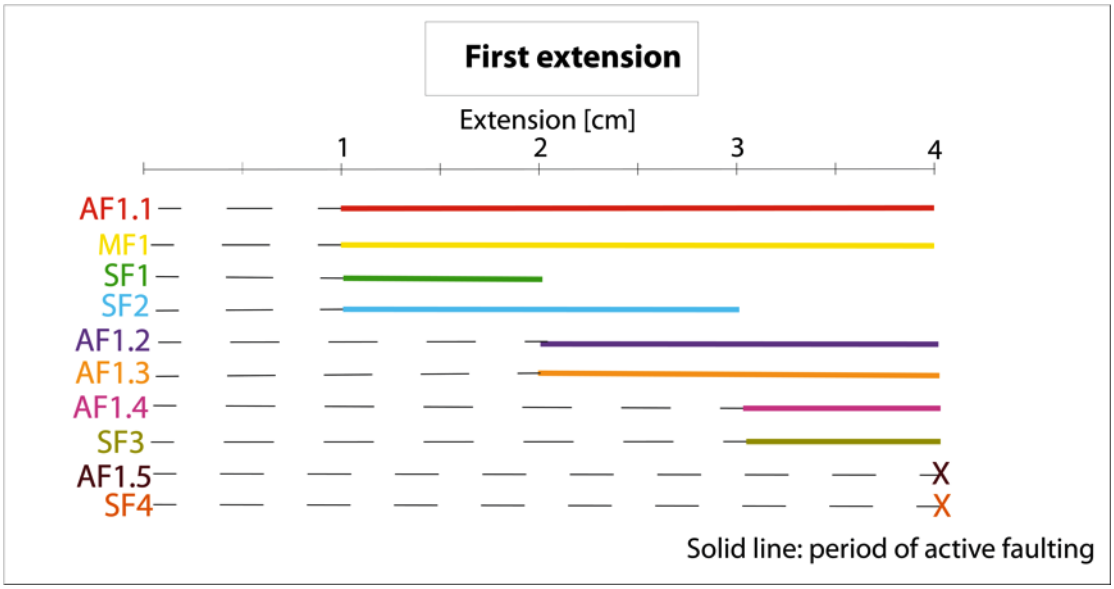

Figure 4.18: Timing of activation and development of structural features of the Deeper Graben during the first extension of Experiment #3. Total extension was 4 cm for this rifting.

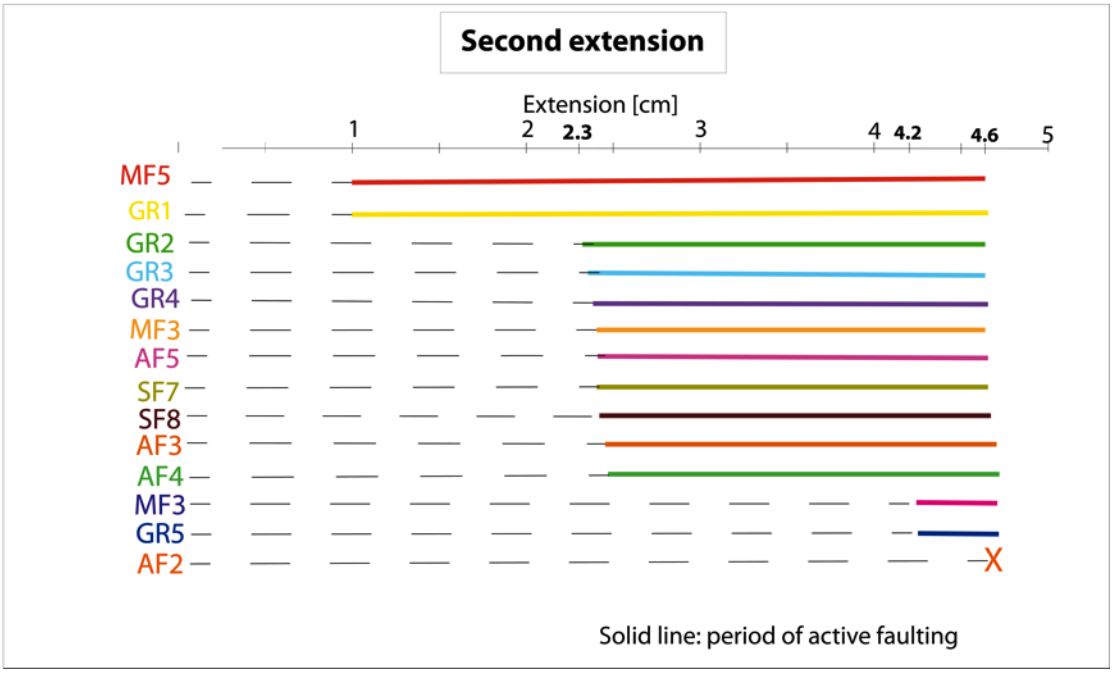

Figure 4.19: Timing of activation and development of structural features during the second extension of Experiment #3. Total extension was 4,6 cm for this rifting.

Summary and Comparison of the models

The similarities and differences between the three experiments will be emphasized in this chapter. Two general development patterns were seen in the experiments, and will first be presented with the similarities between the experiments. Afterwards the differences between the experiments inside each of these two general patterns will be presented.

Experiment #1 and the graben underneath the silicon putty in Experiment #2 and #3 had the same overall structural development but they experienced different amount of extension and the dimension of the structural features became different. The graben in Experiment #1 and the Deeper Graben in Experiment #2 and #3 seen in top view were first defined by the master fault towards east and the first antithetic fault in the west. From the first onset of the graben the development of synthetic faults on the eastern side developed towards west and left an old fault inactive when a new fault developed. Terraces were made between the synthetic faults. Antithetic faults developed from east towards west on the western side of the graben, but here all the antithetic faults made out a zone of deformation and acted together from their activation and all through the experiment.

The general structural development above the silicon putty in Experiment #2 and Experiment #3 were the same, but the structural features were different in dimensions between the two experiments. The general development of the structures in Experiment #2 and Experiment #3 seen in top view, started with the bounding faults of each individual graben. Internal uncontinous faults developed at the surface in the grabens with increasing extension. The uncontinous internal faults in the grabens became linked and developed into terraces with persistent extension.

It is natural to compare the parts of the experiments with similar development and consequently similar structural features and geometries. The graben in Experiment #1 and the Deeper Graben in Experiment #3 were extended respectively 9cm and 8,6 cm, whereas the Deeper Graben in Experiment #2 were extended only 4,7cm. The major difference between Experiment #2 and the other two experiments, were the width of the graben and the amount of developed synthetic faults and hence number of fault blocks, Table 4-5.

Table 4-5: Differences and comparison of the Deeper Graben in the three experiments.

	Experiment #1	Experiment #2	Experiment #3
Amount of extension [cm]	9	4,7	8,6
Graben width, measured at the top of the graben [cm]	17,9	8,1	14,7
Number of synthetic faults	7	4	6
Graben width/cm	1,99	1,72	1,71

Table 4-5 shows that Experiment #1 had the greatest graben width independent of total amount of extension. However, Experiment #2 and Experiment #3 show the same graben width/cm. Number of developed synthetic faults increased with increased amount of extension. Asymmetric extension was performed in the experiments and consequently a big amount of extension give a much larger eastern part of the graben in relation to the western part of the graben.

The structural development of the brittle part above the silicon putty in Experiment #2 and Experiment #3 experienced respectively 4,7cm and 4,6cm of extension. Graben 3 and Graben 1 and the relation to the Deeper Graben of the two experiments will be compared here. Graben 3 of the two experiments had the same width but the distance from the eastern limit of Graben 3 and eastern limit of Graben 1 was 4 cm longer in Experiment #3. Graben 3 developed at the same place in both experiments, 16 cm into the model from the east. The eastern bounding fault of Graben 1 in Experiment #2 developed at 20 cm into the model, whereas Graben 1 in Experiment #3 developed at 24 cm in to the model from the east. MF1 in Experiment #2 was located under the horst between Graben 1 and Graben 3. MF1 in Experiment #3 was located more directly under Graben 3.

MF4 did not develop in all the cross sections in Experiment #3, however the comparable MF3 in Experiment #2 was present in all the cross sections in Experiment #2.

Graben 5 in Experiment #3 was not present in Experiment #2.

Chapter 5; Discussion

The observed structural features in the seismic interpretation will in this chapter be discussed in relation to some main topics. The four topics are (1) whether or not detachments exist in the Ringvassøy- Loppa Fault Complex, (2) a comparison between the structures observed in the seismic data and the structural features obtained in the analogue experiments, with a particular focus on the role of detachments in the development of the Ringvassøy- Loppa Fault Complex, (3) timing of faulting and (4) regional implications in relation to literature of the area. The topics will be presented in this order to deal with the conceptual topics first and correlate them to the regional topics further on.

5.1. Detachments

Previous work has been done regarding multiple detachments both in the Barents Sea (Gabrielsen, 1984; Fitriyanto, 2011) and other places such as Sudanese rift basin (Craig Mann, 1989), from the Niger delta (Maloney et al., 2011) and the North Sea (Fossen et al. 2000). It was proposed by Gabrielsen (1984) that Ringvassøy- Loppa Fault Complex had three possible detachment zones. Only Base Cretaceous and Base Palaeocene were marked in the figure presented there, but to relate the detachment zones to this study the names of the key reflections of this study have been correlated in the modified illustration in Figure 5.1. One upper detachment zone was proposed between the Top Kolmule Formation reflection and Top Kolje Formation reflection, and one intermediate detachment zone was proposed between Top Kolje Formation reflection and Base Cretaceous reflection. The faults affecting Base Cretaceous reflection were suggested to connect to a deeper detachment zone, but this zone was not mapped out in that study. The detachment zones could not be distinguished in the seismic section, but they were inferred from the fault plane geometry (Gabrielsen, 1984).

A detachment zone was interpreted in the southern part of Bjørnøyrenna Fault Complex (Gabrielsen et al., 1997). Listric faults are making out rotated fault blocks above a northwesterly dipping detachment. The deepest reflection

affected by the listric faults is the presumed base Ladinian, Mid Triassic (Gabrielsen et al., 1997). Steep planar faults are interpreted underneath the detachment zone and are part of a horst and graben topography underneath the lowermost extensional detachment in the area (Grunnaleite et al., 1991 as cited in Gabrielsen et al., 1997; Faleide et al., 1993a).

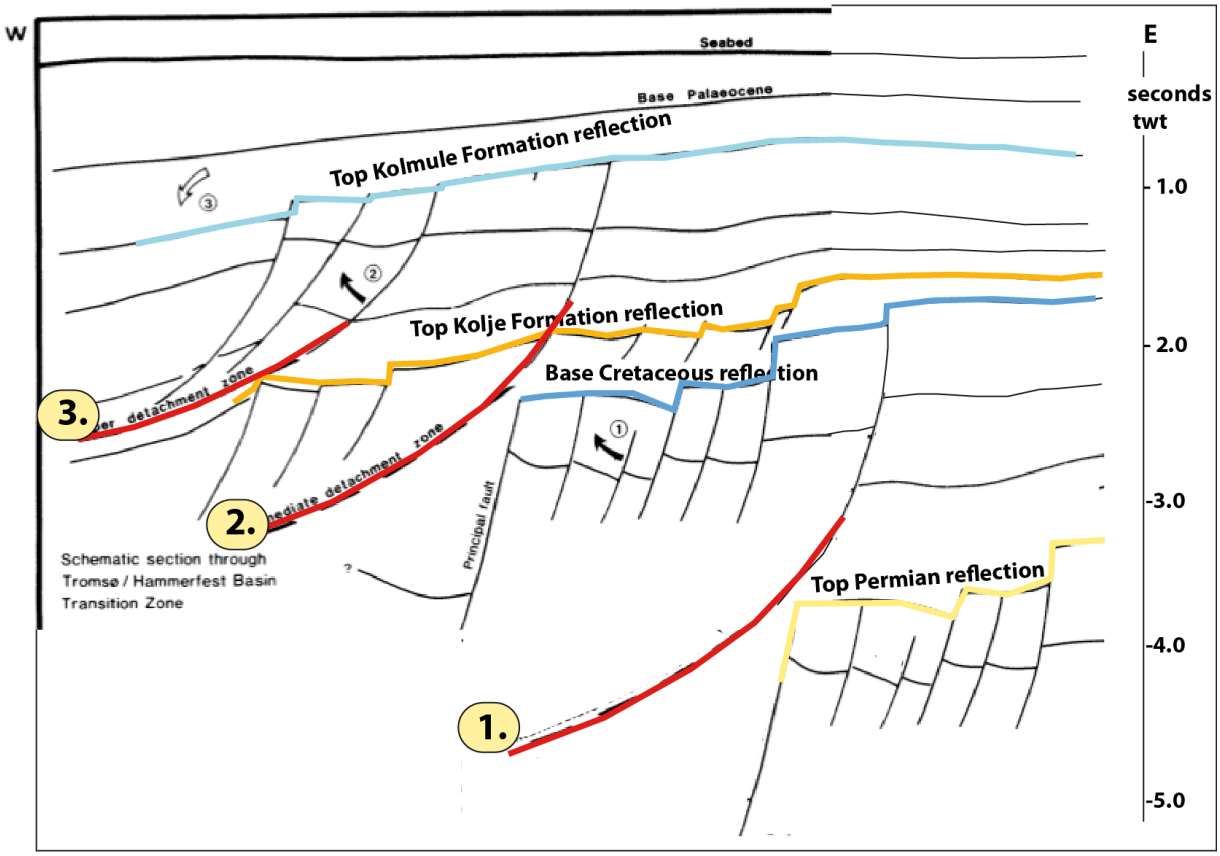

Figure 5.1: Illustration of the three possible detachments (red lines) in the study area and their positioning in relation to the interpreted key profiles (Modified from Gabrielsen, 1984).

This chapter will discuss whether these possible detachments are present or not in the study area. This will be discussed by emphasizing the differences in geometries and structures above and below a possible detachment zone. The typical characteristics to be compared are (1) the fault plane geometry and it´s continuity in depth, (2) the number of faults and the amount of faults with down-to-west displacement in relation to the amount of faults with down-to-east displacement, (3) rotation of the reflections in a fault block and (4) signs of reactivation. The deepest detachment zone (no.1) will be discussed first, then the

intermediate detachment zone (no.2), and finally the upper detachment zone (no.3).

The fault plane of shallow detachment faults can be detected as a low angle reflection cutting near horizontal reflections if they are present. However, the position of the reflection is often more as an approximation than exact location, because it might not be correctly migrated.

Possible Detachment 1

Two contrasting models can present the linkage between the structural geometry of the Late Permian level of faulting and the Mid Jurassic- Early Cretaceous level of faulting. Model 1 (Figure 5.2), is arguing for a thick-skinned detachment, whereas Model2 (Figure 5.2) is arguing for a thin-skinned detachment zone separating the two levels of faulting.

Model 1 shows no thin-skinned detachment zone and the interpreted faults in the Late Permian level of faulting are linked to the interpreted faults in the Mid Jurassic- Early Cretaceous level of faulting. The fault geometry of the linked fault b5-a4 appears to have listric geometry and the Intra Permian reflection shows larger rotation than the Top Stø Formation reflection does. The linked fault between a2 and b1 has near planar geometry, and this fault show an increase in throw with increasing depth, which indicate that the same fault was reactivated several times. If there were a thin-skinned detachment we would expect to see greater rotation of the reflection of Mid Jurassic- Early Cretaceous age. The fault a1 in Key profile 2 and 3 are interpreted to cut all key reflections, and clearly show that reactivation occurred along that fault, (Figure 3.13, Figure 3.14).

Model 2 shows one deep detachment zone approximately in the sequence between Top Permian reflection and the Intra Permian reflection. The number of faults and their listric geometries in the Mid Jurassic- Early Cretaceous level of faulting is an important argument for this Model 2. The fault plane of a normal fault with listric geometry is shallowing with increasing depth, and many listric fault planes will merge together with depth and form a detachment level (Maloney et al., 2011). To get the number of faults in the Mid Jurassic- Early Cretaceous level of faulting to match the number of faults in the Late Permian level of faulting, the deep faults must be splaying into several faults during the

reactivation of the fault in the Mid Jurassic. If this is the case we would expect the throw in the Permian reflections to be larger than the sum of the throws of at least two of the faults in the Mid Jurassic- Early Cretaceous level of faulting, which is not the case. Thus the different number of faults between the two levels of faulting cannot be corrected for by arguing for a splay fault. MF10 and b8 have a down-to-east displacement, whereas all the faults in the Late Permian level of faulting have a down-to-west displacement. The overall geometry differences with the three sub-areas in the Mid Jurassic- Early Cretaceous level of faulting in contrast to the geometry of the Late Permian level of faulting is implying that a detachment zone is present. The reflections of the hanging wall block of a2 is dipping towards southwest, whereas the reflections in the fault blocks above in the Mid Jurassic- Early Cretaceous level of faulting have an north-easterly dip, which seem unlikely if there is no detachment present in between.

In case of reactivation of the deeper faults an increase in throw with increasing depth is expected. Not all the deeper faults indicate this, as the Intra Permian reflection across a3 has a smaller throw than any of the reflections across the fault blocks of the Mid Jurassic- Early Cretaceous level of faulting.

A final conclusion whether Possible Detachment 1 is present or not cannot be made based on the observations done in this study. Both Model 1 and Model 2 have strong evidence against the opposing model, and cannot be neglected. Thus, the Possible Detachment 1 is not concluded on.

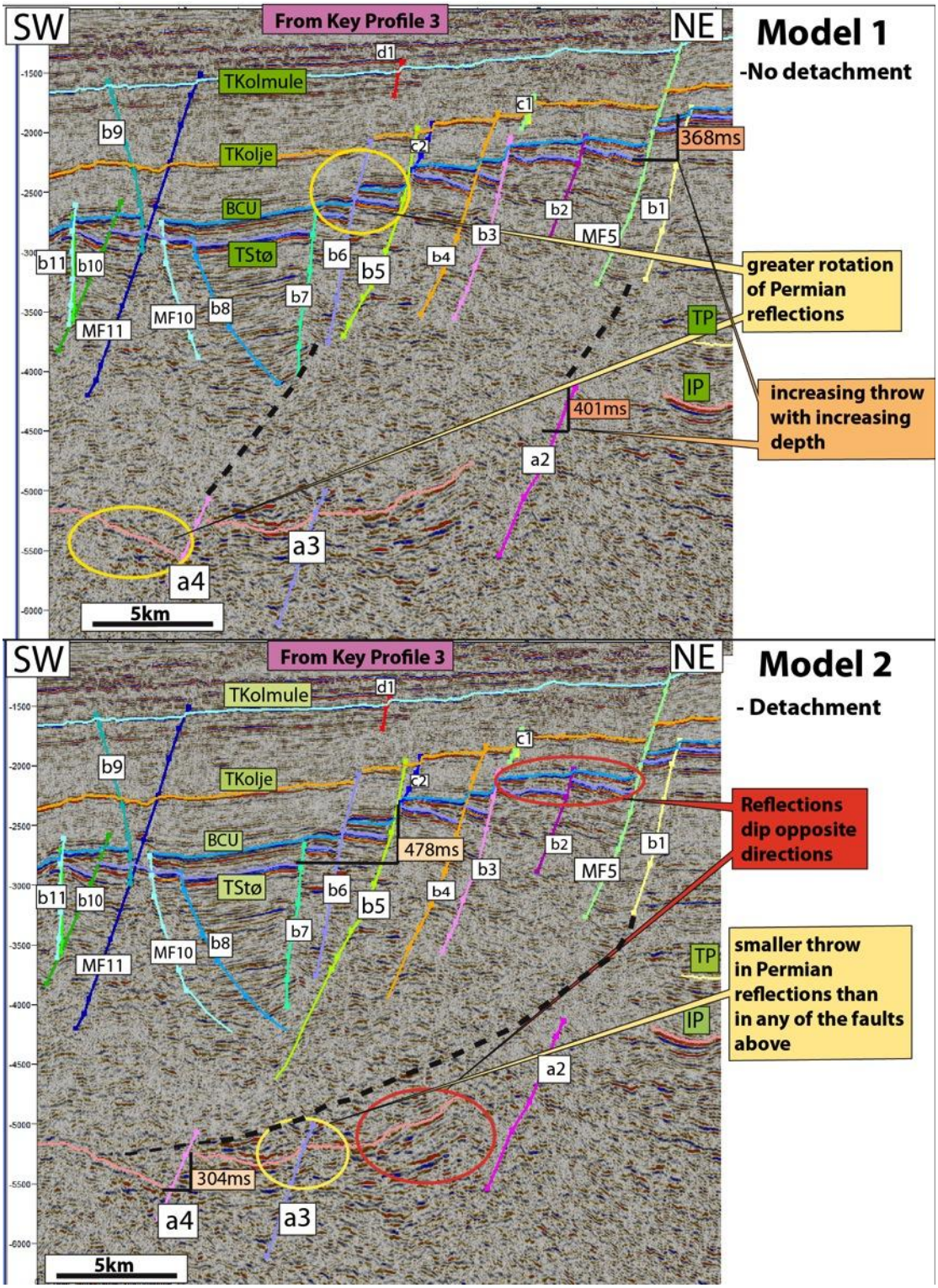

Figure 5.2: Focused area from Key Profile 3, red dashed square in Figure 3.14. Model 1 (top) illustrating the link between the Late Permian level of faulting and the Mid Jurassic- Early Cretaceous level of faulting without a detachment zone in between. Model 2 (bottom) illustrating the link between the Late Permian level of faulting and the Mid Jurassic- Early Cretaceous level of faulting with the presence of a detachment zone.

Possible Detachment 2

The Possible Detachment 2 can be seen in Figure 5.3. Two listric faults are cutting down from the Top Kolmule Formation reflection through the Top Kolje Formation reflection in Key profile 3. The fault geometries of the two faults are listric and the reflections in the fault block between c3 and c4 show rotation of 9° relative to the reflections in the footwall block. Top Stø Formation reflection and Base Cretaceous reflection in Key Profile 4, are clearly faulted in sub-area C. The Top Kolje Formation reflection appear to be undisturbed by these faults, which indicate that the Top Kolje Formation reflection is detached from the Mid Jurassic- Early Cretaceous level of faulting in sub-area C. However, farther east on the platform it is clear that the faults of the Mid Jurassic- Early Cretaceous level of faulting is reactivated and cut the Top Kolje Formation reflection. The Knurr Formation would be the location of the Possible Detachment 2. The lithology of the Knurr Formation contains dark grey to greyish brown claystone with thin limestone and dolomite interbeds (FactPage NPD, www.npd.no), which could be typical lithology for a thin-skinned detachment (Maloney et al., 2011).

Based on the observations discussed above, the Possible Detachment 2 appears to be real. However, the detachment is only present in the area far west on the platform of the fault complex, above sub-area C. The faults affecting the Base Cretaceous reflection is clearly reactivated and affect Top Kolje Formation reflection farther east on the platform.

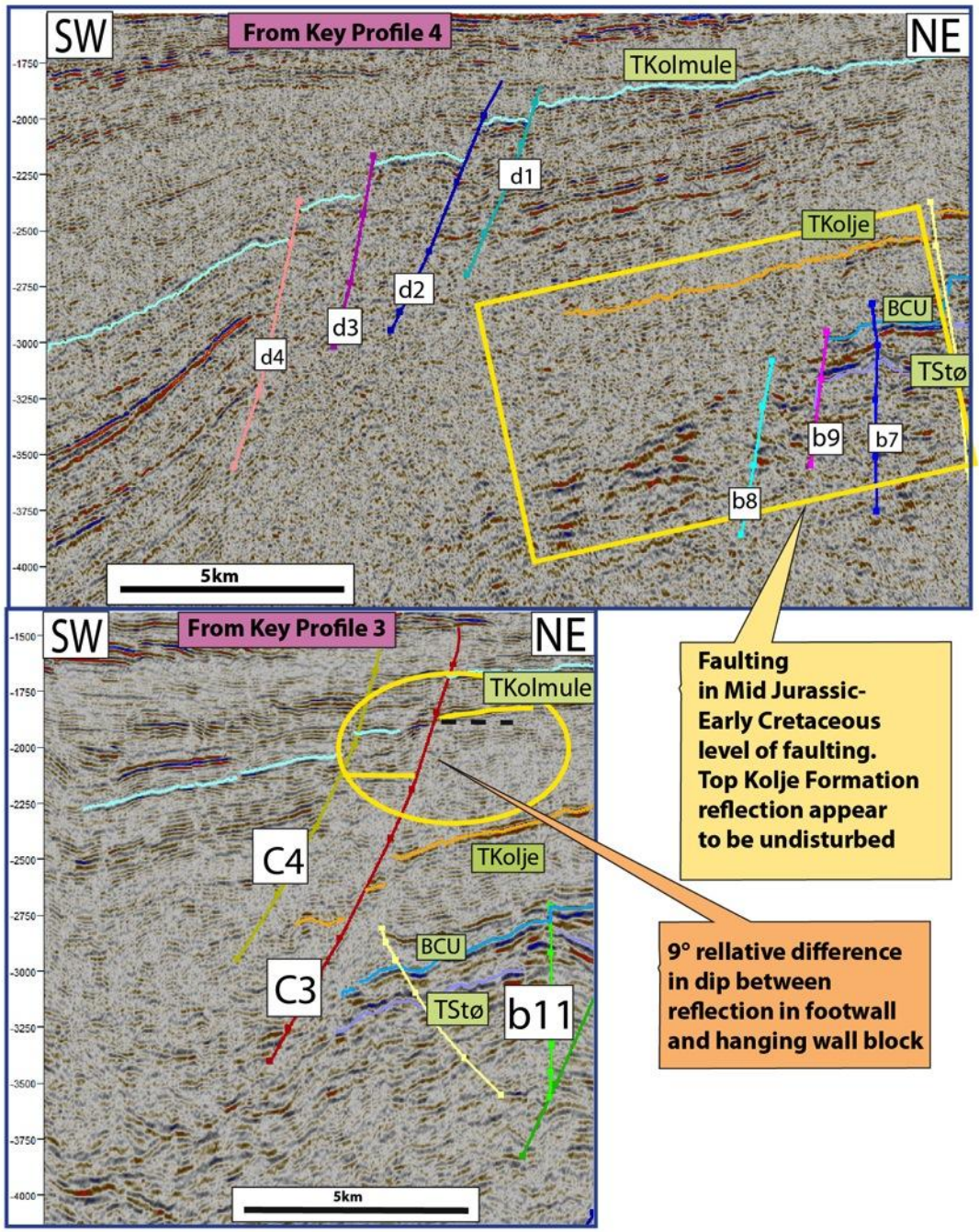

Figure 5.3: Top: focused area marked by red dashed square in Key Profile 4 (Figure 3.15). Faults affecting Base Cretaceous do not affect Top Kolje Formation reflection. Bottom: focused area marked by yellow full square in Key Profile 3 (Figure 3.14). Faults with listric geometry detached from the faults affecting Base Cretaceous reflection.

Possible Detachment 3

Key profile 1 has a low angle reflection interpreted to be the reflection of a fault plane, Figure 5.4. This reflection is located above the Top Kolje Formation reflection and indicates the Possible Detachment 3. The western boundary fault of the fault complex at Mid Jurassic- Early Cretaceous level of faulting is located approximately vertically underneath d1 and d2 (Figure 3.15). This implies that the faults in the Early Tertiary level of faulting have developed independently from the Mid Jurassic-Early Cretaceous level of faulting, and the presence of a detachment in between are likely.

The observation of the reflection of the fault plane, F1, is a strong implication that the Possible Detachment 3 must be real, and a conclusion that the faults affecting the Top Kolmule Formation reflection are detached from the faults affecting Top Kolje Formation reflection can be done.

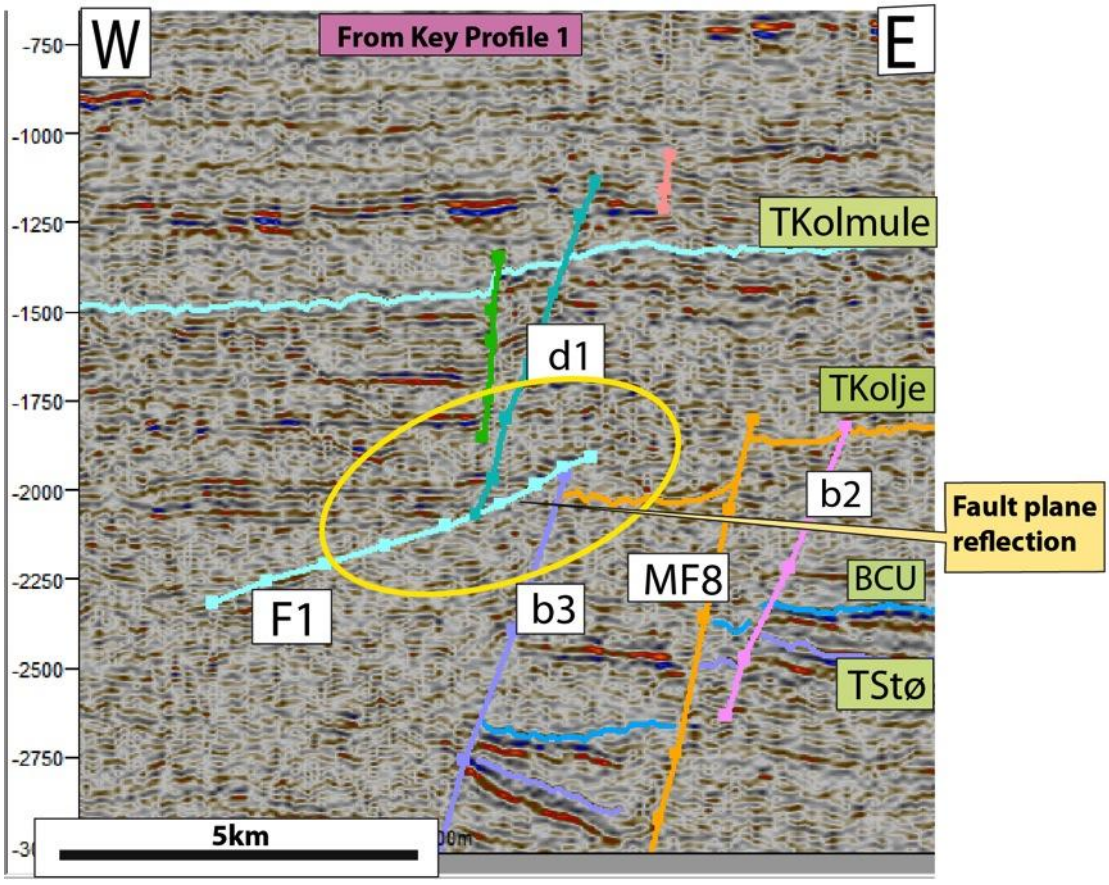

Figure 5.4: Focused area marked by red full square in Key Profile 1,Figure 3.12. Low angle fault plane reflection, F1, indicate Possible Detachment 3.

5.2. Analogue models

The Experiments presented in subchapter 4.3 is part of a bigger project about the influence of detachment zones in extensional regimes. The Experiments of this study allow for a general observation of the development of structures above and below the detachment zone.

A comparison between the structures observed in the seismic data and the structural features obtained in the analogue experiments will be done in this chapter with a particular focus on the role of detachments in the development of the Ringvassøy- Loppa Fault Complex. The general structural pattern will first be presented followed by examples from the analogue models and the Key Profiles.

The overall structural pattern seen in Experiment #2 and #3 is two independent sets of fault blocks separated by a detachment zone (Figure 4.9 and Figure 4.15). A conceptual figure of this general structural geometry is presented in Figure 5.5a. Figure 5.5b shows an example from Experiment #3 of cross section 2 where the two vertically independent sets of fault blocks have developed. An example from the Possible Detachment 3, taken from Key Profile 4 illustrates the same structural independency between vertically separated fault block developments (Figure 5.5c).

By recognising the same structural pattern in the 2D seismic lines as in the analogue models, the presence of detachment zones are possible. However, due to a much more complicated tectonic history in Ringvassøy- Loppa Fault Complex than in the analogue models, farther investigation of the influence of detachments needs to be done.

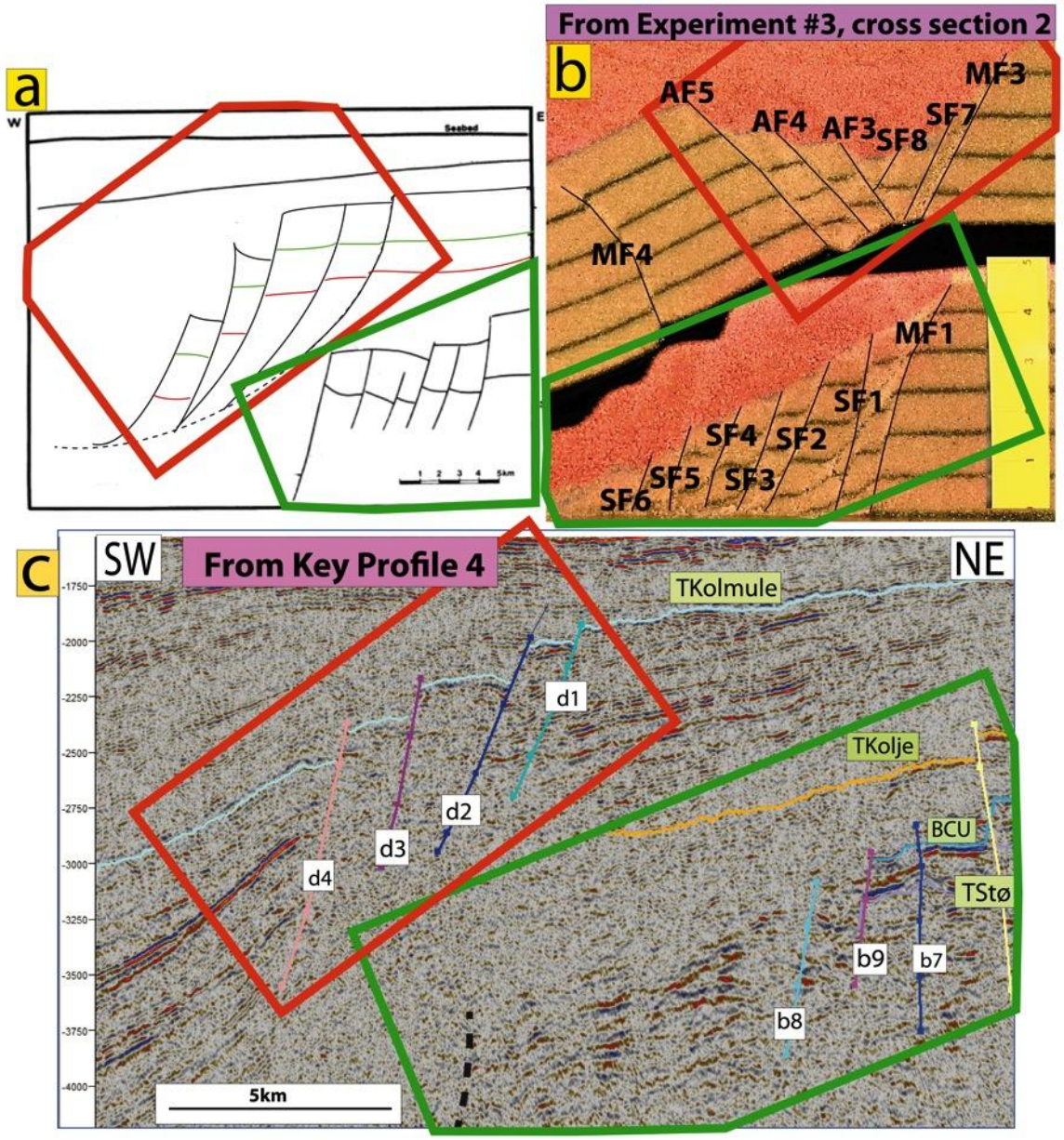

Figure 5.5: a) Illustration of the general structural geometry when a detachment is present (Modified from Gabrielsen, 1984) .b) example from Experiment #3 of cross section 2 where the two independent fault developments are present. c) Focused area marked by red dashed square in Key Profile 4, Figure 3.15. Illustration shows the same structural independency between vertically separated fault block developments in the seismic section. Green squares and red squares are marking comparable areas in the three different examples.

5.3. Timing of faulting

Five phases of extensional tectonics are described for the South Western Barents Sea (Gabrielsen et al.; 1990; Faleide et al., 1993a; Gudlaugsson et al., 1998), namely during the Carboniferous, the Late Permian, the Late Jurassic- earliest Cretaceous, the Early Cretaceous and the Early Tertiary. The identification of wedge-shaped sequences, drag folds, thinning towards the fault in the footwall block, and thickening towards the fault in the hanging wall block, are indications of growth faults and active extensional tectonics. Growth faults are characterized by an abrupt thickening of the sequence between two reflections across the fault, and indicate that the fault was active during the sedimentation of the sequence (Edwards, 1976).

The Carboniferous

The Carboniferous structural phase cannot be unequivocally confirmed in the present study area since no wells are penetrating to that depth and sedimentary sequences/ structures of this age are deeply buried and not well imaged by most of the seismic data. However, a wedge-shaped sedimentary sequence is seen underneath the intra Permian reflection in Key Profile 2 (Figure 5.6). The exact age of the sequence cannot be determined with certainty but it must be older than Intra Permian and accordingly there must have been a period of active faulting before the Late Permian. The literature says that an extensional event of regional importance happened in Carboniferous time (e.g. Gudlaugsson et al., 1998), and it is natural to expect that this Carboniferous event caused the wedge-shaped sequence under the Intra Permian reflection.

The Late Permian

The Late Permian structural event is identified by the Permian sequence between the Top Permian reflection and the Intra Permian reflection in Key Profile 2. Thickening of the sequence across the fault a1 is 176ms twt, and clearly indicate that a1 is a growth fault (Figure 5.6). The Top Permian reflection is seen as a clear unconformity in the hanging wall block, with the underlying reflections toplapping onto it. The reflections above Top Permian reflection have eastern dips around 3°, whereas the reflections below Top Permian reflection have eastern dips around 16°. The sequence between Top Permian reflection and Intra Permian reflection is thinning towards a1 in the footwall block. This is an

indication that the original fault scarp has been eroded, which indicate that the sedimentation rate could not keep pace with the fault displacement (Craig Mann, 1989). Normal drag is identified in the Top Permian reflection along a1 in the hanging wall block. The throw across a1 is larger for the Permian reflections than for the Triassic reflections that indicate active periods of faulting before Triassic times (Figure 5.12).

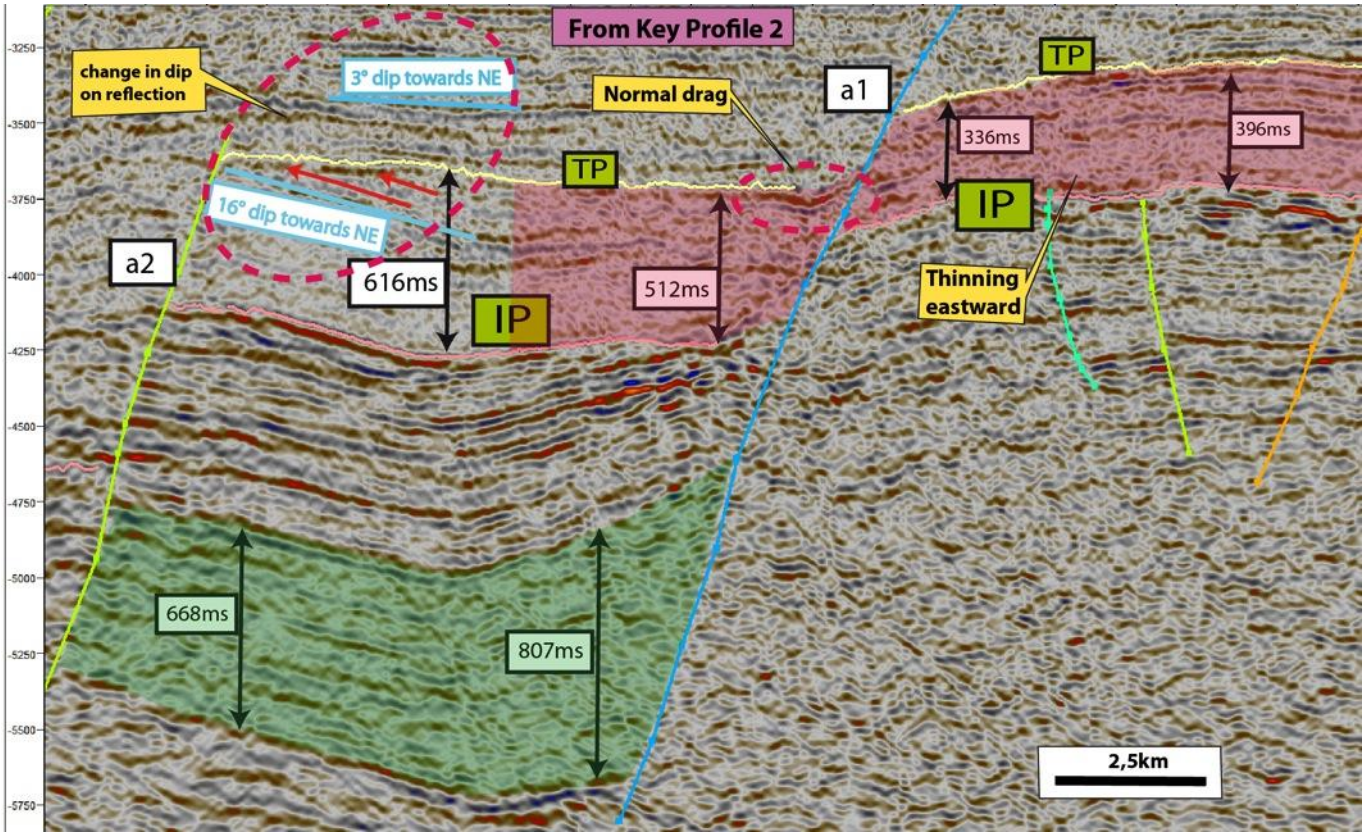

Figure 5.6: Focused area marked by blue dashed square in Key Profile 2, Figure 3.13. Identified active periods of faulting are marked by green area (Carboniferous?), and red area (Late Permian).

The Late Permian extensional event is in correlation with the literature (e.g. Dengo & Røssland, 1992; Gudlaugsson et al., 1998). It is already described in chapter 2 that the Selis Ridge was a narrow N- S trending ridge in Late Permian until Early to Mid Triassic time (Glørstad- Clark et al, 2011). Figure 5.7 shows the position of the Selis Ridge in relation to the tectonic structural elements of the Western Barents Sea. The Asterias Fault Complex was not an important hinge line until Mid Jurassic (Gabrielsen et al., 1990). The salt in the Tromsø Basin (Faleide et al., 1993a) and the salt in the Nordkapp Basin (Gabrielsen et al., 1990) have been dated to Late Carboniferous. These evaporites are not present

in the Hammerfest Basin positioned in between the two basins. This observation indicates that parts of the area in between these two salt basins were a structural high at the deposition time of the salt. Thus, the Selis Ridge of Late Permian age might have been a positive structural high farther south into the Hammerfest Basin.

Figure 5.7 indicates the suggested prolonged Selis Ridge southward. The a1 fault is located in this zone and could have been one of the western bounding faults of a Late Permian positive structural feature in the west of the Hammerfest Basin.

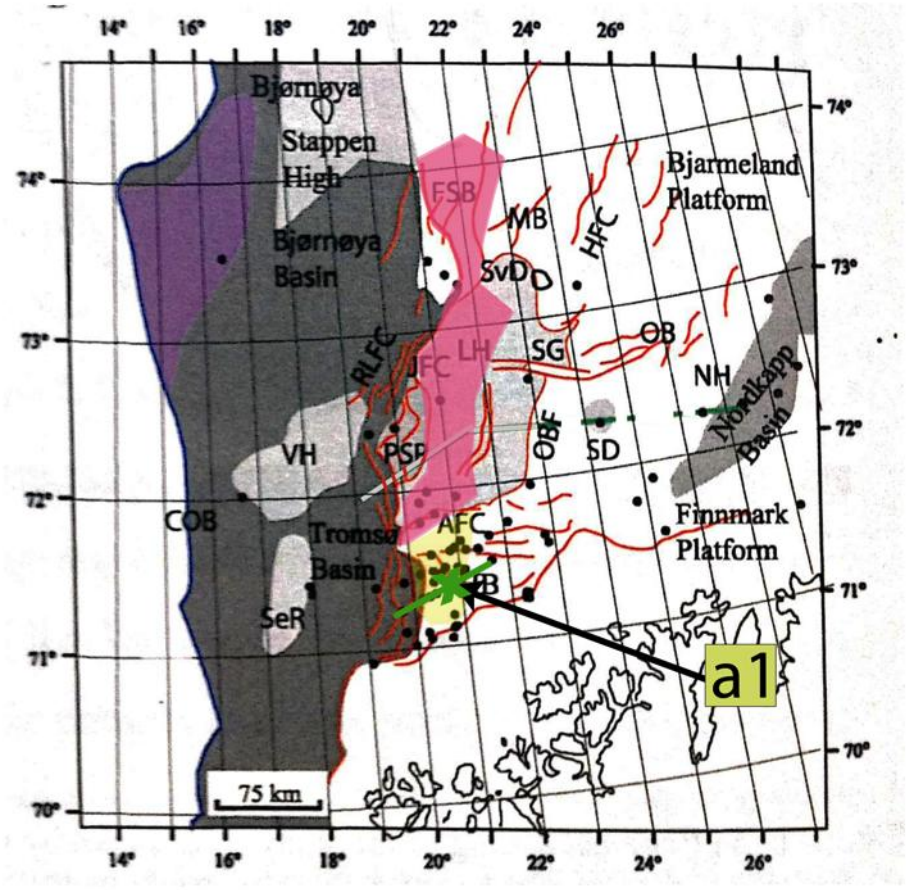

Figure 5.7: Location of the Selis Ridge (pink filled area) in relation to the structural elements of the Barents Sea. Yellow filled area show the proposed extension of the Selis Ridge southward into the Hammerfest Basin. Green line show the position of Key Profile 2 (Figure 3.13), and green x show the location of the a1 fault.

The Late Jurassic- earliest Cretaceous

The extension in the Late Jurassic- earliest Cretaceous is the most evident tectonic event in the study area. The Top Stø Formation reflection is parallel with the reflections below and the onset of the faulting must have happened after the deposition of that formation. The sequence between The Base Cretaceous reflection and Top Stø Formation reflection is seen as a wedge-shaped sequence in many of the fault blocks (Figure 5.8). The sequence also show abrupt thickening from 86ms twt to 181ms twt across fault b7, which indicates a growth fault. The Base Cretaceous reflection has normal drag towards the faults in many of the hanging wall blocks, e.g in the hanging wall block of b5. The faults cutting up through the Top Kolje Formation reflections have larger throws at the Top Stø Formation reflection and Base Cretaceous reflection than in the Top Kolje Formation reflection, which also indicate that the fault was active previous to the faulting of Top Kolje Formation reflection.

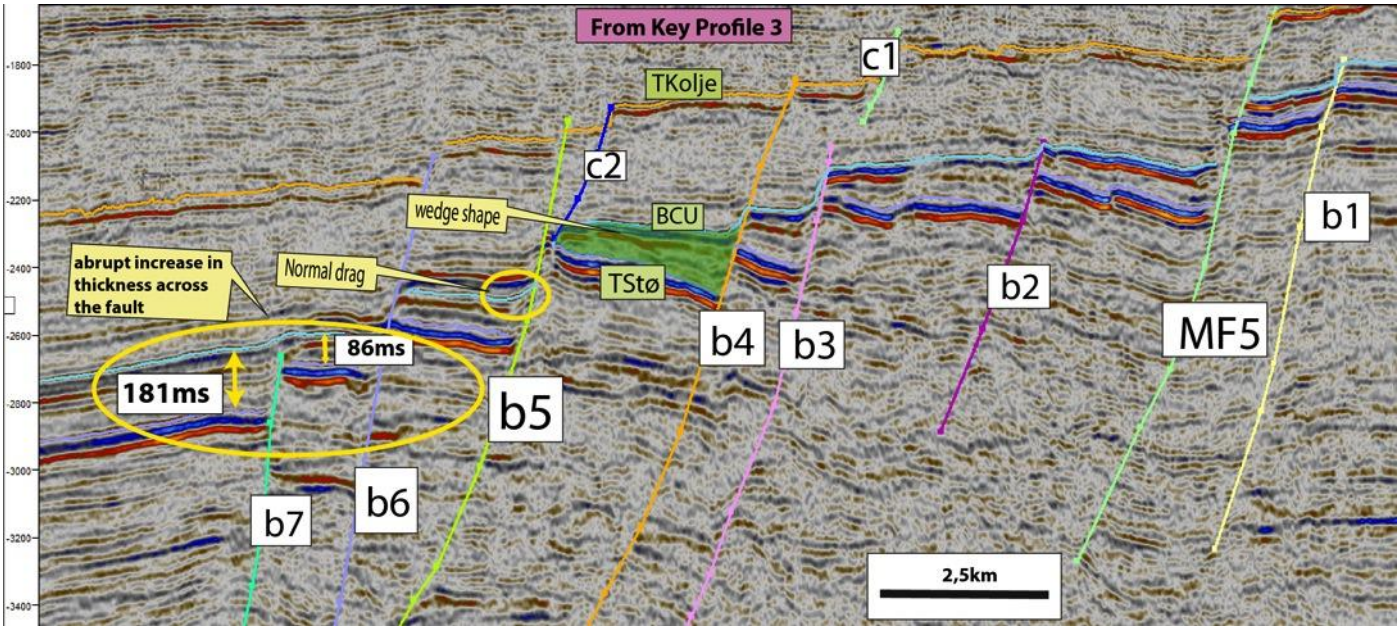

Figure 5.8: Focused area marked by yellow dashed square in Key Profile 3, Figure 3.14. Active faulting of Mid Jurassic- earliest Cretaceous is supported by wedge-shape sequences (green area), normal drag (small yellow circle), and abrupt increase in thickness across the fault (big yellow circle)

The Early Cretaceous

In Figure 5.9 the Top Kolje Formation reflection has small throws across the eastern faults (e.g. 34ms twt across MF4). More into the platform farther SW, the throws become greater up to 191ms twt across MF7. The development of bigger

throws farther out on the platform shows that the Hammerfest Basin was gradually abandoned in the Cretaceous. The evidence of an Early Cretaceous period of active faulting is seen in the relative throw between reflections of different age. The b4 fault is affecting the reflections from Top Stø Formation reflection up to Top Kolmule Formation reflection and show that the throw increases with depth. Thus, the Top Kolje Formation reflection has a smaller throw than the deeper reflections but a larger throw than the Top Kolmule Formation reflection above. This indicates that the fault must have been active after Base Cretaceous and before Late Cretaceous (Top Kolmule Formation reflection). The sequence between The Top Kolje Formation reflection and Base Cretaceous reflection has a wedge-shape in the fault block between b2 and b3, and a normal drag in the Top Kolje Formation reflection is seen towards b3. This sequence is also showing an abrupt increase in thickness of 256ms twt across b5. These observations indicate the presence of growth faults and hence a period of active faulting in Early Cretaceous.

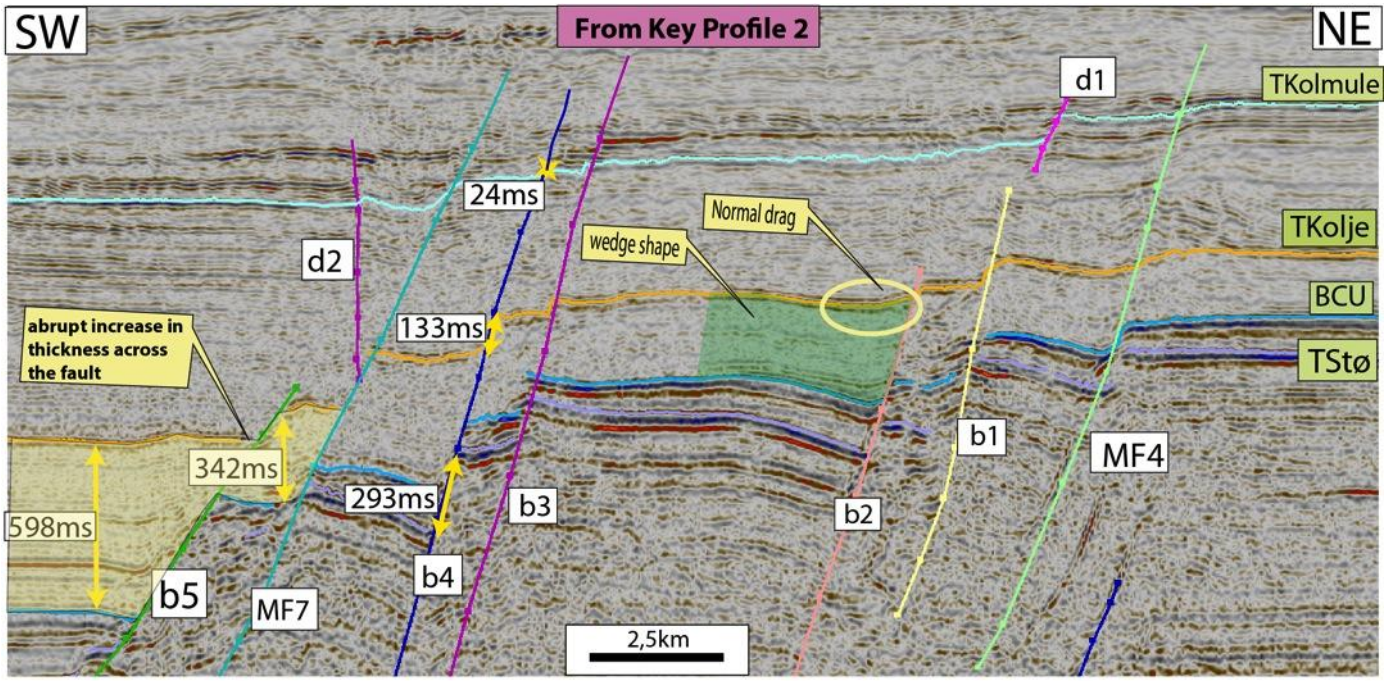

Figure 5.9: Focused area marked by purple dashed square in Key Profile 2, Figure 3.13. Active faulting in Early Cretaceous is supported by wedge-shaped sequences (green area), normal drag (yellow circle), and abrupt increase in thickness across faults (yellow area)

The Early Tertiary

The Top Kolmule reflection is of Late Cretaceous age (Figure 2.4). This key reflection is not affected by many faults until far out on the platform as seen in Figure 3.15. Faults d1, d2, d3 and d4 are most likely detached from the underlying levels of faulting as argue for in chapter 5.1. The presence of the detachment supports that there must have been a period of active faulting later than Early Cretaceous. Growth fault appear to affect the Top Kolmule Formation reflection, and is seen as an abrupt increase in thickness of the sequence above Top Kolmule Formation reflection across a1 (Figure 5.10). This growth fault is only identified in the Late Cretaceous sequences, but a1 is clearly cutting through the whole Tertiary sequence (Figure 5.12), and it is likely that the growth fault was active into the Early Tertiary, but cannot be seen due to lack of amplitudes of those representing reflections. This tectonic event can be correlated to the final break up of the Norwegian Greenland Sea that happened in the Early Tertiary (e.g. Faleide et al., 1984; Faleide et al. 1993a).

The throw across a1 is less for the Top Kolmule Formation reflection than for the Top Kolje Formation reflection, which indicate that the fault was reactivated after the Early Cretaceous tectonic event.

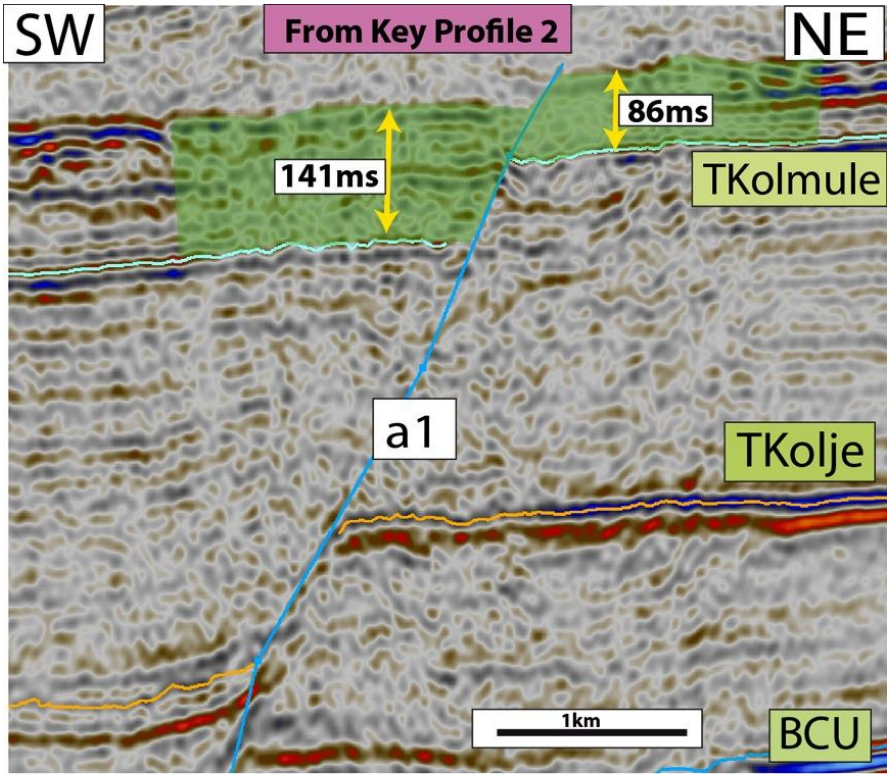

Figure 5.10: Focused area marked by yellow dashed square in Key Profile 2, Figure 3.13. Active faulting in Late Cretaceous is supported by abrupt increase in thickness across the fault (green area)

A Compressional event

Two compressional events are suggested to have affected Bjørnøyrenna Fault Complex. The first suggested event was in Hauterivian- Aptian (left- lateral (?) transtension), and the second in Late Cretaceous- Early Tertiary (head on inversion), These compressional events were suggested to be of regional significance (Gabrielsen et al., 1997).

Structures indicating a possible inversion event are seen in an area in the continuation towards SW of Key Profile 2 (Figure 5.11). A fold is seen towards the hanging wall block of b7. This contractional structure cannot be distinguished in any of the other 2D seismic lines, and a conclusion whether it is caused by a strike-slip event or a head on contraction cannot be made. The fold axis of the compressional structure has to be mapped and related to the trending strike of the fault complex to establish the tectonic event that caused the compression. If the fold axis is parallel to the strike of the fault complex a head on contraction is likely, whereas if the fold axis is located with an angle to the strike of the fault complex, a strike-slip event is likely (Woodcock et al., 1994). Top Kolmule Formation reflection and Top Kolje Formation reflection are affected by the compressional event, however the Tertiary reflections appear to be unaffected. If the Late Cretaceous- Early Tertiary compressional event had caused the structure we would expect the Tertiary reflections to be affected as well. If the Hauterivian- Aptian compressional event caused the structure the Top Kolmule Formation reflection would be unaffected. By these observations the contractional structures appear to be caused by a local compressional event independent of the two compressional events in Bjørnøyrenna Fault Complex. The exact timing of the compressional event has not been made, but since both Top Kolje Formation reflection and Top Kolmule Formation reflection is affected, the compressional event must have occurred in Cretaceous. The compressional event is not affecting farther into the platform and cannot be distinguished in any of the other 2D seismic lines. The compressional structure might be caused by an oblique component in an extensional phase, which would then have worked as a transtensional system (Woodcock et al., 1994).

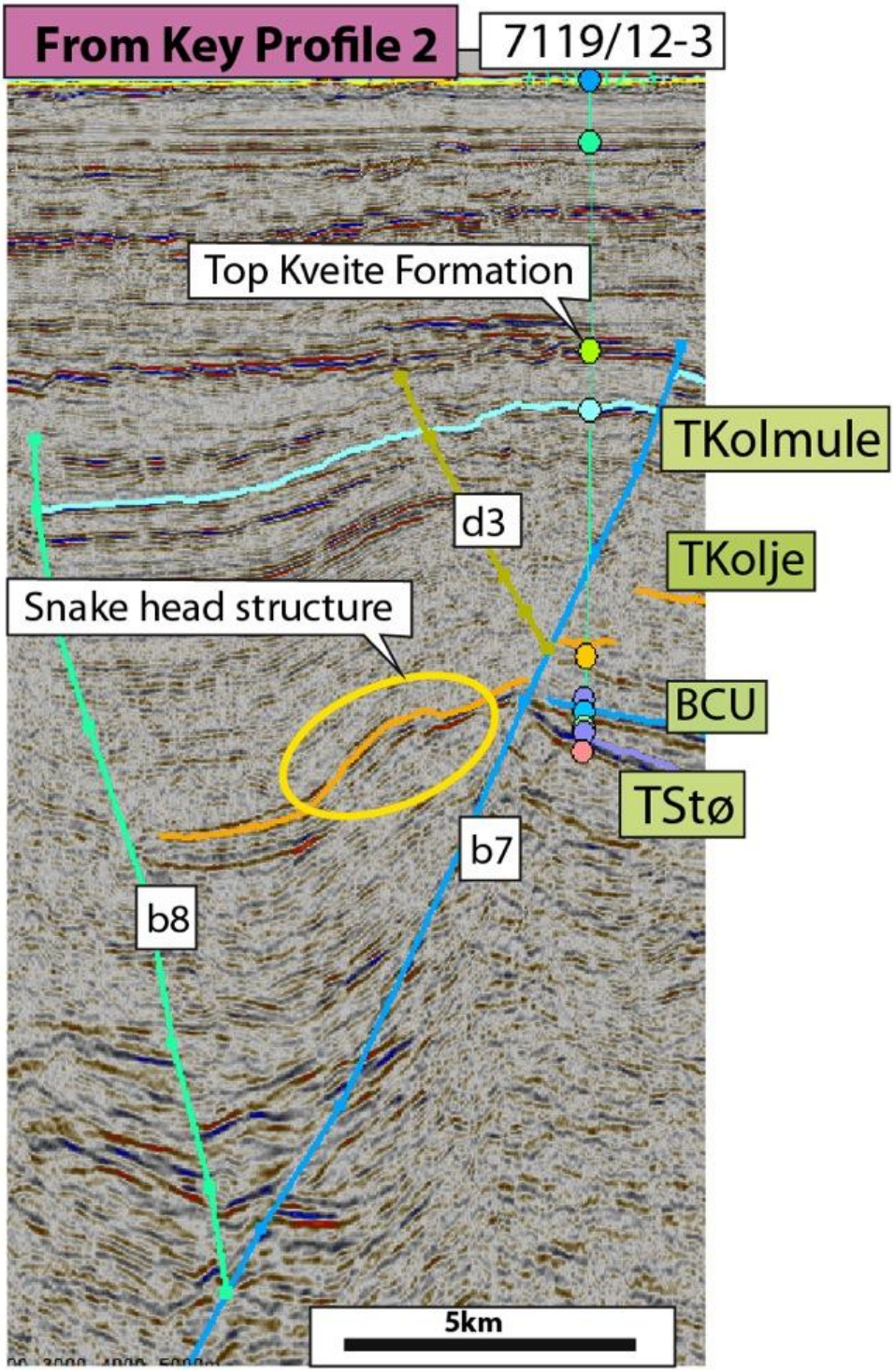

Figure 5.11: Focused area marked by yellow full square in Key Profile 2, Figure 3.13. Compressional event supported by a fold (yellow circle). Top Kveite Formation reflection correlated to Base Tertiary, appear to be unaffected.

Summary of active faulting

Five phases of active extensional faulting have been identified in the study area and they are in correlation with the tectonic extensional phases described in the literature (Faleide et al., 1984; Dóre et al., 1991; Dengo & Røssland, 1992; Faleide

et al., 1993a; Gudlaugsson et al., 1998). The five phases were in Carboniferous?, Mid Jurassic- earliest Cretaceous, Early Cretaceous and Early Tertiary (growth faults in Late Cretaceous). All the phases can be identified in Key Profile 2 along a1, which apparently have been reactivated several times (Figure 5.12). Each phase is represented by wedge-shaped sequences in the hanging wall block or an increase in thickness of the sequence across the fault. The throw across the fault is increasing with increasing depth.

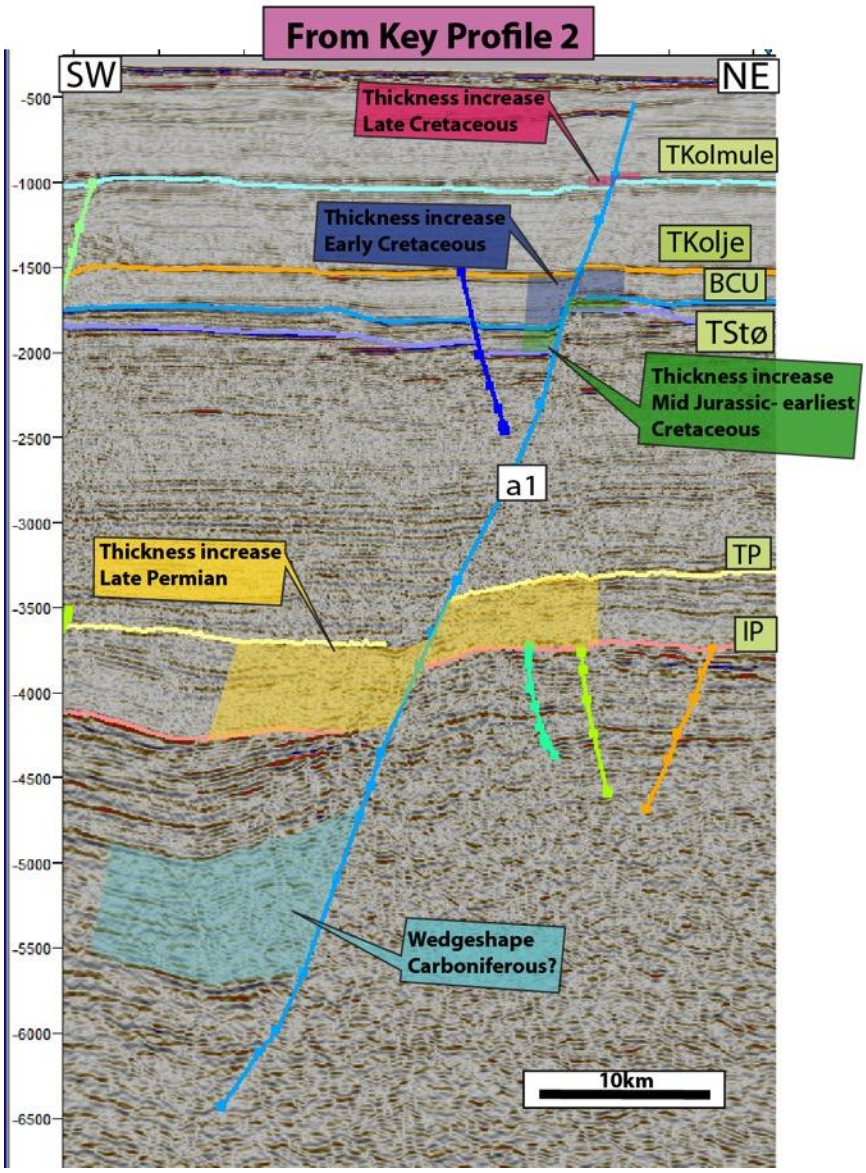

Figure 5.12: Focused area marked by red dashed square in Key Profile 2, Figure 3.13. Active faulting in Carboniferous? (wedge-shape blue area); active faulting in Late Permian (abrupt increase across the fault marked by yellow area); active faulting in Mid Jurassic- earliest Cretaceous (abrupt increase across the fault marked by green area); active faulting in Early Cretaceous (abrupt increase across the fault marked by blue area); active faulting in Late Cretaceous (abrupt increase across the fault marked by red area).

5.4. Fluid communication

Studies of open fractures in cores from the Snøhvit field done by Wennberg et al. (2008), is important when analysing the fluid flow in the study area. The fractures formed in relation to the faulting develop both parallel to, and cut the main fault core. The width of the damage zone, which contains a network of fractures, is proportional to the total fault throw. However, the latest reactivation of the fault is more important in generation and preservation of fractures than the total displacement on a fault (Wennberg et al., 2008).

Residual oil has been found both above the present gas oil contact and below the present oil water contact in the reservoir units in the Stø Formation in the Snøhvit field. There are indications that oil was spilled from the petroleum traps during expansion of gas during uplift (Nyland et al., 1992). Kristiansen (2011) identified bright zones (Løseth et al., 2009) along fault planes and in shallow areas (Torsk Formation) in the Snøhvit field area. These bright zones were located around dry structures and might be the result of the leakage described by Nyland et al. (1992).

This chapter will discuss the fluid communication in the area based on 1) reactivation of faults (2) presence of detachment (3) the geometric relation between the different levels of faulting.

Reactivation of faults was discussed in relation to the timing of faulting in subchapter 0. Reactivation of faults is known to be important to preserve open fractures (Wennberg et al., 2008), which can serve as a migration path for hydrocarbons (e.g. Bjørlykke, 2010a).

The presence of possible detachments were discussed in subchapter 5.1. Thin-skinned detachments may form in sequences containing clay, and the clay might be smeared along the fault plane. The ceiling property of the detachment depend on the amount of clay smear (Bjørlykke. 2010b), and hence the displacement along the detachment fault. However, if the detachment is ceiling, migration might happen along the fault plane of the detachment, and if the detachment is not ceiling migration through weak points in the fault plane might occur (Ligtenberg, 2005).

Both presence of detachments and reactivation of faults are important when discussing the fluid flow in the fault complex. The discussions in subchapters 5.1 and 0 lead to the illustration in Figure 5.13. The three possible detachments are included where the Possible Detachment 1 is placed farthest east, with a gradually westward location of the younger possible detachments 2 and 3. In each individual level of faulting the eastern faults appear to be reactivated and affecting younger sequences above that level of faulting. The westernmost faults in the individual fault levels appear to be detached from the faults affecting the younger sequences above.

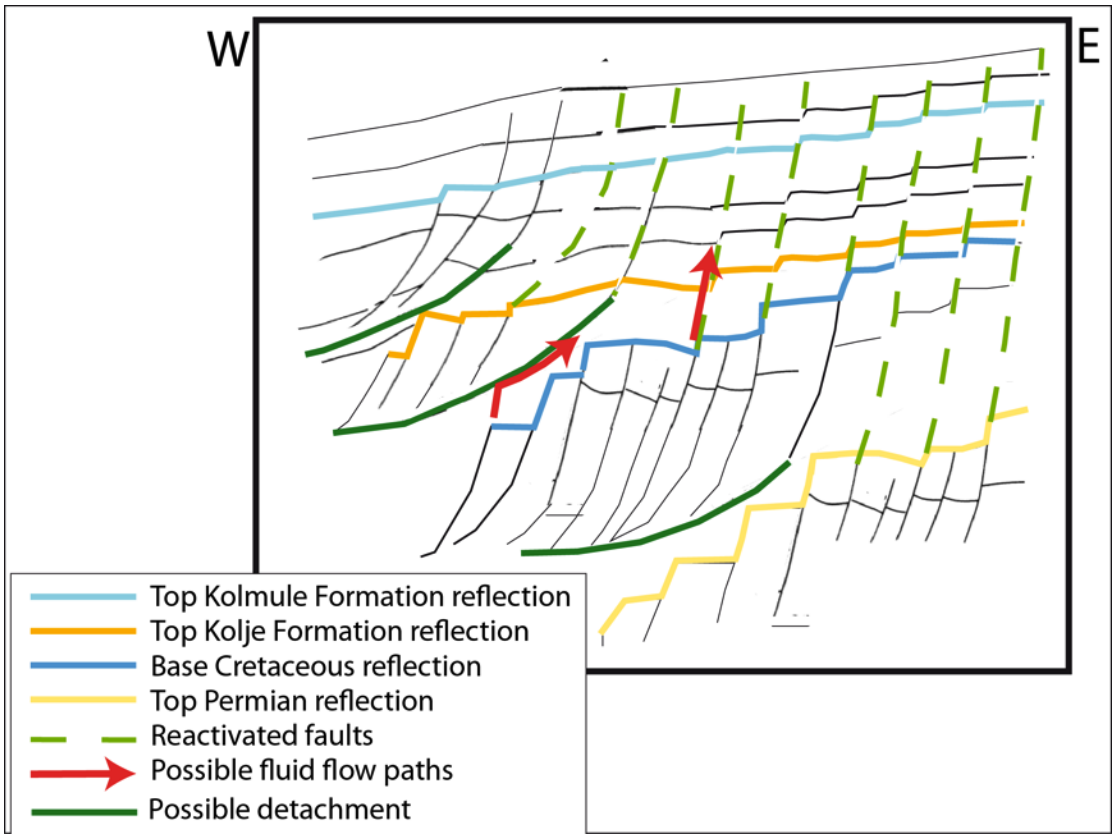

Figure 5.13: Illustration with the relation between reactivated faults and detachments between the different levels of faulting. Possible fluid flow paths are marked with red arrows. Legend of the coloured lines in the figure is given in the bottom left. (Modified from Gabrielsen, 1984)

5.5. Correlation to regional tectonic events

A correlation of the local tectonic events to the regional tectonic events is presented in this chapter. This is done in order to establish which regional tectonic events have influenced the Ringvassøy- Loppa Fault Complex. The scheme in Figure 5.14 is presenting the correlation in relation to the timeline. The five active periods of faulting discussed in subchapter 0 is in correlation to regional extensional tectonic events in the South Western Barents Sea (Faleide et al., 1984; Gabrielsen et al., 1990; Dóre et al., 1991; Dengo & Røssland, 1992; Faleide et al., 1993a; Gudlaugsson et al., 1998). Those five periods were identified by the presence of *growth faults* (Edwards, 1976). No overall regional compressional tectonic event have affected the South Western Barents Sea. However two compressional events affecting the Bjørnøyrenna Fault Complex were suggested to be of regional significance (Gabrielsen et al., 1997), but the local compressional event interpreted in the study area is not correlated to the compressional events in the Bjørnøyrenna Fault Complex.

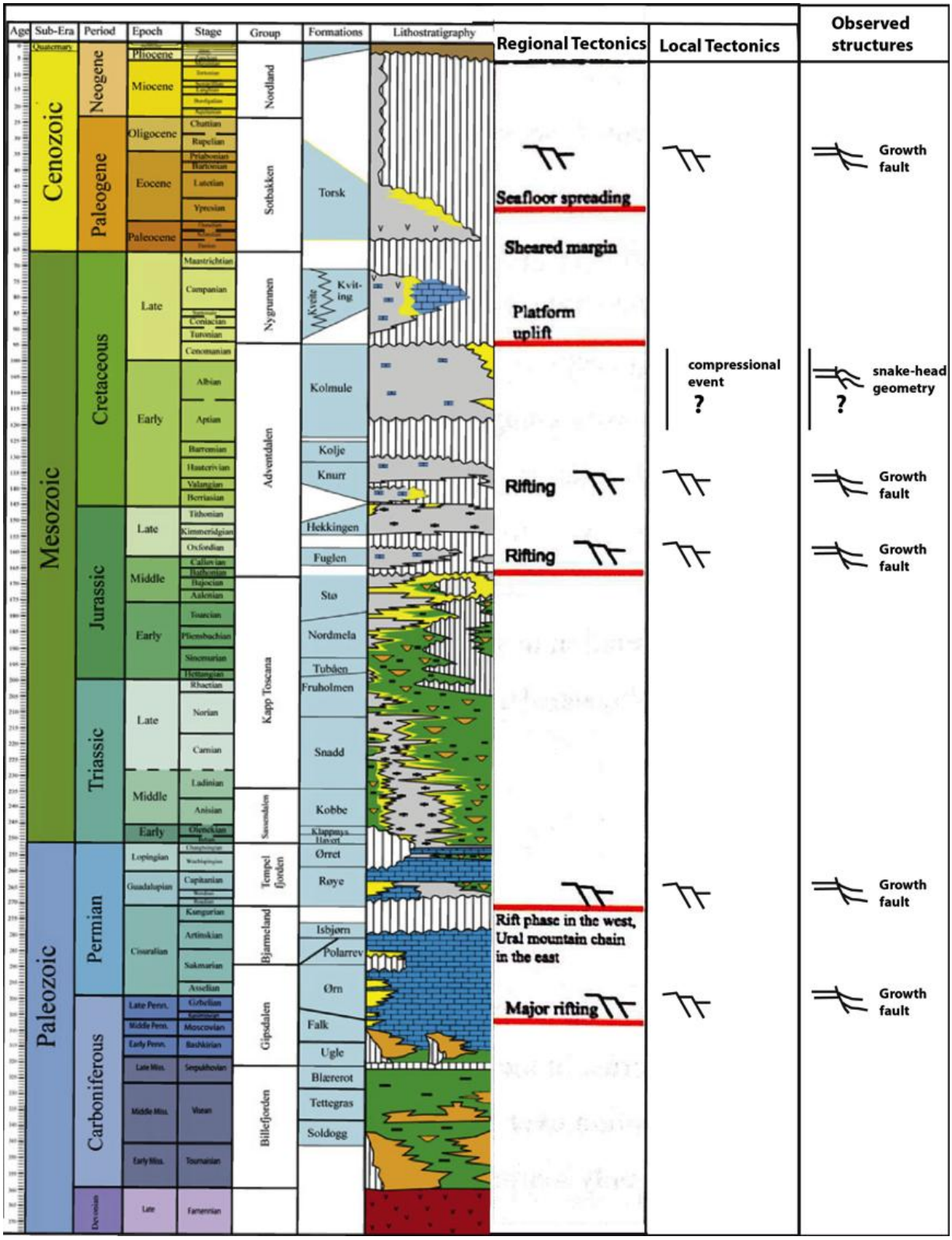

Figure 5.14: Comparison of regional tectonic evolution in SW Barents Sea (modified from Glørstad-Clark et al., 2011) to the local tectonic events in study area together with the observed structures in the seismic sections.

Chapter 6; Conclusion

Structural analysis of the Ringvassøy- Loppa Fault Complex with special focus on structural geometries, timing of faulting, reactivation of faults, whether detachments are present or not and fluid communication have been done for this study. Seismic interpretation of 2D seismic lines and interpretation of the results of analogue experiments with multiple rifting and presence of detachments, have been the two complementary parts of the data used for the analysis.

Ringvassøy- Loppa Fault Complex have vertically been divided into three levels affected by faulting with contrasting geometries, namely Late Permian level of faulting, Mid Jurassic- Early Cretaceous level of faulting and Early Tertiary level of faulting.

Three possible detachments were suggested by analysing fault plane geometries, amount of rotation of reflections in the faults blocks and overall structural geometry of the vertically separated fault levels. Two possible models for the relation between the faults in the Mid Jurassic- Early Cretaceous level of faulting and the Late Permian level of faulting are presented. Both models include important structural observations that support their presence, and no conclusion whether it is present or not can be done. The Possible Detachment 2 appears to be real far west in the fault complex above sub-area C. We can therefore conclude that the faults with listric geometries affecting both Top Kolmule Formation reflection and Top Kolje Formation reflection are detached from the faults in sub-area C in the Mid Jurassic- Early Cretaceous level of faulting. The Possible Detachment 3 was presented by a low angle fault plane reflection, and we can conclude that the faults with listric geometry affecting Top Kolmule reflections are detached from the faults affecting Top Kolje Formation in parts of the study area.

The overall structural geometry in the analogue Experiment #2 and #3 is two independent sets of fault blocks separated by a detachment zone. This overall geometry was identified in the seismic key profiles.

Five tectonic extensional phases are identified by the presence of growth faults in the study area, namely Carboniferous?, Late Permian, Mid Jurassic- earliest Cretaceous, Early Cretaceous and Early Tertiary. These are in correlation with regional tectonic events in the South Western Barents Sea. One folding was proposed to be the result of a compressional event. This event appears to be of local importance and the genesis of it cannot be concluded based on the available data.

The structural geometries, the presence of detachments, and reactivation of faults are believed to influence the fluid flow in the area. Detachments are likely to have ceiling properties, whereas reactivation of faults are likely to cause preservation of open fracture in the damage zone around the fault plane. Both Detachment 2 and 3 are only present in a limited area in the western part of the fault complex and evidences of reactivation of older faults are seen eastward in the fault complex. Two possible migration paths were indicated based on these observations.

Chapter 7; Future work

Ringvassøy- Loppa Fault Complex is a structural complex area, and future work will increase the knowledge and the understanding of the fault complex. Recommended future work for the topics in this thesis can be summarized in the following points.

- A more concentrated structural analysis of the fault complex with interpreting of 3D seismic data would improve the understanding of the linkage between the faults in area. The understanding of the fault interaction is important for the understanding of the fluid flow.
- A denser grid of interpreted seismic lines gives the opportunity to make good resolution maps, which provide important information about the structures in the fault complex.
- 3D seismic cubes give the opportunity to investigate structures in relation to detachment in chosen orientations and locations, and will most certain reveal more reliable structures that can confirm or reject the presence of a detachment with stronger evidences.
- Further investigation of analogue models with detachment zones and multiple tectonic events will probably provide more detachment related structures to compare with the structures seen in the seismic cross sections.
- Depth conversion of some seismic lines with important structural features would reveal whether the fault plane geometries are real or artefacts of the seismic velocities.
- Structural analysis of the fault complex northward and southward of the study area of this thesis will be important investigations to be done in the future.

References

Barnett, J. A. M., Mortimer, J., Rippon, J. H., Walsh, J. J., Watterson, J. (1987), *Displacement geometry in the volume containing a single normal fault.* AM. Assoc. Petrol. Geol. Bull. **71**, p. 925- 938

Barere, C., J. Ebbing, and L. Gernigon, (2009) *Offshore prolongation of Caledonian structures and basement characterisation in the western Barents Sea from geophysical modelling. Tectonophysics* **470**,p. 71-88.

Berglund, L. T., Augustson, G., Færseth, T. & Ramberg. Moe, H., (1986), *The evolution of the Hammerfest Basin*. In: A. M. Spencer (ed): Habitat of Hydrocarbons on the Norwegian Continental Margin, Norwegian Petrol. Soc. (Graham & Trotman), p. 319- 338.

Bjørlykke, K., (2010a), *Introduction to Petroleum Geology*, In: Bjørlykke, K., Petroleum Geoscience: From sedimentary Environments to Rock Physics, Springer Verlag Berlin Heidelberg, 2010,p. 1-26

Bjørlykke, K., (2010b), *Subsurface Water and Fluid Flow in Sedimentary Basins*. In: Bjørlykke, K., Petroleum Geoscience: From sedimentary Environments to Rock Physics, Springer Verlag Berlin Heidelberg, 2010,p. 259-279.

Brekke, H., & Riis, F., (1987), *Mesozoic tectonics and basin evolution of the Norwegian shelf between 60 °N and 72 °N*. Norsk Geologisk Tidsskrift, **v. 67**, p. 295-322.

Brun, J. P, T. Virginie, (1993), *Development of the North Viking Graben: interferences from laboratory modelling*. Sedimentary geology **86,** p. 31-51.

Craig Mann, D., (1989), *Thick-skin and Thin-skin Detachment Faults in Continental Sudanese Rift Basins*. Journal of African Earth Sciences, **Vol. 8**, p- 307-322

Dalland, A., D. Worsley, and K. Ofstad, (1988), *A lithostratigraphic scheme for The Mesozoic and Cenozoic Succession Offshore Mid- and Northern Norway*. Norwegian Petroleum Directorate Bulletin **4,** 65.

Dengo, C. A., and K. G. Røssland, (1992), *Extensional Tectonic History of the Western Barents Sea.* Vol. 1, In: Structural and tectonic Modelling and Its Application to Petroleum Geology, edited by R. Larsen, H. Brekke, B. Larsen and E. Gallerias, p. 91-107. Amsterdam: Elsevier, 1992.

Doré, A. G., (1991), *The structural foundation and evolution of Mesozoic seaways between Europe and the Arctic*. Paleogeography, Paleoclimatology, Paleoecology, **87**, p. 441-492.

Edwards, M. B. (1976), *Growth Fault in Upper Triassic Deltaic Sediments, Svalbard*. The American Association of Petroleum Geologists bulletin, **vol. 60**, p. 341- 355

Ellis P. G, K. R. McClay (1988), *Listric extensional fault systems- results of analogue model experiments*, Basin Research **1**, p. 55-70.

Faleide, J. I., E. Vågnes, and S. T. Gudlaugsson, (1993a), *Late Mesozoic- Cenozoic Evolution of the Southwester Barents Sea.* Vol. 4, In: Petroleum geology of Northwest Europe, Proceedings of the 4th Conference, edited by J. R. Parker, p. 933-950. London: The geological Society of London

Faleide, J. I., E. Vågnes, and S. T. Gudlaugsson, (1993b), *Late Mesozoic- Cenozoic Evolution of the South Western Barents Sea in a Regional Rift Shear Tectonic Setting*. Marine and Petroleum Geology **10**, p. 186-214.

Faleide, J. I., Tsikalas, F., Breivik, A.J., Mjelde, R., Ritzmann, O., Engen, O., Wilson, J., Eldholm, O. (2008), *Structure and Evolution of the Continental Margin Off Norway and Barents Sea.* Episodes **31**, p. 82-91.

Faleide, J. I., K. Bjørlykke, and R. H. Gabrielsen. (2010), *Geology of the Norwegian Continental Shelf*. In: Petroleum geoscience: From sedimentary Environments to Rock Physics, by K. Bjørlykke. Springer- Verlag Berlin Heidelberg.

Faleide, J. I., S. T. Gudlaugsson, and G. Jacquart. (1984), *Evolution of the Western Barents Sea.* Marine and Petroleum Geology **1**, p. 123-150.

Fitriyanto, A. (2011), *Structural Analysis of The Hoop Fault Complex, SW Barents Sea*. Master thesis, University of Oslo.

Fossen, H. & Gabrielsen, R. H., (1996), *Experimental modelling of extensional fault systems by use of plaster*. Journal of Structural Geology, **vol 18**, no. 5, p. 673- 687.

Fossen, H., Odinsen, T:, Færseth, R. B., Gabrielsen, R. H., (2000), *Detachments and low- angle faults in the northern North Sea rift system*. Geological society, London, Special publications 2000, **vol 167,** p. 105-131

Gabrielsen, R. H. (1984), *Long- lived fault zones and their influence on the tectonic development of the South Western Barents Sea*. J. geol. Soc. London **141**, p. 651- 662.

Gabrielsen, R. H., I. Grunnaleite, and E. Rasmussen. (1997), *Cretaceous and Tertiary inversion in the Bjørnøyrenna Fault Complex, south western Barents Sea*. Marine and Petroleum Geology **14**, p. 165- 178.

Gabrielsen, R. H., I. Grunnaleite, and S. Ottesen. (1993), *Reactivation of fault complexes in the Loppa High area, South Western Barents Sea*. Arctic Geology and Petroleum Potential, p. 631-641.

Gabrielsen, R. H., R. B. Færseth, L. N. Jensen, J. E. Kalheim, and F. Riis. (1990), *Structural elements of the Norwegian continental shelf, Part 1, The Barents Sea Region*. NPD- Bulletin (Oljedirektoratet) 6

Gabrielsen, R. H., J. A. Clausen (2001), *Horses and duplexes in extensional regimes: A scale-modelling contribution* In: Koyi, H.A., and Mancktelow, N.S., eds., Tectonic Modeling: A Volume in Honor of Hans Ramberg: Boulder, Colorado, Geological society of America memoirs **193**, p. 207- 220.

Gabrielsen, R.H., (2010), *The Structure and Hydrocarbon Traps of Sedimentary Basins*, in Bjørlykke, K., Petroleum Geoscience: From sedimentary Environments to Rock Physics, Springer Verlag Berlin Heidelberg, 2010,p. 299- 329

Gabrielsen, R. H., (2012), *Personal communication*

Glørstad- Clark, E, S. a. Clark, J. I. Faleide, S. S. Bjørkesett, R. H. Gabrielsen, J. P. Nystuen, (2011), *Basin Dynamics of the Loppa High area, SW Barents Sea: A history of complex vertical movements in an epicontinental basin*. In: Basin analysis in the Western Barents Sea area: The interplay between accommodation space and depositional systems, Phd thesis, University of Oslo, Oslo, p. 11-178.

Gudlaugsson, S. T., J. I. Faleide, S. E. Johansen, and A. Breivik. (1998), *Late Palaeozoic structural development of the south western Barents Sea.* Marine and Petroleum Geology **15**, p. 73-102.

Hamblin, W. K., (1965), *Origin of "reverse Drag" on the Downthrown Side of Normal Faults.* Geological Society of American Bulletin, **vol.76**,p. 1145- 1164

Kristiansen, K., (2011), *Vertical Fault Leakage in the Western Part of the Hammerfest Basin.* Master thesis, University of Bergen, Bergen

Larssen, G. B., Elvebakk, G., Henriksen, L. B., Kristensen, S. –E., Nilsson, I., Samuelsberg, T. J., Svånp, T.A., Stemmerik, L., Worsley, D., (2005), *Upper Palaeozoic lithostratigraphy of the Southern Norwegian Barents Sea*. NPD- Bulletin (Oljedirektoratet) 9

Ligtenberg, J. H., (2005), *Detection of fluid migration pathways in seismic data: implications for fault seal analysis.* Basin Research, Vol **17**, p. 141-153

Løseth, H., Gading, M., Wensaas, L., (2009), *Hydrocarbon leakage interpreted on seismic data.* Marine and Petroleum Geology, **26**, p. 1304- 1319

Maloney, D.,Davies, R., Imber, J., King, S., (2011), *Structure of the footwall of a listric faults system revealed by 3D seismic data from the Niger Delta*. Basin Research **24**, p. 107- 123.

McClay, K. R., P. G. Ellis (1987), *Analogue models of extensional fault geometries.* Geological society, London, Special Publications 1987, **v.28**, p. 109- 125

McClay, K. R., (1990), *Deformation mechanics in analogue models of extensional fault systems*. Geological Society, London, Special Publication 1990, v.54, p. 445- 453.

Nyland, B., Jensen, L. N., Skagen, J., Skarpnes, O. & Vorren, T., (1992), *Tertiary uplift an erosion in the Barents Sea: Magnitude , timing and consequences*. In: R. M. Larsen, H. Brekke, B. T. Larsen & Talleraas: Structural and Tectonic Modelling and its Application to Petroleum geology. NPF Special Publication (Elsevier, Norwegian Petroleum Society), 1, p. 153- 162.

Norwegian Petroleum Directorate, 2012, FactPage, Available at: http://factpages.npd.no/factpages/Default.aspx?culture=en (accessed 31th May 2012)

Olaussen, S., Gloppen, T. G., Johannessen, E., Dalland, A., (1984), *Depositional environment and diagenesis of Jurassic reservoir sandstone in the eastern part of Troms I area.* In: A.M. Spencer (ed.), Petroleum Geology of the North European Margin., Norw. Pet. Soc., Graham and Trotman, London, p. 61-80

Passchier, C. W., D. Sokoutis, (1993), *Experimental modelling of mantled porphyroclasts*. Journal of Structural Geology, **Vol. 15**, No. 7, p. 895- 909

Rønnevik, H. C. (1981), *Geology of the Barents Sea*. In: Petroleum Geology of the Continental Shelf of North. West Europe, edited by L.V. Illing and G.D. Hobson, London, p. 395-406.

Rønnevik, H. C., B. Beskow, and H. P. Jacobsen. (1982), *Structural and stratigraphic evolution of the Barents Sea. .* Offshore North Seas 1982. Technology Conference and Exhibition, Stavanger 1982, 29.

Rønnevik, H., and H. P. Jacobsen. (1984), *Structural Highs and Basins in the Western Barents Sea.* In: Petroleum geology of the North European margin, by Spencer A.M. et al., p. 98-107. Norwegian petroleum society, Graham & Trotman, 1984.

Schlumberger (2010), *Petrel 2010 manual, Seismic Visualization and Interpretation*. Schlumberger

Stemmerik, L. (2000), *Late Paleozoic Evolution of the North Atlantic Margin of Pangea.* Palaeogeography Palaeoclimatology Paleoecology **161**, p. 95- 126.

Twiss, R.J., E.M. Moores (2007) *Structural geology*. second edition, W. H. Freeman and Company, England.

Van Nunen, A. P., (2011), *Analogue modelling of extensional tectonics with a curved basal plate*. Master thesis, VU Universiteit Amsterdam.

Vrije universiteit Amsterdam. 2012. *Tectonic modelling laboratory*. Available at: http://www.falw.vu.nl/nl/onderzoek/laboratoria/labs-aardwetenschappen/Tectonic-Laboratory/index.asp (accessed 31th May 2012)

Walsh, J. J., &Watterson, J., (1991), *Geometric and kinematic coherence and scale effects in normal fault systems.* In: A. M., Yielding, G., and Freeman, B., (Eds.), The geometry of normal faults: Geological Society of London Special Publication, **v. 56**, p. 193-206.

Waqas, A., (2012), *Structural Analysis of the Troms-Finnmark Fault Complex, SW Barents Sea.* Master thesis, University of Oslo

Wennberg, O.P., Malm, O., Needham, T., Edwards, E., Ottesen, S:, Karlsen, F:, Rennan, L. & Knipe, R., (2008), *On the occurrence and formation of open fractures in the Jurassic reservoir sandstones of the Snøhvit Field, SW Barents Sea.* Petroleum Geoscience, **14**, p. 139-150. (tk)

Willingshofer, E., D. Sokoutis, J. P. Burg, (2005), *Lithospheric- scale analogue modelling of collision zones with a pre- existing weak zone*, In: Tectonics: from Minerals to the Lithosphere, Geological Society, London, Special Publications **243**, p. 277- 294.

Wood, R. J., S. P. Edrich, and I. Hutchison. (1989), *Influence of North Atlantic tectonics on the large scale uplift of the Stappen High and the Loppa High, Western Barents Shelf.* American Association of Petroleum Geologists Memoir **No. 46**, p. 559- 566, .

Woodcock, N. H., Scubert, C., (1994), *Continental strike-slip tectonics.* In: P. L. Hancock (ed.), Continental deformation, pergamon press, Great Britain, p. 251-263.

Worsley, D., (2008), *The post-Caledonian geological development of Svalbard and the Barents Sea.* Polar Reasearch 27, 298-317.

Zalmstra, H., (2011), *The effect of plate boundary geometry on the evolution of crustal structures in the Norwegian continental margin. An Analogue modelling study*. Bachelor thesis, VU Universiteit, Amsterdam.

Ziegler, P. A., (1988), *Evolution of the Arctic- North Atlantic and the Western Tethys.* American Association of Petroleum Geologists Memoir, **43**.